MACHINING OF FIBRE COMPOSITES AND DEVELOPMENT OF A QUICK STOP DEVICE

by

M. SATHEESHA
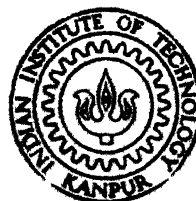
DEPARTMENT OF MECHANICAL ENGINEERING

INDIAN INSTITUTE OF TECHNOLOGY KANPUR

SEPTEMBER, 1988

MACHINING OF FIBRE COMPOSITES AND DEVELOPMENT OF A QUICK STOP DEVICE

A Thesis Submitted
In Partial Fulfilment of the Requirements
for the Degree of

MASTER OF TECHNOLOGY

by

M. SATHEESHA

to the

DEPARTMENT OF MECHANICAL ENGINEERING

INDIAN INSTITUTE OF TECHNOLOGY KANPUR

SEPTEMBER, 1988

ME-1988-M-SAT-MAC

CERTIFICATE

This is to certify that this thesis entitled, "Machining of Fibre Composites and Development of A Quick Stop Device", by M. Satheesha is a record of work carried out under our supervision and has not been submitted elsewhere for a degree.

(Dr. Prashant Kumar)
Professor
Department of Mech.Engg.
IIT Kanpur

(Dr. V.K. Jain)
Assistant Profess
Dept. of Mech. En
IIT Kanpur

Dated: September, 1988.

CERTIFICATE

This is to certify that this thesis entitled,
"Machining of Fibre Composites and Development of A Quick
Stop Device", by M. Satheesha is a record of work carried
out under our supervision and has not been submitted
elsewhere for a degree.

(Dr. Prashant Kumar)
Professor
Department of Mech.Engg.
IIT Kanpur

(Dr. V.K. Jain)
Assistant Professor
Dept. of Mech. Engg
IIT Kanpur

Dated: September, 1988.

ACKNOWLEDGEMENTS

CONTENTS

ABSTRACT

The present work consists of two parts. In first part i.e. Section I, development of a Quick Stop Device (QSD) has been discussed. Section-II deals with the machining of fibre composites.

SECTION I: Quick Stop Devices are used in machining of materials to obtain chip samples which are representative of the deformation taking place during dynamic conditions. DYnamometers are used for the measurement of cutting forces

In the present work, a safe, easy to operate and very fast retracting QSD, a concept new to this field where energy is stored as strain energy, has been designed and fabricated. The QSD has been combined with the dynamo-meters to form a single device which can be used in machini research for the study of the mechanism of chip removal. The time taken for the withdrawal of the tool from the work piece has been estimated theoretically and experimentally determined through oscilloscope by considering the front wave propagation mechanism. The chip roots have been collected at different cutting conditions and the photograp of the shear deformation zone are given.

SECTION-II: Fibre reinforced composites, though relatively new materials, have already become important engineering materials. So far the main emphasis of research has been the development of materials, but nowadays more attention i

drawn to the industrial production of products made of composites. In this work an attempt is made to study the machining of composite material through experimental investigation, in order to understand the machinability of the composites.

The effect of different cutting conditions such as cutting speed, feed rate and spindle speed on feed force, cutting force, temperature and tool wear during facing and longitudinal turning of a glass fibre composite bar has been discussed. Longitudinal turning has been conducted according to "Design of Experiments" technique while facing been conducted using 'one variable at a time' approach. For longitudinal turning the analysis has been done using the software package CADEAG-1. The effects of different factors on the responses are shown in various graphs and photographs.

LIST OF TABLES

LIST OF FIGURES

SECTION-I

CHAPTER-1

INTRODUCTION

1.1 Quick Stop Device:

Machining process is the most important of all manu-
facturing processes for the production of precision machine
components and has received considerable engineering attention
in the past few decades. With increasing introduction of new
materials in industries it is essential to understand the
mechanism of chip formation of such materials. The study of
mechanism of chip formation leads to investigate important
phenomena such as crater wear and flank wear of cutting tools
or plastic deformation associated with chip formation. The
machinability of a material can be analysed with the proper
study of the chips.

Much useful information on the mechanism of cutting
can result from a study of the chip root after rapidly
stopping a cut. The objective here is to stop the cutting
process quickly, such that the 'frozen' specimen does portray
what is happening during the cutting process. These frozen
specimen are helpful in studying the plastic deformation that
occurs in the shear zone.

Quick Stop Devices (QSD) are used in machining to
obtain chip root samples which are representative of the
deformation taking place during dynamic cutting conditions.

This device provides rapid acceleration (or deceleration) of the tool relative to the work. This withdraws tool quickly such that the chip root is not affected much during the withdrawal. So far various QSD's have been designed and used. But still the researchers are emphasising the modification of earlier QSD's.

1.2 Dynamometer:

The study of tool work interaction forces is of a great practical interest in all the chip forming operations. Specifically, the study of forces involved in the cutting process could be useful in efficient designs of machine tools and jigs and fixtures. They are also useful in studying the machining process.

For the measurement of cutting forces, dynamometers are used. It is based on the principles of modern transducer techniques, in which the cutting forces are calibrated in terms of measurable quantity such as voltage, pressure, etc. Different types of dynamometers have been developed by investigators.

1.3 Quick Dtop Device cum Dynamometer:

In machining process the study of mechanism of chip formation and the cutting forces involved are dependent parameters, which plays an important role in understanding the machinability of a material. Hence, instead of having QSD and dynamometer as separate devices, it is decided to

combine both devices as QSD cum dynamometer. The proposed device enables the simultaneous study of the forces on the tool and the instantaneous separation of the tool and workpiece for the investigation of a chip root.

1.4   Literature Survey:

1.4.1 Quick Stop Device

The idea of suddenly withdrawing the tool from cutting zone, so as to observe the zone for the correct evaluation of the process is fairly old one, already tried by Rosenhein and Sturney [1] in 1925, in connection with their studies on built up edges. However, serious investigations devoted to the chip root deformation started much later by various types of QSD.

Basically, there are two design strategies available for QSD's.

1.   Accelerating the cutting tool out of the cutting position and away from the workpiece.

2.   Abruptly decelerate the workpiece, with the tool in contact.

Both of these strategies have been used in the design of QSD.

For the design of QSD the above strategies can be approached in two ways:

        1. Mechanically operated QSD and

        2. Explosive QSD's.

1.4.1.1 Mechanically Operated QSD

A QSD involves the techniques such as action of spring pressure and the machining force to shear a pin and release the tool or action of sudden impulse loading either due to a falling mass, or a directed blow.

The QSD designed by Kocecioglu [2] is of simple construction and very easy to use. The mechanism used to 'freeze' the process of chip formation is shown in Fig.(1.1 The mechanism consists of a shortened tool pivoted about a heavy pin, and the pin fitted in a yoke. The end of the tool opposite the cutting edge is held against a sear pin by a spring. The tool is tripped by manually pulling up a handle which rotates the sear pin. The rotation of the sear pin releases the cutting tool, which swings out of the way of the chip almost instantaneously under the push of the cutting force and the pull of the spring. But this device produces a very low acceleration of the tool, so that the contact distance of the tool and the workpiece was large after the withdrawal of the tool.

For a study of the chip contact zone, Das and Bhattacharya [3] reported the use of a device similar to the Koceicoglu's QSD [2], but of heavier construction. But this device could not improve the performance of QSD.

For high speed machining and rubbing, Black and James [4] have designed a hammer QSD. This hammer QSD

A Tool
B Sear Pin
C Heavy Pin
D Spring
E Tripping Rod
F Yoke
F_c Cutting Force
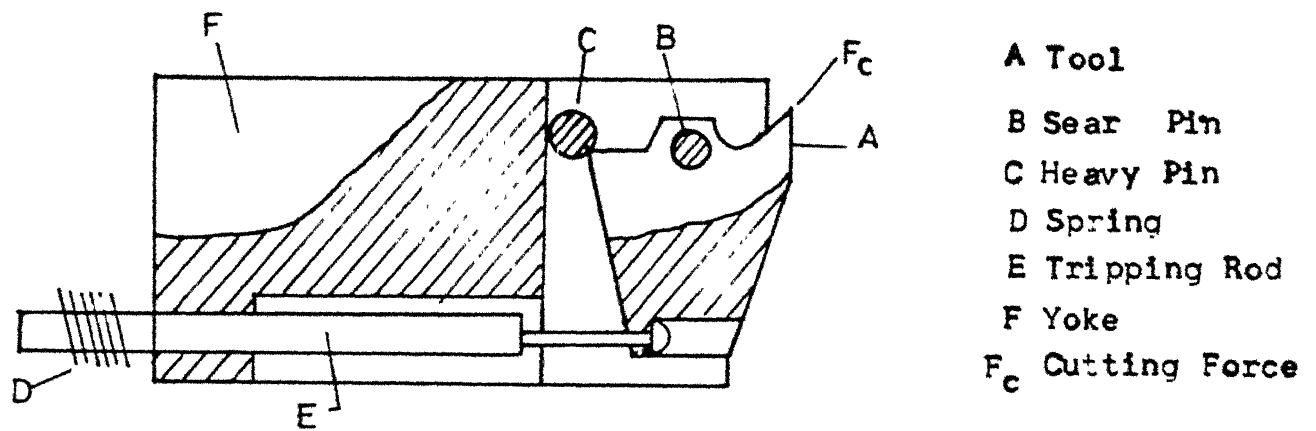
Fig. 1.1 Q S D Developed by Kocecioglu.

A Impact Bar
B Workpiece
C Tool
E Shock wave
F Guiding Blocks
G Holding Blocks
H Support
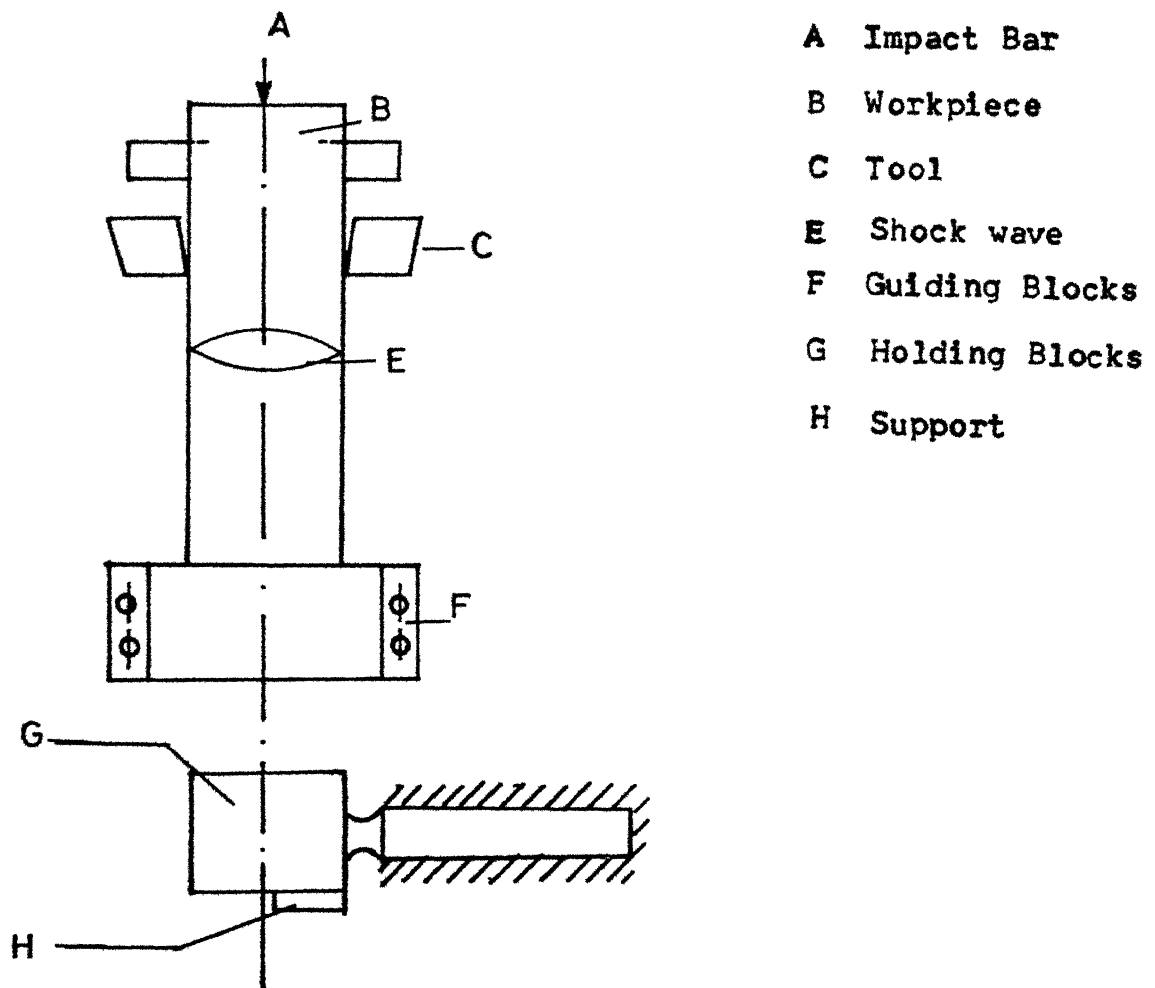
Fig. 1.2 Q S D Developed by

accelerate the tool by positive means and employs a
hammer that travels with the workpiece to accomplish
the objective. Thus, the rate at which the tool is
removed is keyed to the rate of cutting, so that the
cutting velocity never outruns the tool removal mech-
anism. The tool has a small mass composed to the
hammer, so that the tool can be drawn out of the
cutting position and away from the workpiece at the
cutting velocity. This device is mainly useful for
high speed machining.

Vorm [5] has developed a QSD to obtain the
shortest possible separation time which requires a high
initial acceleration. He has tried to obtain high
initial acceleration of the tool by transferring
energy through an elastic impact and accelerating the
workpiece from zero to the cutting velocity. His device
consists of a drop hammer of 75 kg mass falling from a
height of 600 mm corresponding to velocity of 200 m/min,
as a driving system. Figure (1.2) shows the principle
of Vorm's QSD. Orthogonal cutting is carried out symme-
trically on to the two edges of a sheet workpiece, which
is positioned relative to the cutting tools by means
of two guiding blocks. The workpiece with its holder are
hanging in the guiding blocks during the falling of
the hammer until the workpiece holder hits the shearing
punch. Thereby, the workpiece is stopped and the two

cutting processes are now carried out with the workpiece sliding in the guiding blocks. After passing the cutting length the impact bars hit the workpiece holder and a shock wave propagates through it into the shearing punch which cuts off the shear pin and then the impact forces accelerate the workpiece, thus stopping the cutting process quickly.

A QSD in which the workpiece is accelerated to the cutting velocity has been designed by Okushima and Hstomi [6]. It comprises a jig in which the travel of the shaper ram has been used to release a pin, the workpiece holder being then free to travel with the tool. The acceleration forces are provided by the cutting resistance.

Heginbotham and Gogia [7] have designed a QSD in which workpiece is brought to rest. It is relatively complex and has a large rotating mass.

1.4.1.2 Explosive QSD

In this type of QSD generally the tool is accelerated away from the workpiece after fracture of a shear pin. The fracture of a shear pin is usually achieved by a small explosive charge which is detonated at an appropriate position during the cut. These devices may be categorised into two basic ways:

1.   Those in which the exploding gas pressure acts
        directly on a piston in contact with the tool
        holder and

2.   Those in which an explosively driven bolt impacts
        top of the tool holder.

Hastings [8] has developed an explosive QSD.
The principle of operation of this device is explained
with respect to the Fig. (1.3). The force generated by
the explosive charge A located in the chamber B is used
to shear the holding pin C. The piston D transmits
the force from the burning charge to the tool block E.
The outside of the piston is threaded for the lower two
threads of its length and a knurled ring F is located on
this thread. Tightening of this ring against the body
of the tool holder forces the piston firmly against
the top of the tool block which is in turn held securely
in contact with the shear pin. This prevents free
movement of the tool block during cutting on firing of
the charge, the charge start to burn after a short delay
time. When the pressure in the explosive chamber causes
the shear pin to break, the tool block is free to move
in a downward direction under the influence of their
accelerating force. This shearing process of a pin
has been approximated as an instantaneous release mechanism

By adopting straight line retraction of the tool
Ellis, Kirk and Barrow [9] have designed a QSD on the
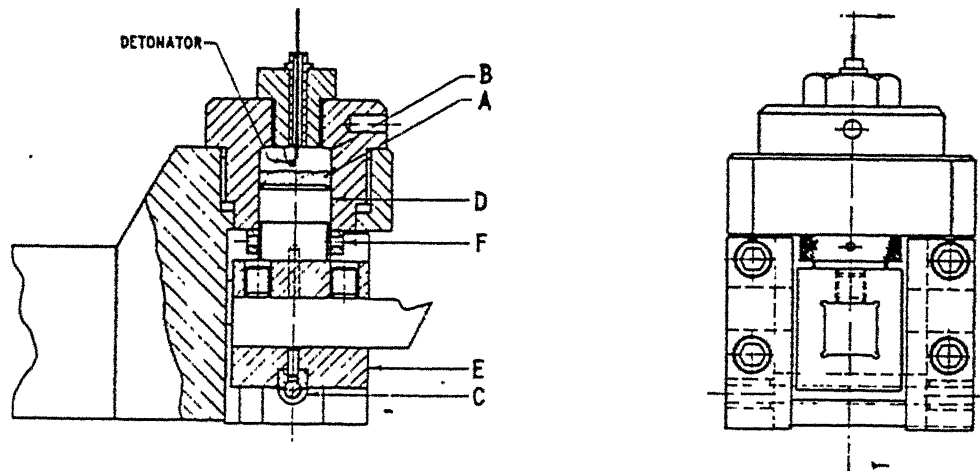
Fig.1.3   QSD developed by Hasting
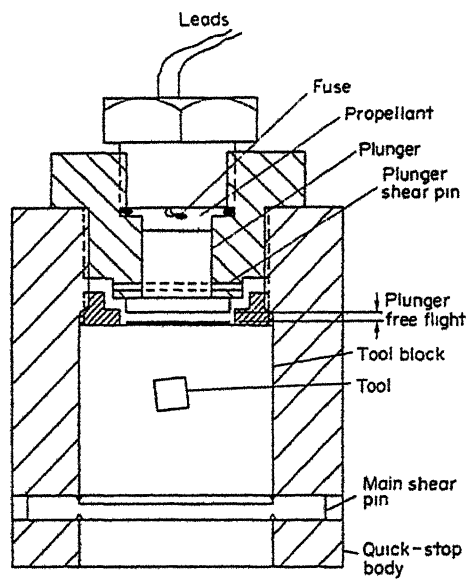
Fig. 1.4   QSD developed by Brown

pattern of the Hastings [8] QSD. Ellis et al. have used a gun with captive bolt to provide a large tool accelerating force.

Brown [10] modified Ellis et al. QSD [9] by employing double shear pin. The schematic diagram of this QSD is shown in Fig. (1.4). In this device the energy for tool acceleration is obtained from both the kinetic energy of the plunger and the direct explosive gas pressure. The double shear pin permits to obtain high tool acceleration.

A QSD for turning operation on the lines of Hastings [8] has been developed by Philip [11]. A schematic view of the device is shown in Fig. (1.5). The tool is held in a hollow cylinder A with the help of allen screws B. The upper portion of this unit serves as a piston inside a bush screwed into the holder C. D is the combustion chamber. The shear pin E resting in bushes F is used to take up the cutting force and helps in initial build up of gas pressure in the combustion chamber. The inserts G in conjunction with sharp-edged bushes create a stress concentration in the plane of the shear. The ignition assembly H holds the two terminals I and serves to vary the combustion chamber volume. A thin copper wire is strung across the termin to ignite the charge. The acceleration of the tool is achieved by breaking of the shear pin which happens after explosion of the charge by connecting the two terminal wires I.
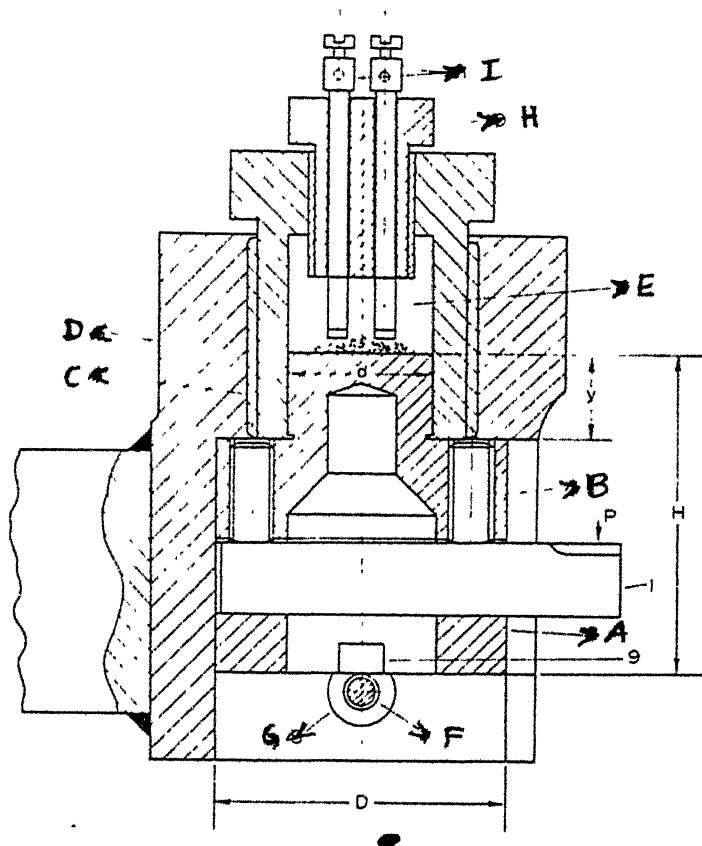
Fig. 1.5   QSD developed by Philip

Brown and Komanduri [12] have investigated the performances of all types of QSD's and have given merits and demerits of each QSD.

1.4.2 Dynamometer

The method of measuring cutting forces using dynamometer is quite old and many investigators have worked on this to develop different types of dynamometers. Basically, the design of dynamometers depend upon the type of transducers used for converting the cutting force, to measurable quantities such as voltage, pressure etc.

The different types of transducers which may be used in design of dynamometers are

1. Mechanical type
2. Pneumatic and hydraulic type
3. Electrical type
4. Piezoelectric type.

Successful practical designs, however incorporate combination of the above types and by far the most common one is the electro-mechanical type where the transducer output is in the electrical form.

One of the early successful application of electro-mechanical type dynamometer used for measuring forces in turning is reported by Merchant and Zlatin [13] . He has used strain gauge technique in which there will be change in resistance corresponding to changes in force. The dynamometers is calibrated for cutting forces in terms of

change in resistance which can be recorded.

Boothroyd [14] has developed a two-component turning dynamometer by employing strain gauges as transducers.

Shaw [15] has developed a mechanical type dynamometer. He has used a beam as cantilever for this purpose. In his design, making successful use of the principle of dimensional analysis, Shaw has given an empirical expression connecting the dimensions for the choice of the slot and hole sizes for practical design consideration.

The design and working of other strain gauge type of dynamometer for the measurement of cutting forces could be found in literature [16-18]. Among these Albrecht [17] has used a special right angled cantilever design with semiconductor strain gauges.

1.5 Objective of the Present Work:

From the above literature survey it is seen that nobody has tried to develop a QSD cum dynamometer, though extensive work has been done in both QSD and dynamometer individually. Hence it is decided to combine both QSD and dynamometer to form a single device which can be used in the investigation of material behaviour during machining process.

For a safe, easy to operate, very fast retracting and compact QSD a concept new to this field is applied where energy is stored as strain energy. This energy is released suddenly by fracturing a brittle screw with a sharp notch so as to achieve the quick withdrawal of the tool. The design utilises pivoted tool retraction. For measuring cutting forces (horizontal and vertical) a crossed ring dynamometer has been considered. The QSD is fitted to the dynamometer to enhance the moment arm of the combined device.

The present QSD cum dynamometer has been designed and fabricated in the laboratory. Theoretical and experimental analysis has been made for the estimation of the time taken by the QSD for the withdrawal of the tool from the workpiece. This device can be used only as a dynamometer, whenever needed, and this facility has been utilised in machining of composite materials. Experiments on thin mild steel tube (considering orthogonal machining) have been conducted to determine the primary shear deformation zone (PSDZ) using this QSD cum dynamometer device.

Design consideration has been discussed in Chapter 2. Chapter 3 deals with the experimentation. Results and discuss: are present in Chapter 4. Chapter 5 is the conclusion and scope for future work.

DESIGN DEVELOPMENT AND PERFORMANCE OF QSD CUM DYNAMOMETER

2.1 General Background:

Ideally, the quick stop device should accelerate the tool at an infinite rate [19] , so as to effect instantaneous withdrawal. Thus, an enormous force should act upon a negligible mass to produce large deformation of tool to move it away from the cutting zone. To achieve this, a practicall conceived QSD should satisfy the following requirements:

1.   The time from start to the finish of the separation process, i.e., the separation of tool from the work-piece, should be very small.

2.   The distance to be travelled by the tool relative to the workpiece during the separation process should be small.

3.   Geometrical and metallurgical changes in the chip and the workpiece surface produced by the action of the device should be minimum.

4.   The device should be safe, and easy to operate and should be reliable and give reproducible results.

An efficient dynamometer should satisfy the followin requirements:

1.   Dynamometer should be sensitive as well as rigid.

2.   It should be capable of measuring forces without
        any appreciable cross-sensitivity.

3.   Its performance should be unaffected by the change
        in humidity and temperature.

4.   The response time of the dynamometer should be
        small enough.

In the present design of a QSD cum dynamometer, an attempt has been made to achieve some of the above characteristics.

2.2   Principle of Operation:

The schematic diagram of the QSD cum dynamometer is shown in Fig. (2.1).

Initially, the tool holder G is held horizontal by tightening the notched allen screw by a long L shaped allen key. Whenever it is needed to withdraw the tool from the cutting position the notched allen screw H is tightened further (the rotation required for breaking of this screw, after initial tightening has to be pre-estimated by slightly rotating the allen screw.   The screw breaks and the tool holder instantaneously falls down swining about the pin K. The potential energy stored in the tool holder by holding it through the notched allen screw is converted to kinetic energy by breaking this screw.
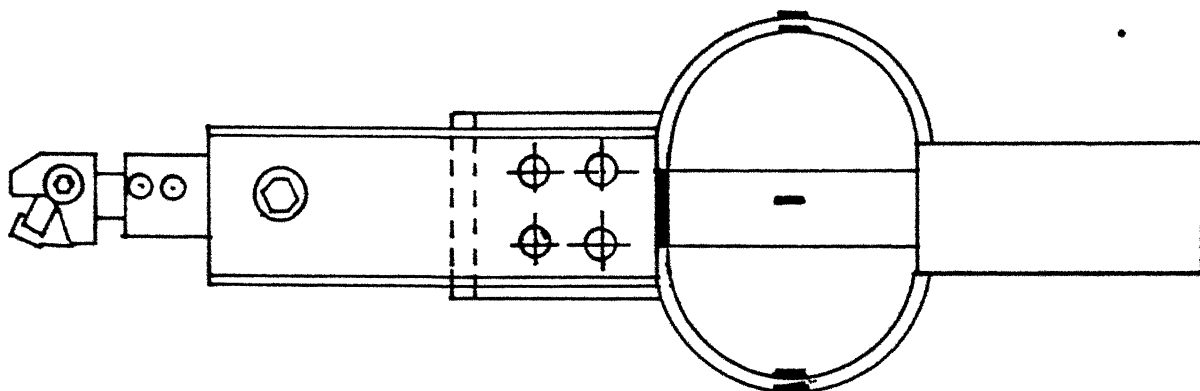
Top View
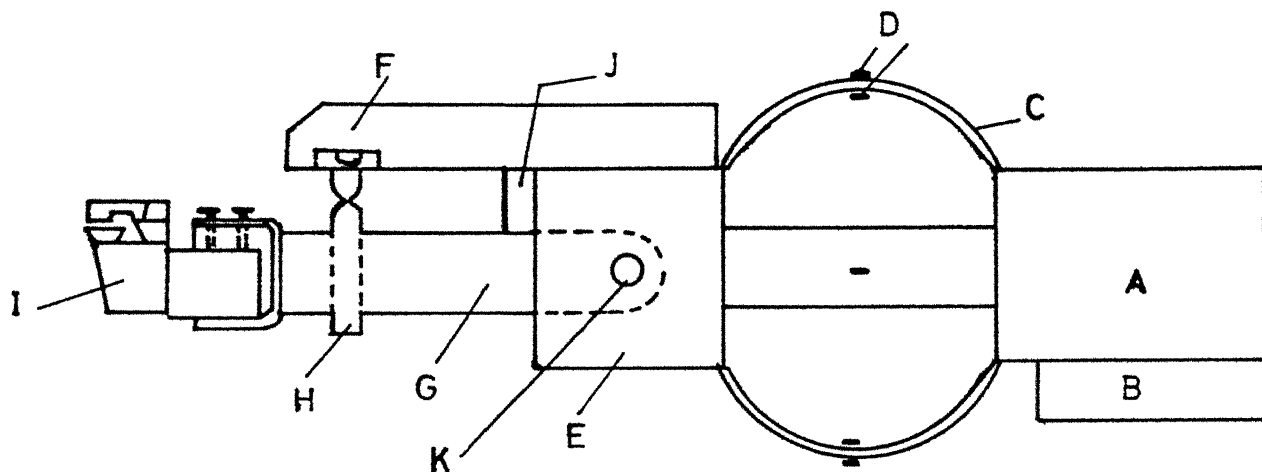
Front View

A Base
B Base Plate
C Crossed rings
D Strain gauges
E Body

F Top Plate
G Tool Holder
H Notched Screw (allen)
I Carbide bit tool holder
J Support
K Pin (hinge)

Fig.2.1 Quick Stop Device Cum Dynamometer.

The forces acting at the carbide tool bit, while machining, are sensed by the strain gauges mounted on the ironed rings of the dynamometer. The change in resistance of the strain gauges corresponding to the change in cutting forces is converted to electrical signal by wheatstone bridge. The pen recorder records the millivolts corres- ponding to cutting forces. Through calibration of the dynamometer, the forces are estimated by noting the milli- volts recorded by the pen recorder.

The QSD cum dynamometer can also be used only as a dynamometer, if desired, by using an allen screw in place of 'notched allen screw'.

2.3 Parts - Description:

The main parts of the QSD cum dynamometer are as follows:

Allen Screw: The allen screw H used is made of hardened alloy steel commonly available with tensile strength of 1000 MPa. The allen screw is of 8 mm diameter and has a notch of 3 mm diameter. The allen key used for the allen screw is ground to give hemispherical shape at its tip to have only torque and no force transmits while tightening. Figure (2.2) show the allen screw.
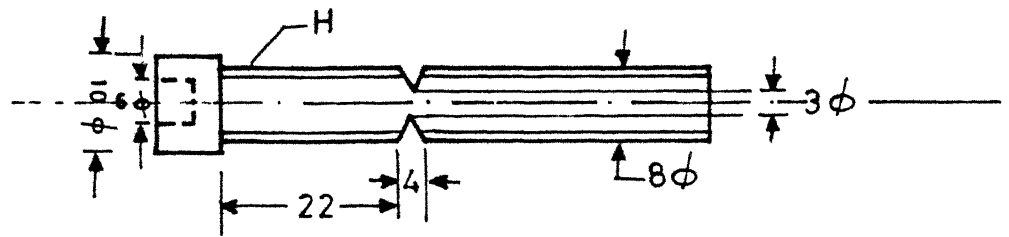
Fig. 2.2 Notched Allen Screw.

Cavity for
Tool Holder
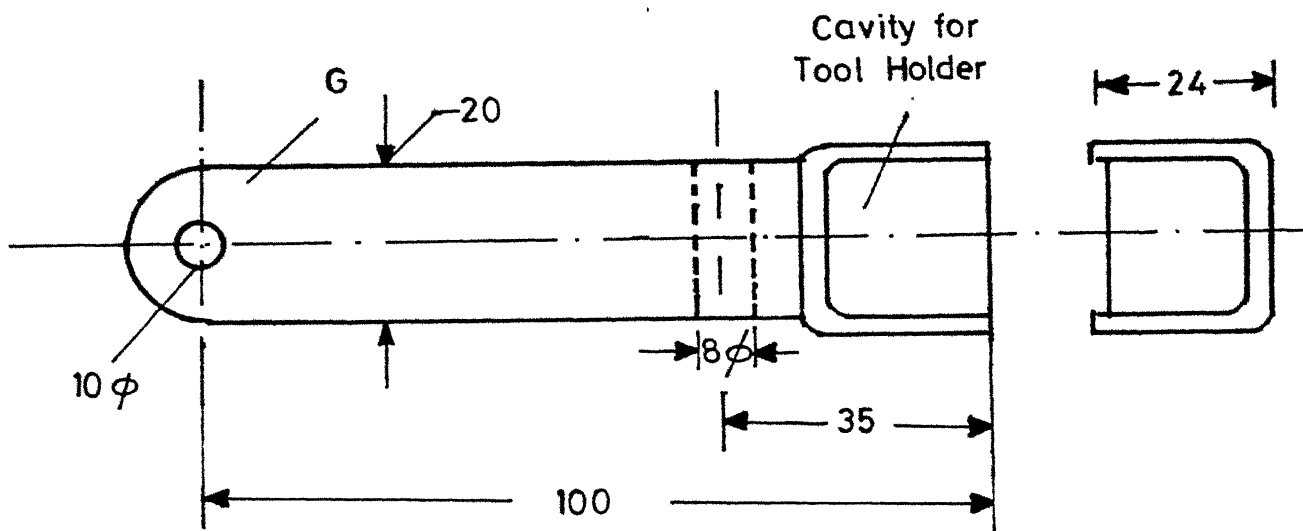
All Dimensions in m.m.

Fig. 2.3 Tool Holder.

Tool Holder: The tool holder G is made of mild steel. It is of rectangular cross-section with a rectangular cavity in front to hold the carbide bit tool holder which is tightened with the help of two screws. At the distance of 35 mm from the tool end, a tapped hole of 8 mm diameter is made. The tool holder swings about a pin K by which it is connected to the body E. The tool holder is shown in Fig. (2.3).

Body: The body E of QSD is made of mild steel. It is connected to the top plate which is also made of mild steel. Top plate (channel type) has a through hole to project the allen screw. A mild steel rectangular block is connected to the top plate and body in order to restrict the upward movement of tool holder.

Dynamometer: It is designed for orthogonal cutting for measuring two mutually perpendicular cutting forces (cutting and feed forces) in turning. The material of the dynamometer does not yield when subjected to the design load. Eight strain gauges of 120 resistance (R_g) and gauge factor 2.0 are mounted on the crossed rings for the measurement of two forces. Strain gauges coupled with wheatstone bridges are used to measure forces in orthogonal direction. The forces are measured in terms of millivolts recorded by the pen recorder. The wheatstone bridge circuit-1 is shown in Fig. (2.4).
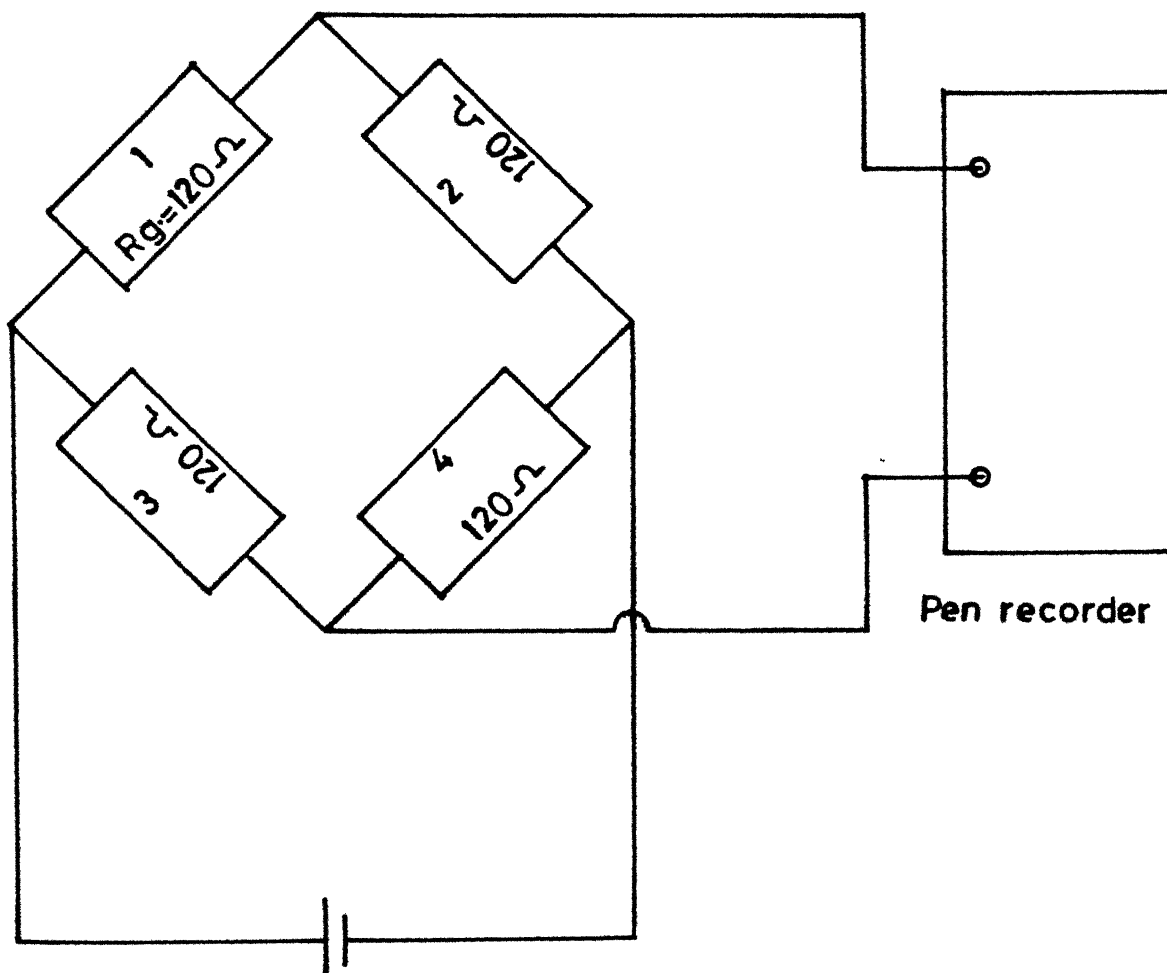
Fig. 2.4 Wheatstone Bridge Circuit - I.

2.4 Performance of QSD:

The tool holder swings about a pin after instantaneously release of the tool from the workpiece by breaking a notched allen screw. In order to determine the time taken for the withdrawal of the tool from the workpiece, the natural frequency of the tool holder is estimated by considering the forces acting on the tool holder.

In the analysis, the tool holder with tool is considered as a beam.

The schematic diagram of the beam is shown in Fig. (2.5).
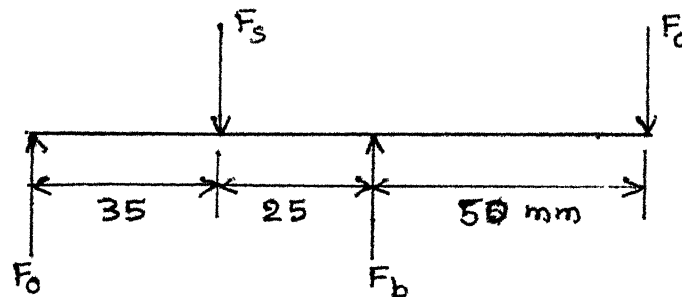
Fig. (2.5). Schematic Diagram of the
                    Beam

where,

F_o is the force at the pin K of the tool holder

F_s is the force acting by the support M

F_b is the allen screw

F_c is the cutting force.

Since sum of all the moments about F_o, before breaking of the screw is zero, we have

$$F_c (115) - F_b (60) + F_s (35) = 0$$

or

$$F_s = \frac{F_b (60) - F_c (115)}{35} \qquad (2.1)$$

But, F_b is equal to the force required to break the screw, which can be written as,

$$F_b = \pi(\frac{d^2}{4}) \times \sigma_b \qquad (2.2)$$

where, d is equal to 3 mm and σ_b, the breaking strength of the screw and is about 1000 MPa.

By substituting values of d and σ_b in Eq. (2.2), we obtain,

$$F_b = \frac{(0.003)^2}{4} \times 1000 \times 10^6 \text{ N} \simeq 7069 \text{ N}$$

If the dynamometer is designed for the maximum load of 500N, then substitution of Eq. (2.2) in Eq. (2.1) gives,

$$F_s = 10,475 \text{ N}$$

Also, since sum of all the forces in vertical direction is zero, we obtain,

$$F_o + F_b = F_s + F_c$$

or

$$F_o = F_s + F_c - F_b$$

$$= 10,475 + 500 - 7069$$

$$= 3906 \text{ N}$$

2.4.1 Determination of Deflection of the Beam

After initial tightening of the screw, the deflection of the beam will be as shown in Fig. (2.6).
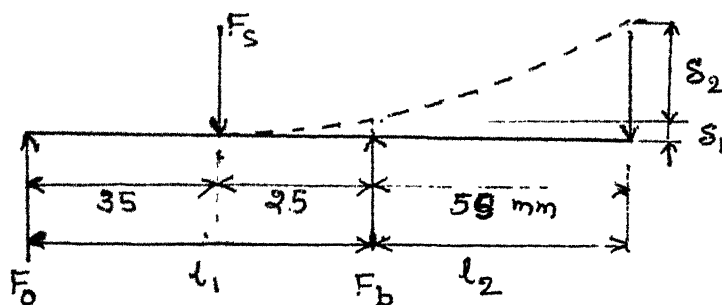
Fig.(2.6). Mode of Deflection of the Beam After Tightening of the Allen Screw.

Here, it is assumed that the cutting force acting at the end of the beam is negligible. Also, it is assumed that the beam acts as a cantilever between F_s and tip of the tools. The total deflection (δ) of the beam will be equal to the deflection of the beam due to force F_b and due to overhanging length, l_2.

Therefore, total deflection at the tip of the tool is

$$\delta = \delta_1 + \delta_2$$

where,

$$\delta_1 = \frac{F_b (l_1)^3}{3EI}$$

$$\delta_2 = \Theta \cdot l_2$$

$$= \frac{1}{2} \frac{F_b (l_1)^2}{EI} \times l_2$$

where,

l_1 = length between hinge and centre of the screw = 0.06 m

l_2 = length between F_b and tip of the tool = 0.05

E = Young's modulus of the beam = 210 MPa

I = Moment of inertia of the beam = $1.73 \times 10^{-8} m^4$

Θ = Slope of the beam.

For the configuration of this study,

$\delta_1 = 1.4 \times 10^{-4} m$

$\delta_2 = 1.93 \times 10^{-4} m$

$\delta = \delta_1 + \delta_2 = 3.3 \times 10^{-4} m$

2.4.2 Estimation of Time taken by the QSD to Withdraw Tool from the Workpiece

Natural frequency [20] of the beam is given by

$$\omega = (\beta_1 l)^2 \sqrt{\frac{EI}{\rho \, l^4}}$$

where $(\beta_1 l)$ is the fundamental mode of vibration with $(\beta_1 l)^2 = 3.52$ for cantilever beam.

l is the overhanding length of the cantilever = 0.08m

ρ is the mass per unit length of the beam = 4.07 kg/m

Therefore,

$$\omega = (3.52) \sqrt{\frac{210 \times 10^9 \times 1.73 \times 10^9}{4.07 \times (0.08)^4}}$$

$$= 1.64 \times 10^4 \text{ rad/sec.}$$

We are interested in the withdrawal of the tool only which occurs in less than T/4 time, where T is the time period. Hence, withdrawal time t_ω is,

$$t_\omega = T/4 = \pi/2\omega \tag{2.3}$$

Substituting the value of ω in Eq.(2.3) we obtain,

$$t_\omega = 9.57 \times 10^{-5} \text{ secs.}$$

Thus, withdrawn time of the tool from the workpiece is less than 96 μs.

2.4.3 Contact Time between Tool and Workpiece:

For the quick withdrawal of the tool from the workpiece the velocity of the tool at T/4 secs should be greater than the velocity of the workpiece. Assuming the motion of the beam (tool holder) to be simple harmonic motion (SHM), the displacement of the beam is given by,

$$X = X_o \cos \omega t \qquad (2.4)$$

where X_o is the maximum deflection of the beam before breaking = 3.32×10^{-4} m.

By differentiating Eq. (2.4), we get velocity,

$$X^o = -X_o \omega \sin \omega t$$

Maximum value of velocity is

$$X^o_{max} = -X_o \omega = 3.32 \times 10^{-4} \times \left(\frac{2\pi}{96 \times 4 \times 10^{-4}} \right)$$

$$= 5.43 \text{ m/sec.}$$

If we design for maximum velocity of the workpiece X^o_{Wp} to be 5 m/sec, then

$$X^o_{max} > X^o_{Wp}$$

To determine the contact time t_c between the tool and the workpiece after the tool starts moving, we equate X^o to 5 m/sec. Then, we have,

$$X^o = 5 = -X_o \omega \sin \omega t_c \qquad (2.5)$$

By substituting the values of X_o and ω in Eq. (2.5), we obtain,

2.4.4 Acceleration of the Tool

To calculate the acceleration a, at the time of withdraw, consider,

$$\int\limits_{0}^{5} dv = \int\limits_{0}^{71} a\, dt$$

or

$$a = + 7 \times 10^4 \text{ m/sec}^2$$

2.4.5 Contact Distance between Tool and Workpiece

The distance moved before complete withdraw of the tool is given by,

$$\int\limits_{0}^{5} v\, dv = \int\limits_{0}^{s} a\, ds$$

or, $s = 1.78 \times 10^{-4} \text{m}$

or $s = 0.178$ mm.

As the distance moved before complete withdraw of the tool is very less i.e. 0.178nm, there will not be much changes in the geometrical changes in the chip and the workpiece surface.

CHAPTER-3

EXPERIMENTATION

The combined Quick Stop Device with dynamometer has
been fabricated in the laboratory according to the design
discussed in Chapter 2. The photograph of this device is
shown in Fig. 3.1. Experimental set-up shown in Fig. (3.2).
was developed with instrumentation and recording system for
the measurement of time taken by the QSD for the withdrawal
of the tool. Using this combined QSD with dynamometer device
orthogonal cutting has been conducted on mild steel tube to
study the primary shear deformation zone (PSDZ). The photo-
graphs of (PSDZ) are shown in Fig. (3.3).

3.1   Experimental Determination of Performance of QSD:
3.1.1 Principle Adopted
        In order to estimate the time taken by the tool to
withdraw from the workpiece, wave propagation is considered in
the body of the tool holder. In elastic materials it is
well known that the longitudinal waves move with the velocity of
$\sqrt{\dfrac{E}{\rho}}$ and shear waves (or flexural waves) move with the velocity
of $\sqrt{\dfrac{G}{\rho}}$ where, E and G are Young's and shear modulus of the
bar respectively and ρ is the density of the bar material. In
case of mild steel, material used for making tool holder,
the longitudinal velocity is 3 mm/μs and shear wave
velocity is 6 mm/μs.
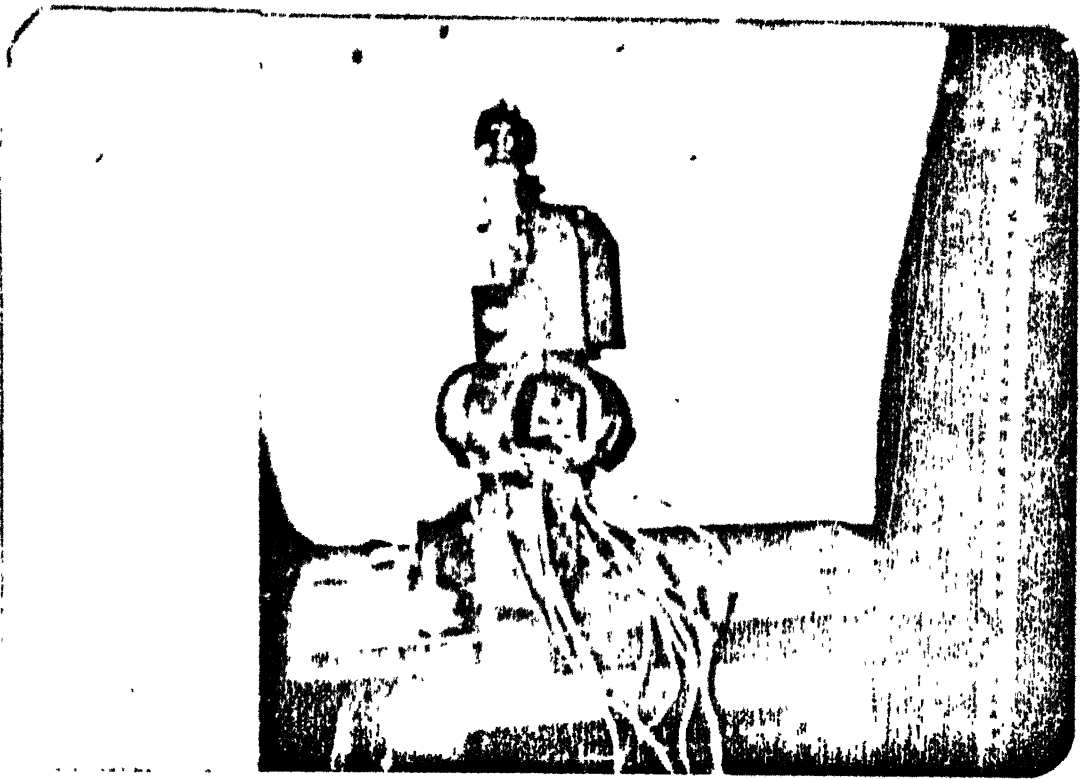
FIG.(3.1) PHOTOGRAPH OF QSD CUM DYNAMOMETER.
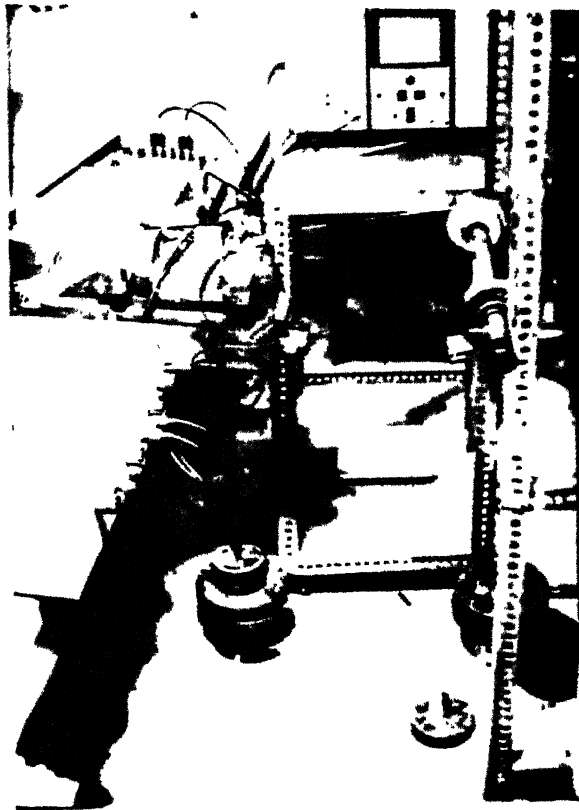
FIG.(3.2) PHOTOGRAPH OF THE EXPERIMENTAL
SET-UP FOR THE ESTIMATION OF TIME
TAKEN BY THE TOOL FOR THE WITHDRAWL
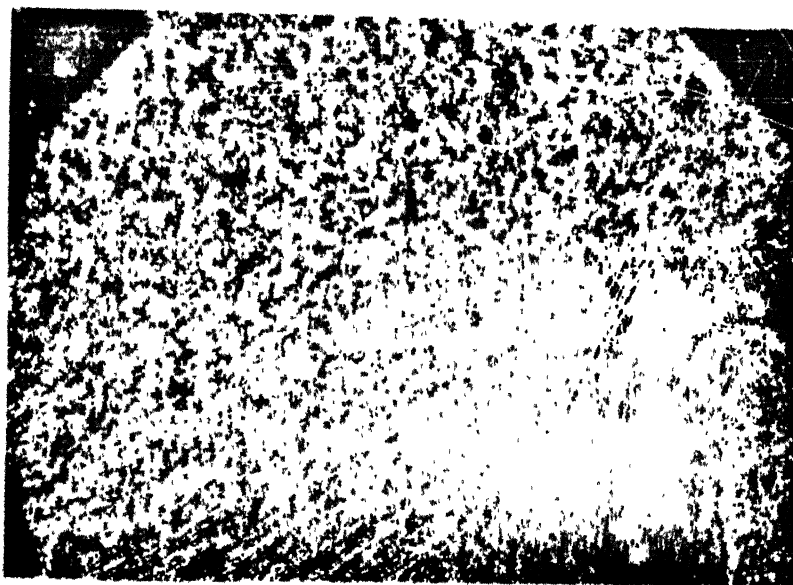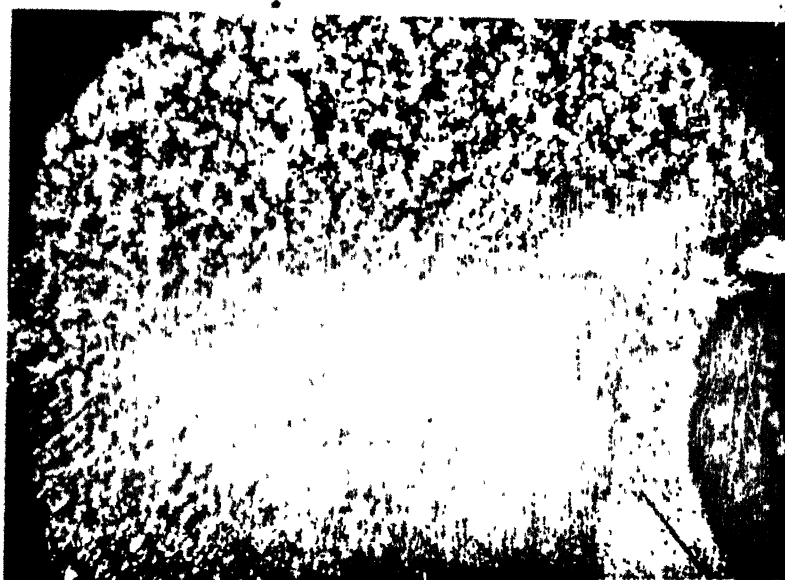
FIG.(3.3). PHOTOGRAPHS OF SHEAR DEFORMATION ZONE

The energy is stored in the tool-holder by tightening the screw in the form of potential energy. As soon as the screw is broken by slight-tightening, the whole energy will be converted into kinetic energy which helps us to withdraw the tool from the workpiece. When the screw breaks, the released waves moves in both directions, towards the hinge of the tool holder and towards free tip of the tool holder. In fact, the body of the tool holder which is made from a rectangular bar, works as a wave guide. The velocity of energy propogation and the shape of the wave front group velocity determines the withdrawal time of the tool from the workpiece.

In the present QSD with dynamometer, as the conserved energy is released suddenly by breaking the notched screw, the above mentioned principle is utilised for the estimation of time taken by the QSD for the withdrawal of the tool.

3.1.2 Experimental Procedure

In order to monitor this wave front strain gauges and wheatstone bridge is used. Two strain gauges of 120Ω resistance and gauge factor 2.0 are mounted on the tool holder adjacent to the notched screw, side by side. The leads of the strain gauges are connected to the wheatstone bridge to record stress on a digital oscilloscope. A triggering pin is held near the strain gauges to receive and

display of the wave front on the oscilloscope. When the notched screw breaks, the wave front is transmitted to the oscilloscope by triggering action and the time taken by this wave to travel and also the stress induced by this wave can be measured on oscilloscope. Hence the time taken by the tool for the withdrawal can be measured by the oscilloscope record.

The wheatstone bridge circuit as shown in Fig. 3.4 is designed and made. The leads from the strain gauge terminals are connected to a bridge circuit housed in an aluminium box. Coaxial wires with BNC connectors are used to minimise the noise. A D.C. battery of 9V is used in the bridge circuit. The two gauges mounted on the tool holder from the two opposite arms of the bridge circuit to cancel the effect of flexural waves, if any. A dummy gauge (same as mounted on the tool holder) mounted on the piece of a material same as the tool holder material forms the third arm of the bridge. This piece of material along with the strain gauge is also enclosed in the aluminium box to minimise the noise. A standard resistance of 100Ω with the potentiometers forms the fourth arm of the bridge. The 50 Ω potentiometer placed in series with 100 Ω resistance is used for coarse balancing and the $1K\Omega$ potentiometer placed parallel to the 50 Ω potentiometer is used for fine balancing. The aluminium box, the outer shield of the coaxial wires and the tool holder
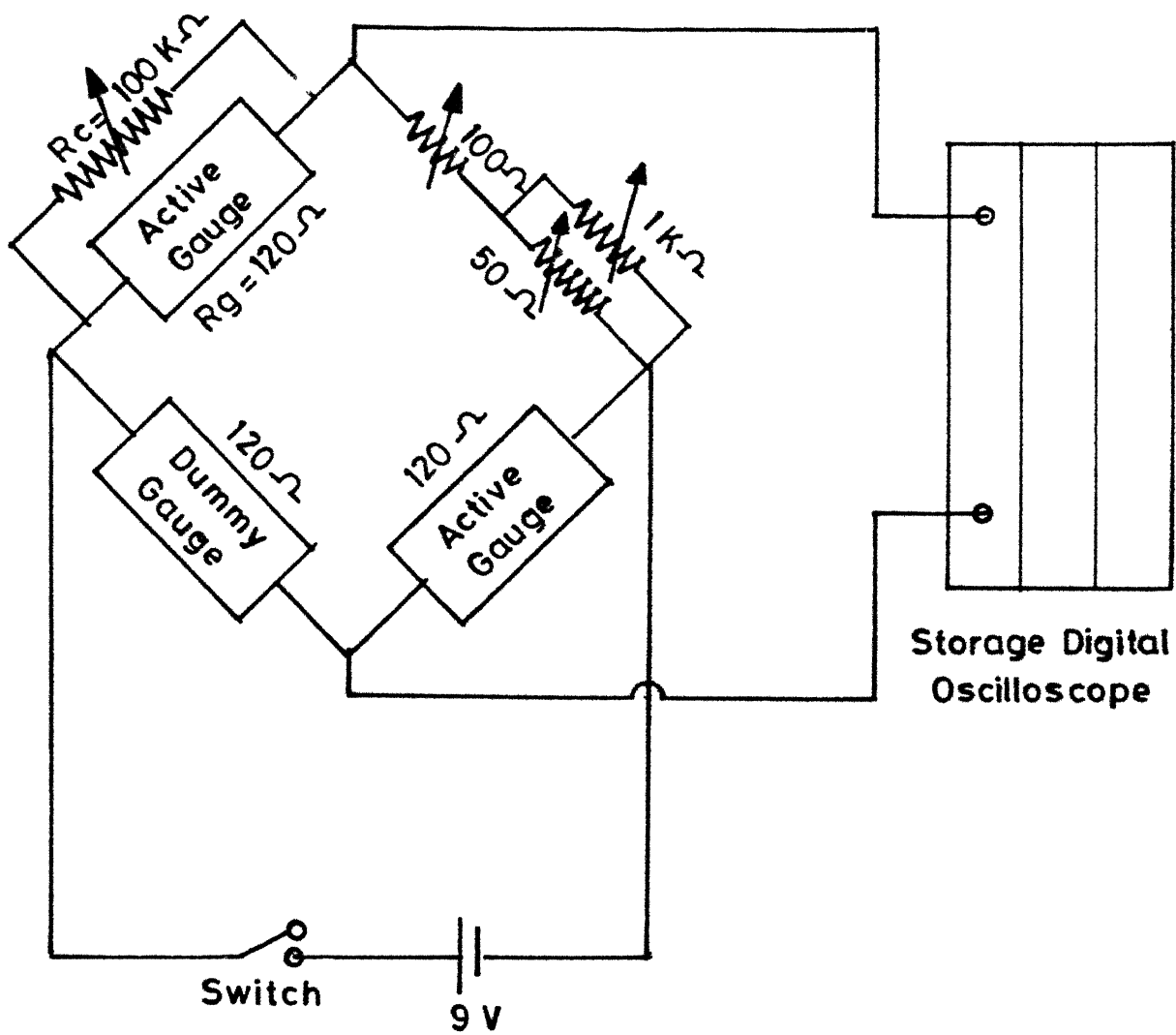
Fig. 3.4 Wheatstone Bridge Circuit - II.

are connected to a common ground for suppressing noise further. The output leads of the bridge are connected to the oscilloscope A storage dual beam digital oscilloscope (Model 2090, Exploer II made by Nicolet Instrument Corporation, U.S.A. is used for measuring the signals.

3.1.4 Measurement of Strain Induced in the Tool Holder

For measuring the strains induced in the tool holder the bridge circuit shown in Fig. (3.4) is calibrated prior to testing. For this purpose a shunt calibrating variable resistance R_c in the circuit is connected in parallel with one of the active gauges. When R_c is included in the circuit by pressing the push button a change in the active gauge resistance is introduced. This change in gauge resistance produces a certain voltage deflection on the oscilloscope screen. In this manner a calibrating relation is obtained between the change in the active gauge resistance and the voltage output of the bridge. Mathematically, the change in the active gauge resistance ΔR_g, is given by

$$\frac{\Delta R_g}{R_g} = \frac{-R_g}{R_g + R_c} \qquad (3.1)$$

The equivalent calibrating strain ε_c, is then directly obtained from the deflection of the gauge factor S_g, of the strain gauge,

$$S_g = \frac{\Delta R_g}{R_g} / \varepsilon_c \qquad (3.2)$$

Substituting Eq. (3.1) in Eq. (3.2) yields,

$$\varepsilon_c = \frac{-R_g}{S_c} \left(\frac{1}{R_g + R_c}\right) \tag{3.3}$$

In the present case, two gauges are mounted on the tool holder to monitor the stress pulses. Hence, the voltage output of the bridge circuit is doubled for the same strain. Thus, by recording the voltage output of the bridge, strains in the tool holder is immediately known.

In order to observe the time taken for the withdrawal of the tool by the QSD, two forces, vertical force and horizontal forces were applied on the tool and the notched screw was broken for different set of these forces the time taken for the withdrawal of the tool have been noted. Hard copies of the recorded wave front signals recorded by the oscilloscope can be plotted on a Hewlett-Packard X-Y recorder. Through this recorded wave front signals the time taken by the tool to withdrawal can be measured directly.

3.2 Study of Shear Zone:

In order to study the PSDZ zone in mild steel, thin mild steel tube was machined at orthogonal conditions and then the chip roots were collected at different cutting conditions as given in Table 2, using the QSD cum dynamometer. The collected chip roots were prepared for microstructure observations by grinding, etching and polishing operations. Afterwards the chip roots have been examined under the microscope.

CHAPTER-4

RESULTS AND DISCUSSION

The time taken by the tool to withdraw from
the workpiece have been estimated at different feed
and cutting forces and are given in Table 1. The
Fig. (4.1) shows the graph of the front waves monitored
by breaking the screw at different cases. Also the
experiments results observations obtained from QSD
cum dynamometer of primary shear deformation zone
(PSDZ) at different cutting conditions are discussed
and are given in Table 2.

4.1 Machining Forces and Tool Withdrawal Time
From the Fig. (4.1) taken by the oscilloscope
X-Y plotter it is seen that in the beginning, the
front wave has attained maximum and minimum value and
then it has become almost steady. As soon as the
screw breaks, the stored strain energy in the tool holder
will be converted to kinetic energy. This maximum
and minimum value may represent the strain energy
storing and releasing condition. The released front
waves will be moving along the tool holder backward
and forward for some period and this is noted by its
steady state. Hence in order to estimate the time taken
by the tool to withdraw we have considered the beginning
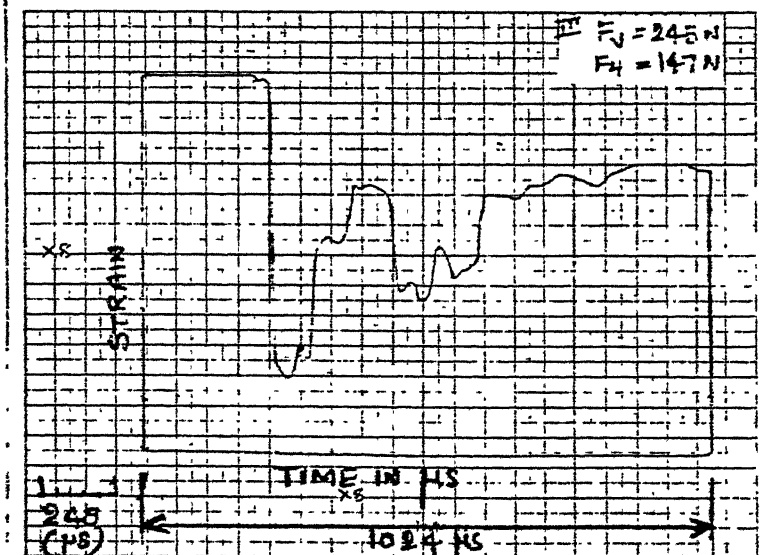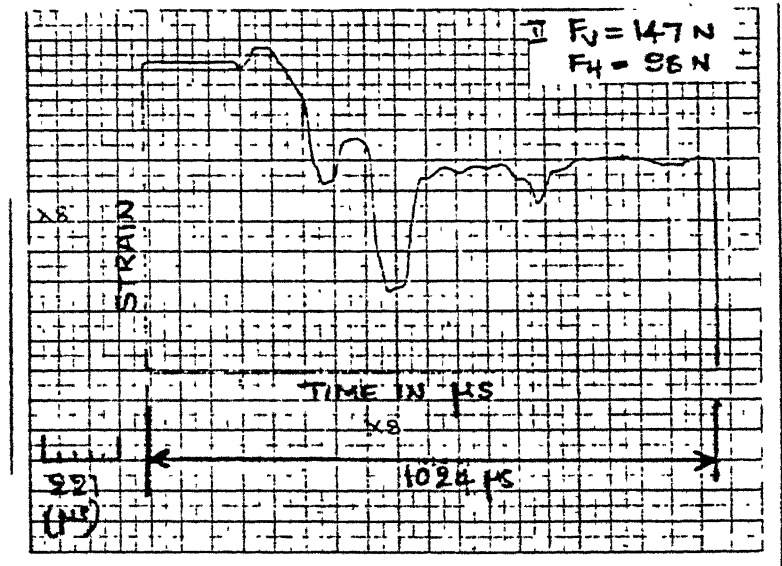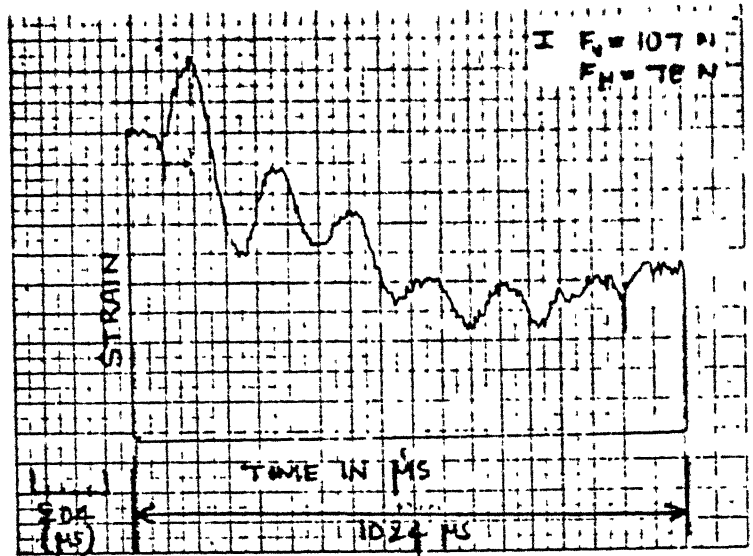
FIG. (4.1). OSCILLOSCOPE RECORD PLOTTED BY
X-Y PLOTTER
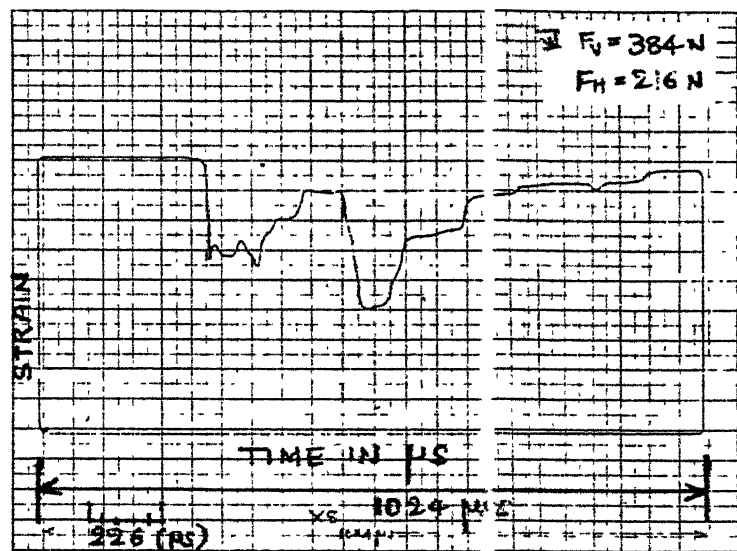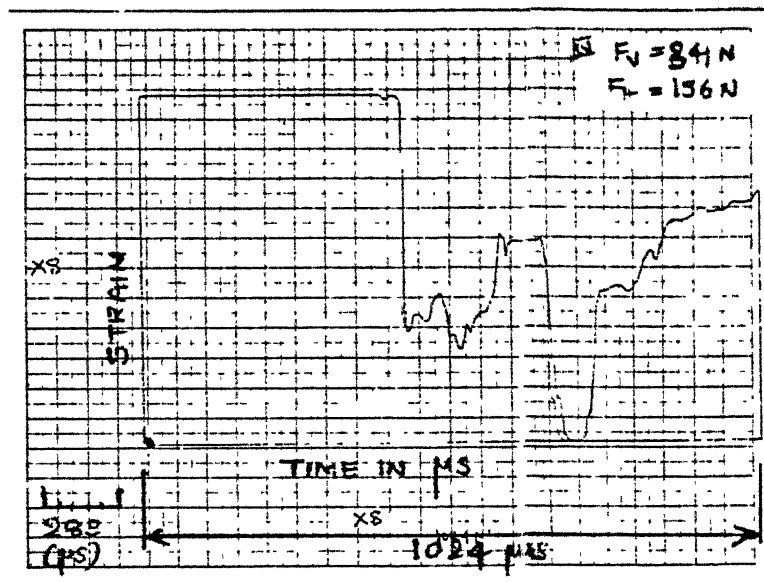
FIG. (4.1) .. CONTINUED

portion of the graph in Fig. (4.1). This time in microseconds is directly noted by the oscilloscope.

From the Table-1 it appears that the withdrawal time of the tool is almost constant for all combination of feed and cutting forces and is found to be around 250 μs.

The photographs of the PSDZ are shown in the Fig. (5.3). From this figure it is clear that the dynamometer cum QSD is very effective in studying the shear zone.

CHAPTER-5

CONCLUSIONS AND SCOPE FOR FUTURE WORK

5.1 Conclusions:

On the basis of analytical and experimental results, the following conclusions may be drawn.

5.1.1 Tool Withdrawal Time

1. The present QSD cum dynamometer would be of a great help for the investigation of material behaviour during machining process by simultaneously measuring the machining forces, and obtaining the frozen chips.

2. The developed QSD cum dynamometer is easy, simple and safety to operate and it consists less number of parts.

3. From the analytical results, the tool withdrawal time is found to be less than 96 μs. While experimentally (considering front wave propagation) it is found to be around 250 μs. This indicates the very fast withdrawal of the tool.

4. The present QSD cum dynamometer is very effective for obtaining chip roots for the study of shear deformation zone.

5.2 Scope for Future Work

1. The dynamometer can be modified for the measurement of all the three cutting forces.

2. Using this QSD cum dynamometer more experimental investigation can be performed for the detailed study of the PSDZ and the secondary shear deformation zone.

CONTENTS

LIST OF FIGURES

SECTION-II

CHAPTER-1

INTRODUCTION AND LITERATURE SURVEY

1.1   Introduction:

1.1.1 Fibre Composites

        A material created by the combination of two or
more constituents differing in form and/or material compo-
sition and that are essentially insoluble in each other
is called a composite material. Composite materials have
been classified on the basis of the geometry of a repre-
sentative unit of reinforcement. Fibre, particles and
laminar are the commonly used geometrical shapes.

        Fibre reinforced composites are relatively new
but they have already become important engineering materi-
als. Since their industrial introduction, composite
materials are replacing metals in many industries. The
main reason for their popularity is the improvement of
physical properties such as light weight associated with
high strength, stiffness, fatigue strength, thermal
resistance and damping capacity. Additional advantages
that composites offer over the conventional materials
include flexibility in design, corrosion resistance etc.
Today, fibre composites have found diverse applications
such as space-vehicles, aircraft, offshore structures,

automobiles, protective armours, chemical containers, sporting goods and electronics. The most widely used fibres are glass, graphite, aramid (Kevlar) and boron. Plastics such as epoxy, polyester, phenolics and metals in certain cases are the commonly used matrix materials.

In the past, the main emphasis of research was only on the development of materials, but nowadays more attention is drawn to the industrial production of products made of fibre reinforced plastics (FRP). In aerospace and shipbuilding industries, which are almost classic fields of application, the production is of large parts in batches, but in automotive, machine-tool and sporting goods-industries, the necessity of fully automated and economic method arises. The substitution of metals by plastics with glass, carbon or aramid fibre reinforcement does not only require change in design philosophy, but also affects both the particular production techniques and the complete production cycle.

1.1.2 Machining of Fibre Composites

Machining of composites has already started taking an important place in the field of manufacturing processes. Products made of composite materials usually need post molding treatment like turning, drilling etc. Economic considerations of different operations to be performed on such products, demand its study in depth.

The machining of FRP differs in many respects from metal working. The material behaviour is not only inhomogeneous, but also dependent on the fibre and matrix properties, fibre orientation and the type of weave. Therefore the machining of FRP puts special demands on the geometry and abrasive resistance of tool material.

For the machining of glass- and carbon- fibre composites, a conventional tool geometry similar to the one used in metal working is usable. Since high abrasion resistance of tool material is necessary while machining these composites, high speed steel (HSS) is unsuitable as a tool material. But, tungston carbide (WC) tools may be used [21].

For the complete utilization of fibre composites in the industries, it is essential to study the machining process of the same in depth. Although at present, the volume of machining of composites required is low but it is still important to estimate the responses such as cutting force, feed force, tool wear, tool-chip interface temperature etc. for full-fledged application in industries. Estimation of cutting forces is needed for proper design of machine tools. For better machinability of composite materials, tool wear evaluation is quite important. As the tool-chip interface temperature affects the tool wear to a greater extent, the study of the temperature has to be given due importance.

1.2 Literature Survey:

Only limited literature is available on conventional machining operations such as turning and drilling of composites. Almost all the processes that are used for the machining of composite materials have been dealt with in references [21] and [22] along with their relative merits and demerits.

Circular sawing uses diamond blades for most composite materials [22]. Cutting speed for composites normally varies from 600 to 3000 m/min. Thicker parts are cut at proportionally lower feed rates. Saber sawing normally cuts aramid-epoxy with a blade which cuts the outermost fibres on both sides of the laminate towards the interior. Blade speeds of 2500 strokes per minute are recommended, but blade speed and feed rates may vary with material thickness.

The machining techniques [23] such as turning, drilling, milling, sanding and grinding, shearing, punching, finishing and polishing, tapping and threading can be applied to fibre composite materials with proper tool design and care.

Rasoto [23] has given the generalised hints for machining of composite materials as follows:

(a)   coolants should be used to avoid over heating and melting.

(b)   operate machine at high speed.

(c)   provide liberal clearance on cutting tools.

(d)   use light cuts and slow feed depending upon the orientation of fibre with respect to feed direction.

(e)   turning tools should be ground to provide rake angle, that minimise cutting and thrust forces.

(f)   tools should be carbide tipped.

(g)   the workpiece should be properly supported to avoid distortion under cutting pressure.

(h)   tools bits and cutters should be sharp.

In machining of aramid (Kevlar) fibre reinforced plastics (FRP)[21] standard tools are not applicable without severe material damage like delamination, i.e., the separation between two layers of a laminate or fuzzing as shown in Fig. (1.1). Aramid fibres require keen cutting edges and a tool geometry which inhibits the fibre displacement in front of the cutting edge. HSS usually achieve insufficient tool life in AFRP. In general, tool life may be increased by coating HSS. Else, by using carbide coated with titanium nitride. In some cases, however, the increase of cutting edge radius due to coating may result in a complete failure of tool performances. Moreover, grinding tools which usually provides a negative rake angle are not suitable for the machining of AFRP.
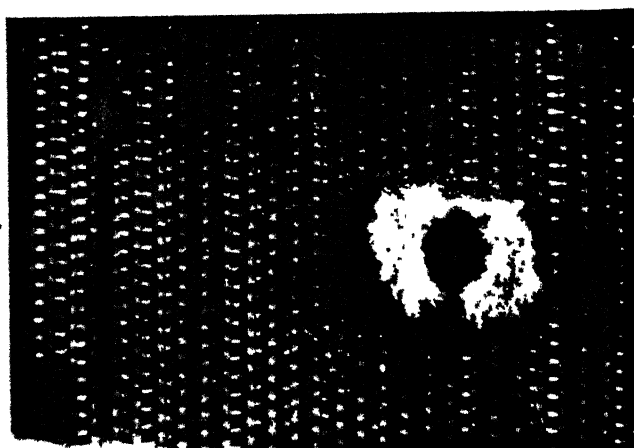
FIG. (1.1). FUZZING PRODUCED WHILE DRILLING
KEVLAR COMPOSITE

Rod Doerr [24] has found that machining of aramid (Kevlar) reinforced laminates with conventional tools produced 'fuzz'. Also, he has analysed that the cost of production has suffered due to ill defined parameters such as feeds, speeds and tool configuration.

Contrary to popular belief, aramid is not appreciably more difficult to machine [24] than graphite or fibre glass. Although the aramid fibres are tough, they are easily cut by sharp tools with the proper cutting angles. It should be noted, however, that temperature over 177°C (350°F) tends to permanently swell edges of the cut, tools must be kept cool during the machining operations.

Radhakrishnan and Wu [25] have worked on the improvement of life of drill bits. They have found that the hole quality deteriorates rapidly with the increasing use of the drill in drilling of composite materials. In order to control the quality of the drilled holes they have established an on-line quality evaluation for drilling composite material using dynamic data.

Machining techniques for thermosets [23] such as glass-epoxy laminates have been evaluated, and well established standard metal and wood working machines may be used with modifications to increase spindle speeds along with reduced feeds. Since standard metal cutting tools are suitable for only short production runs, presently

used tools are carbide or diamond tipped. Tools used on such composites are required to be sharp not only for clean cuts but also to minimise delamination.

For trim-routing of glass and carbon fibre composites, tools with multiple cutting edges made of cemented carbide or polycrystalline cutting materials are recommended [22]. The best machining quality is achieved by upmilling, independent of tool geometry and cutting conditions. Similar to drilling, the amount of cutting force and the surface quality in routing is very much dependent on fibre orientation.

Everstine [26] has derived equations to present a theory of the machining of FRP materials. This analysis is applicable to the plane deformation of incompressible composites reinforced by parallel fibres of high strength. But, no further work is available on theory of machining of composite materials.

Aksel Koplov [27] gives the analysis of the cutting of carbon fibre reinforced plastics (CFRP) using single edge tool with shaping machine. The experiments were carried out on unidirectional CFRP under orthogonal conditions to create a basis for improving the cutting quality, and for understanding the process of cutting. An instrumental shaping machine was used to investigate the workpiece surface, the chips and for measurement of cutting force.

A quick stop device (QSD) was used to investigate the
details of the process near the tool tip and in front
of it. Koplov concluded that in shaping of CFRP
laminate, 90% of the heat was conducted to the tool.
This heat raises the temperatures of the tool-tip
and reduces the wear resistance of the tool. Finally,
the friction can be reduced using a large relief angle.
The cutting mechanism should be considered along and
across the fibre direction. In fact, it is a fracture
process where the cutting is carried out as a series
of brittle fractures. Only negligible plastic defor-
mation takes place.

Koplov has studied [28] the effect of tool
rake angle on horizontal and vertical forces at different
depth of cut in shaping of CFRP. He has found that
there was a close relationship between the chip producing
process at the rake face of the tool, the horizontal
force, the vertical force, the interaction of the surface
of the specimen and the rake face of the tool.

Report from Preuss and McGinly [29] states that
turning of Fibre FP/aluminium, a metal matrix composite,
can be accomplished with standard C-2 uncoated carbide
tool bits with a 1/64 inch corner radius. They have
conducted experiments on turning of bars of two inch
diameter, cutting speed of 30 m/min and depth of cut
as 0.50 mm. They have found that the rate of tool wear

decreased at feeds above 0.32 mm/rev. At feeds above
0.396 mm/rev., the surface finish was unacceptable.
At higher speeds up to 150 m/min and a constant feed
of 0.396 mm/rev., wear rate decreased significantly.
They have noticed that round tool bits having a large
nose radius are helpful in improving surface finish at
higher feed rates.

Unconventional machining processes [21] such as
water-jet machining, laser cutting, electric discharge
machining, ultrasonic machining are also used for
machining of composite materials. But, these processes
are expensive and have their own drawbacks.

1.3 Objectives of Present Work:

From the literature survey it is seen that only
a few researchers have given attention on the evaluation
of cutting forces and performance of cutting tools in
conventional machining such as turning, shaping and
drilling operations. As the conventional machining is
relatively cheaper and simple to unconventional
machining, it is required to study the machining of
composite materials in depth. Also, it is essential
to develop a model for tool wear, cutting forces and
tool-chip interface temperature to get optimised
cutting conditions for better quality components.

The present work is carried out to study
the machining process of a glass fibre-epoxy composite
material. Experiments are conducted using a composite
cylindrical bar as work material. As the performance
of the HSS tools is not satisfactory for machining
composites, tungsten carbide tool bits were used as the
tool material. Also, for the present investigation
a two dimensional force dynamometer was designed and
fabricated to measure feed force and cutting force in
longitudinal turning and facing (accelerated cutting)
operations. This work would help in finding out the
ways to improve the cutting quality, and for under-
standing the mechanics of the cutting process.

Experiments in longitudinal turning have been
planned according to the "design of experiments technique".
For this, central composite rotatable design has been
used. Experiments about facing operation have been planned
according to the "one variable at a time" approach. For
the measurement of flankwear land width, travelling
microscope has been used. Force and temperature measure-
ments are done by pen recorders.

The experimental set-up and procedure are describe
in Chapter 2. Chapter 3 deals with the results and discu-
ssion. Conclusion and scope for future work is presented
in Chapter 4. References are given in Chapter 5.

CHAPTER-2

EXPERIMENTATION

The present work is carried out to estimate the
cutting force, feed force, tool-chip interface temper-
ature and tool wear in longitudinal turning and facing
operations of a glass-epoxy composite cylindrical bar.
The schematic diagram of the experimental set-up is shown
in Fig. (2.1). The dynamometer used for measuring forces
in machining of composites was designed and fabricated in
the laboratory. The design of the dynamometer has been
discussed in Chapter 2, section I.

2.1 Work Material Specification:

A glass-epoxy composite cylindrical bar of length
300 mm and diameter 120 mm was used as a work material. The
composite bar is casted by 'fillament winding process' with
zero degree fibre orientation. This composite bar is
made in FRP centre, IIT Madras, India. The fibre volume
fraction of this composite material is about 52%.

2.2 Apparatus Used:

A lathe machine, Okhla-PTC India make, was used
for   conducting the present experiments. The rated
RPM of this lathe is 1600. The maximum diameter of the
workpiece that can be held in the chuck is 150 mm. The
length of the workpiece that can be held between the
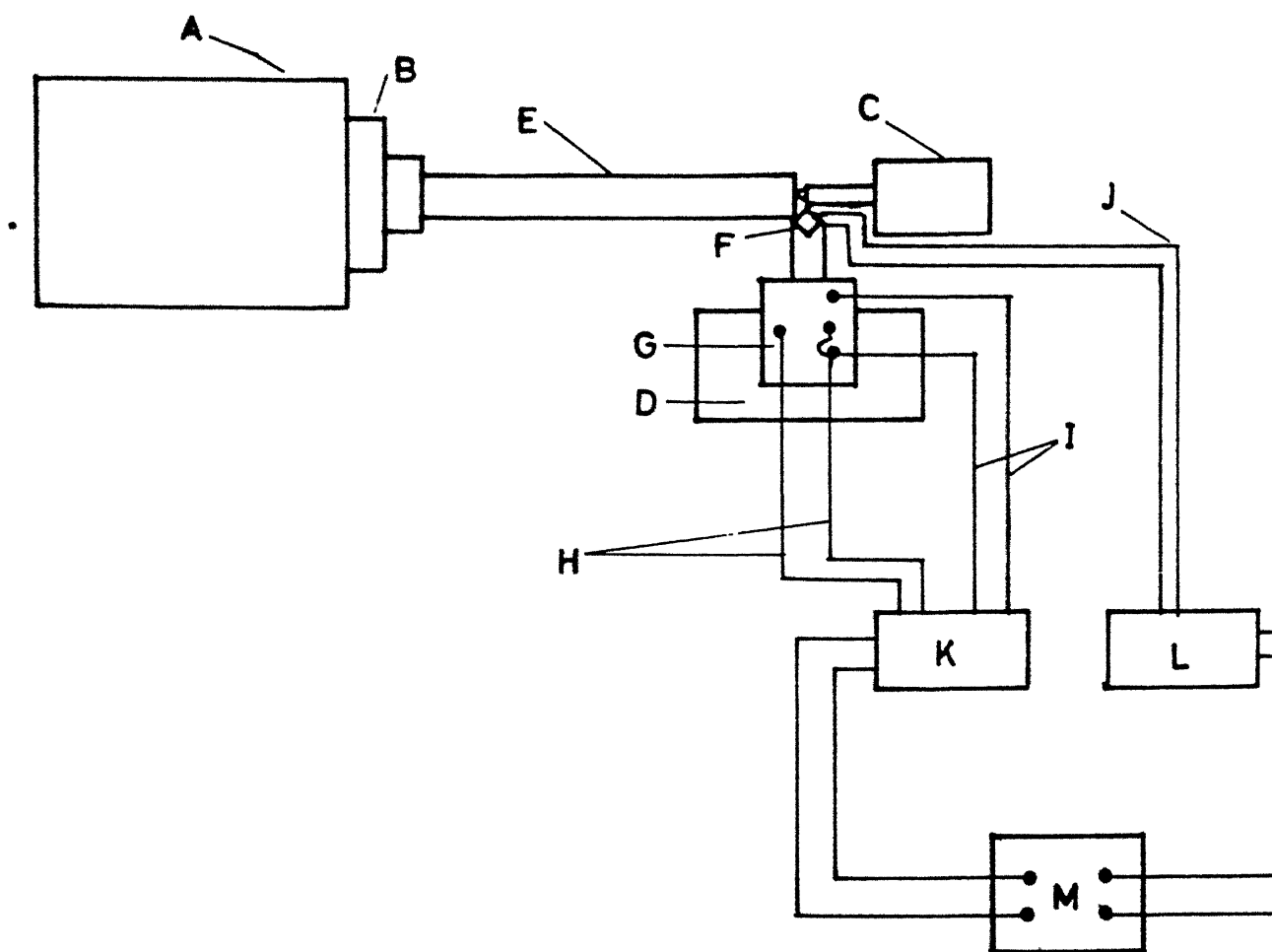
A : Lathe headstock
B : Lathe chuck
C : Lathe tailstock
D : Lathe cross slide
E : Composite bar
F : Tungsten carbide tool bit
G : Dynamometer cum QSD
H : Leads from dynamometer for measuring feed force
I : Leads from dynamometer for measuring cutting force
J : Enamil coated Nickel-chromium thermocouple
K : Pen recorder for measuring forces in machining
L : Pen recorder for measuring temperature
M : Power supply

Fig. 2.1 Schematic Diagram of an Experimental Set-up.
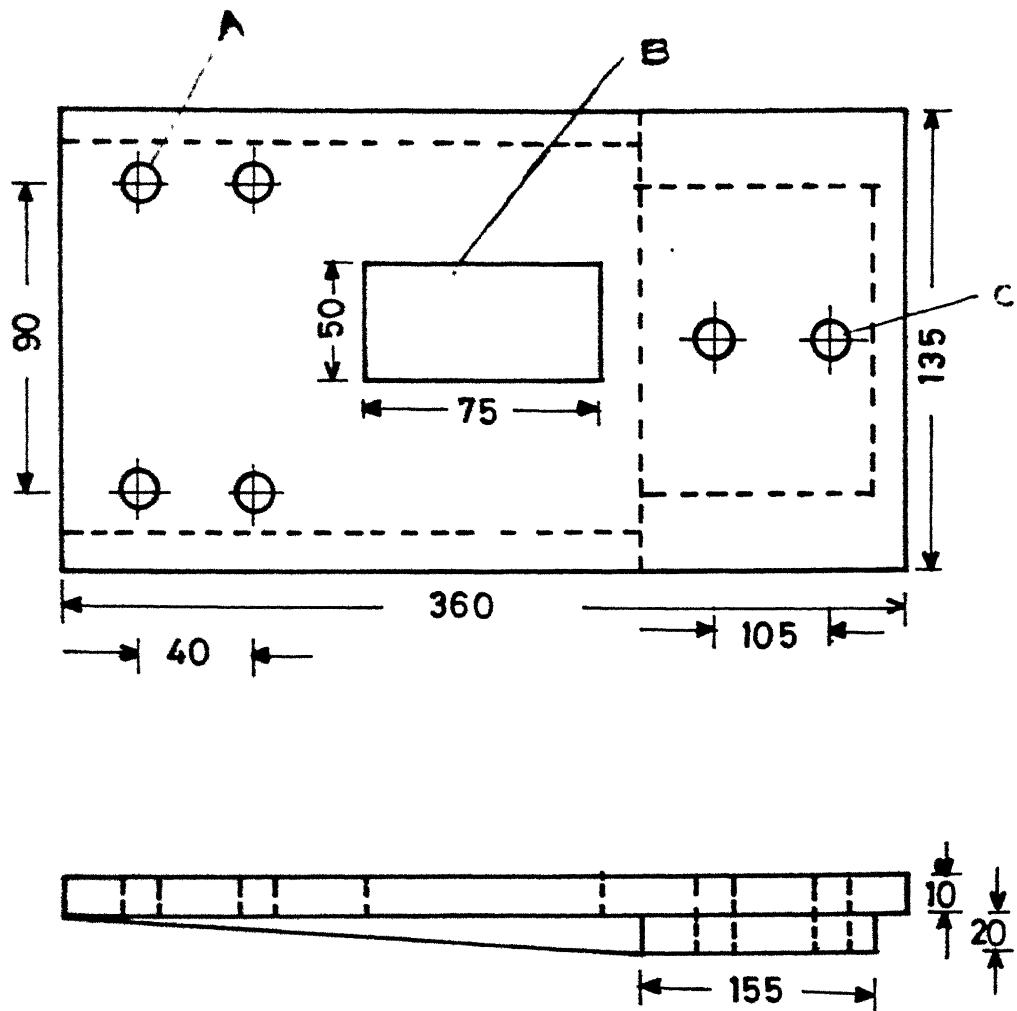
A : Holes for fixing the QSD cum dynamometer holding device
    on the cross-slide of the lathe

B : A slot for projecting the loop of the dynamometer

C : Holes for mounting the dynamometer on the holding
    device by means of bolts.

Fig. 2.2 Two Views of Dynamometer Cum QSD Holding Device

2.3 Estimation of Fibre Volume Fraction of the Work Material:

Fibre volume fraction of glass fibre-epoxy composite rod was 51.9% as found by burn out test.

In this test, a piece of known weight was burnt in the furnace at 850°C for about 12 hours. The epoxy resin burns off and left over glass residue was weighted to obtain the fibre content. The fibre volume fraction is calculated as given below:

W_c = Weight of glass fibre-epoxy composite material = 7.095 gm

W_f = Weight of glass fibre = 4.960 gm

W_m = Weight of epoxy (matrix) = 2.135 gm

ρ_f = Density of glass fibre = 2.54 gm/cm^3

ρ_m = Density of epoxy = 1.18 gm/cm^3

Fibre volume fraction is calculated [30] as follows:

$$V_f = \frac{v_f}{v_c} \qquad (2.1)$$

where,

$$v_f = \frac{W_f}{\rho_f} = \frac{4.960}{2.54} = 1.953 \text{ cm}^3 \qquad (2.2)$$

$$v_c = v_f + v_m \qquad (2.3)$$

where,

$$v_m = \frac{W_m}{m} = \frac{2.135}{1.18} = 1.81 \text{ cm}^3 \qquad (2.4)$$

Therefore, equation (2.3) gives, $v_c = 3.762 \text{ cm}^3$.

Substituting equations (2.2) and (2.3) in equation (2.1), we get,

$$V_f = 0.519$$

or

$$V_f = 51.9\%$$

2.4 Safety Precautions:

Machining of fibre composite may cause a serious problem due to the generation of airborne dust. Glass and carbon fibre composites usually emit a fine powder like dust. The dust has to be extracted and filtered carefully, since it is hazardous to health [21]. Hence, in order to reduce the spreading of the fine glass dust, the experiments were conducted using coolant. The dust mixed with the coolant was collected and filtered out. Also, the 'dust respirator' was used while machining. During machining, precaution were taken by wearing hand gloves and aprons as otherwise it causes itching, because of glass dust. Even the machined workpiece (composite material) should not be touched with naked hands.

2.5 Temperature Measurement:

For the measurement of tool-chip interface temperature, standard thermocouple, Nickel-chromium was used. As the glass fibre-epoxy composite is a bad conductor of heat, the tool alone was considered as a hot junction. In order to fix the beeded thermocouple at the tool tip, a small groove was made on the top of the anvil of the tool holder, so that the thermocouple will be embedded in between tool tip and the anvil. The thermocouple wires were insulated using enamel coating. The cold junction was formed by directly connecting the two wires of the above thermocouple to the pen recorder to measure the generated thermal e.m.f. The recorder was properly set to measure voltage in millivolts. The temperature was directly noted down from the standard chart (for Nickel-chromium) corresponding to the millivolts obtained through the pen recorder.

2.6 Tool Wear Measurement:

The flank wear land widths of carbide tool bits were measured using travelling microscope having a least count of 0.01 mm. In order to mount the sides of the carbide bits horizontal, for measurement, a mounting base made of perspex material was prepared. For the study of crater wear photographic analysis also has been made.

2.7 Force Measurement:

For the measurement of machining forces a two dimensional dynamometer was used. Dynamometer was calibrated prior to use in experimentation. Carbide tool bit holder (which was machined to fix in the dynamometer) was fixed rigidly in the dynamometer. Dynamometer was mounted on the lathe. It was then connected to the pen recorder with each channel sensitivity of 1 mV per full scale and the chart movement was kept at a speed of 25 mm/min. Load on the tool tip was applied, using weight pan in steps of 20N, till a load of 400N was achieved. Corresponding deflections in recorder for each step of increment in weight was noted down. Unloading of dynamometer was done in the same manner and corresponding deflections were also noted. In order to calibrate for horizontal load (feed force), spring balance was used to apply load on the dynamometer and the above mentioned process was repeated. Graphs were then plotted for both vertical load and horizontal load with deflection in pen recorder on the X-axis and the force applied at tool tip on Y-axis as shown in Fig. (2.3). These two curves have been used as the calibration curves for two force measurements, acting in two mutually perpendicular directions.

The deflections recorded by the pen recorder during machining were compared with the calibration chart to measure the forces in machining of composite material.
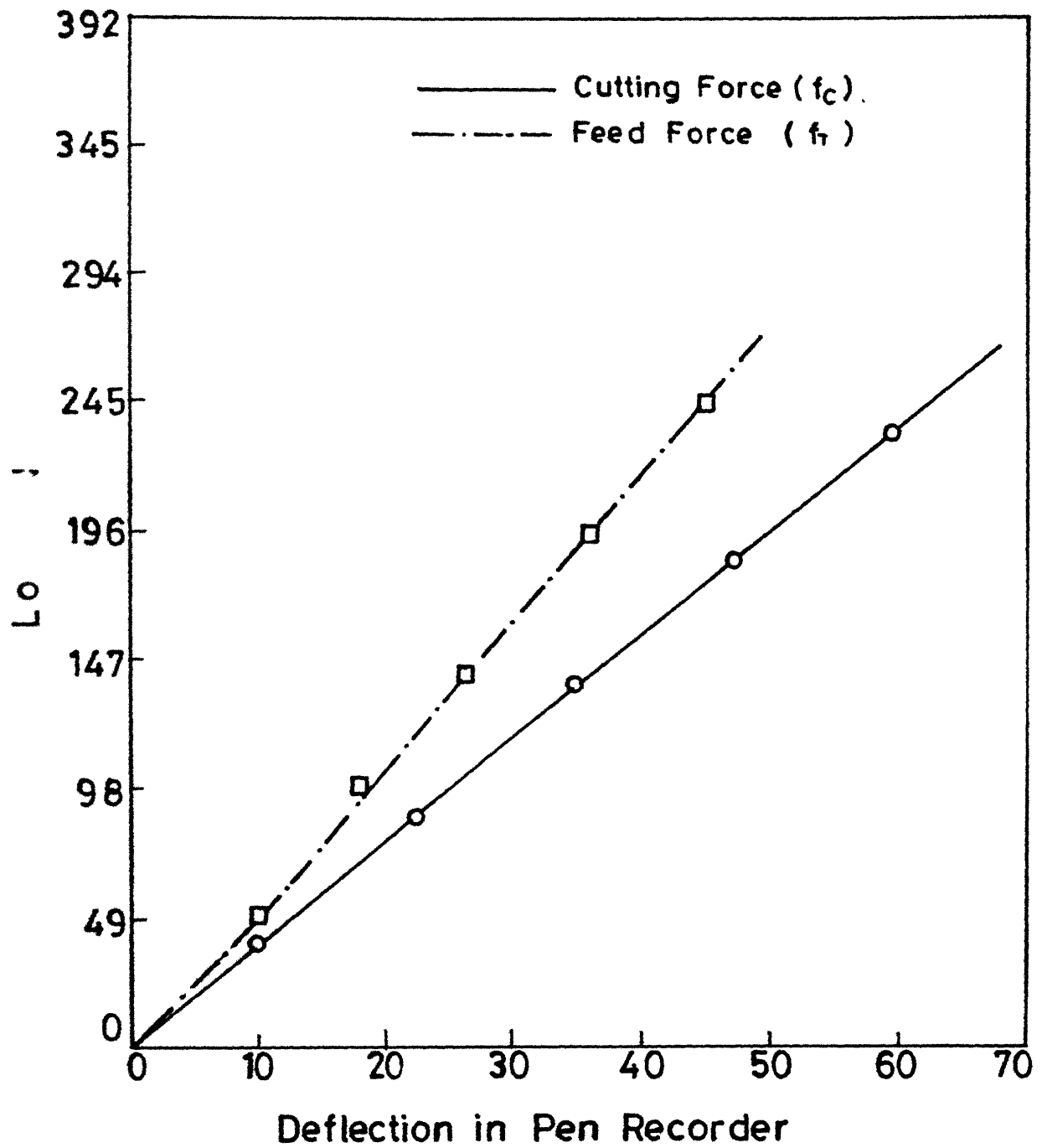
Fig. 2.3   Calibration Curves for Feed and Cutting Force.

2.8 Design of Experiments:

The design of experiments is the procedure [31] of selecting a number of trials and conditions for running them essential and sufficient for solving the problem that has been set with required precision. The folllowing features are of great importance.

1.   Striving to minimise the total number of trials.

2.   Simultaneous variation of all variables, determining

        a process according to the rules of algorithm

        and

3.   The selection of clear cut strategy, permitting the

        investigator, to make substantial discussions after

        each series of trials.

This method is capable to predict independent, quadratic and interactive effects of different parameters on the responses.

In the present investigation, the central composite rotatable design for 2 factors (cutting speed and feed rate) for longitudinal turning was used. The levels for different factors is given in Table - 1.

After conducting the experiments, responses (tool wear, cutting forces, temperature) were measured and/or calculated as given in Table-2 and the second order model 32 was evaluated with the help of the software package CADEAG-1[3

$$Y_r = b_o + \sum_{i=1}^{n} b_i x_i + \sum_{i=1}^{n} b_{ii} x_{ii}^2 + \sum_{i<j} b_{ij} x_i x_j$$

$$\underbrace{\qquad} \quad \underbrace{\qquad} \quad \underbrace{\qquad}$$
independent   quadratic   interactive

(2.5)

where, Y_r is the response and $1,2....n$ are the coded levels of n quantitative variables or factors. The coefficients b_o, b_1, b_2 etc. are known as regression coefficients. The polynomial equation is known as regression function. The values of constants, b_i's are given in Table-3.

2.9 Experimental Procedure:

A glass fibre-epoxy composite cylindrical bar of diameter 120 mm and length 300 mm was rigidly fixed in a 4 jaws chuck. The overall view of the experimental set-up is shown in Fig.(2.4a). For longitudinal turning, the dynamometer cum QSD was mounted on the crossslide of the lathe as shown by photograph in Fig. (2.4b). In order to achieve a desired cutting speed, (according to the design of experiments given in Table - 4) the bar was turned to the required diameter upto a length of 200 mm. Depth of cut for each trial was kept constant as 0.3 mm through out the experiments. The dynamometer was connected to a two-channel pen recorder. The thermocouple wires were connected to a single channel pen recorder.
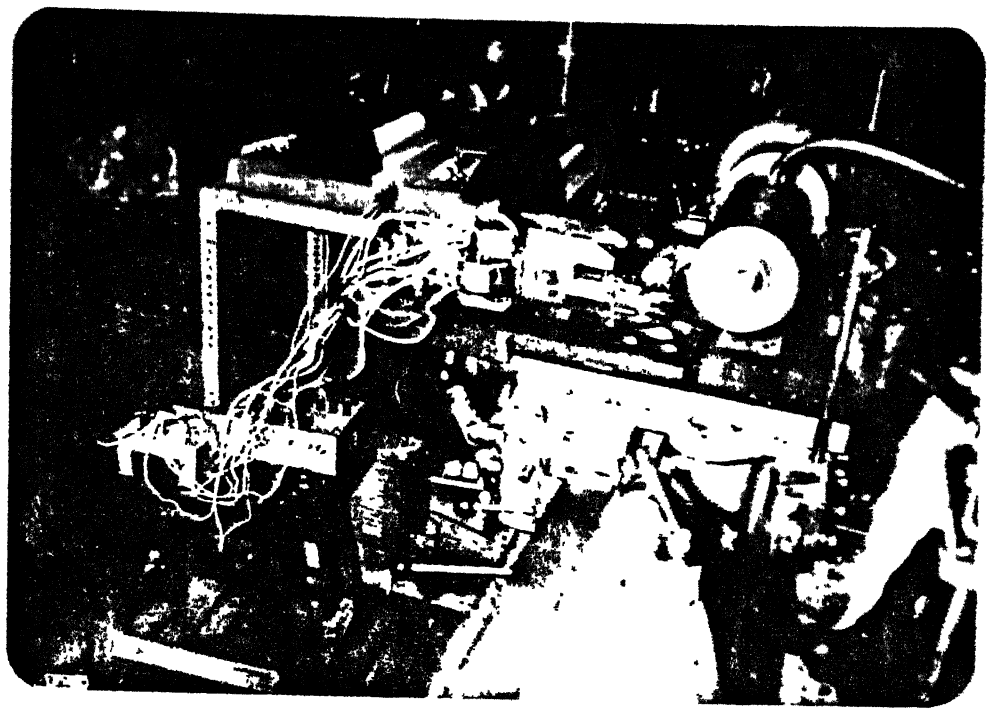
FIG. (2.4a) PHOTOGRAPH OF OVERALL VIEW OF
EXPERIMENTAL SET-UP

FIG. (2.4b). PHOTOGRAPH OF EXPERIMENTAL
SET-UP FOR LONGITUDINAL TURNING

For longitudinal turning, the experiments were conducted according to the plans, given in Table-4. At each trial, the carbide tool bit was taken out after every one minute and the flank wear land width was measured under the travelling microscope having a least count of 0.01 mm. After the measurement of the flank wear the tool bit was replaced in its original position. Feed force, cutting force and temperature were also evaluated from their records obtained during machining. Experiment was conducted for total 6 minutes for each trial. In each trial, for the first half minute the coolant was not used in order to study the effect of machining parameters on machining without coolant. But, for the rest of the period of machining in each trial, the coolant was used at a steady flow rate. A fresh edge of the carbide tool bit was used for each trial.

After each trial, the workpiece was reduced to the required diameter to get the desired cutting speed. The above mentioned procedure was repeated for each of the trials given in Table - 4.

Facing operation was conducted according to one variable at a time approach. The plan for facing operation is given in Table- 5. In facing RPM, cutting speed and feed rate were taken as variables. The diameters of the bore to be drilled in the centre of the job for each trial is decided by the reference cutting speed (36 m/min) and spindle speed of that trial. The reference cutting speed was kept constant for all the trials.

During facing trials, the dynamometer was turned by 90° as shown in Fig. (2.5) so that facing is performed from the centre of the workpiece towards the outer diameter. In facing, for first 5 seconds, the coolant supply was kept off but the rest of the machining was done with coolant supply on for each trial. After each trial the feed force, cutting force and temperature were noted. All the trials in facing were conducted according to the plan given in Table-5. At each trial, the outer diameter of the workpiece was reduced to the required size (see Fig. 2.6) for the design of work-piece) to obtain the desired final cutting speed. For each trial, a fresh edge of the tool bit was used.

In case of facing operation, there was very little flank wear while crater wear was predominant. As there was scattering in the crater wear, photographic analysis has been made for the study of the same and are discussed in Chapter 3.
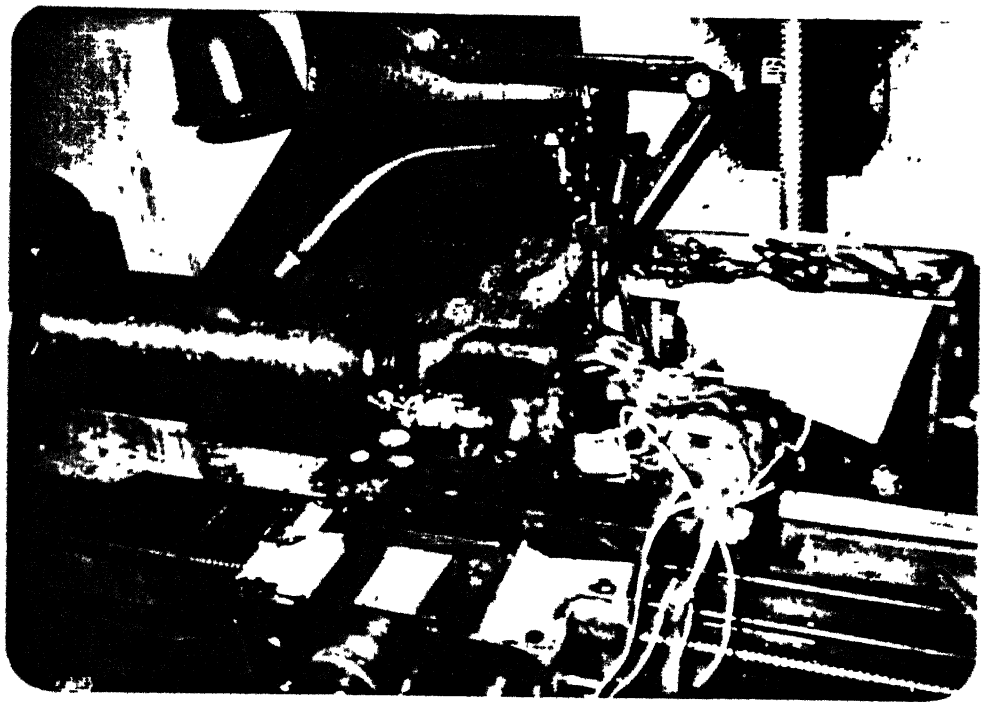
FIG. (2.5) PHOTOGRAPH OF EXPERIMENTAL SET-UP
FOR FACING OPERATION

FACING

FEED FORCE

CUTTING FORCE

Feed rate = 0.132 mm/rev
cutting speed = 54 m/min
Spindle speed = 270 rpm

FEED FORCE

CUTTING FORCE

LONGITUDINAL TURNING

CUTTING SPEED = 60 m/min ; FEED RATE = 0.120 m/min
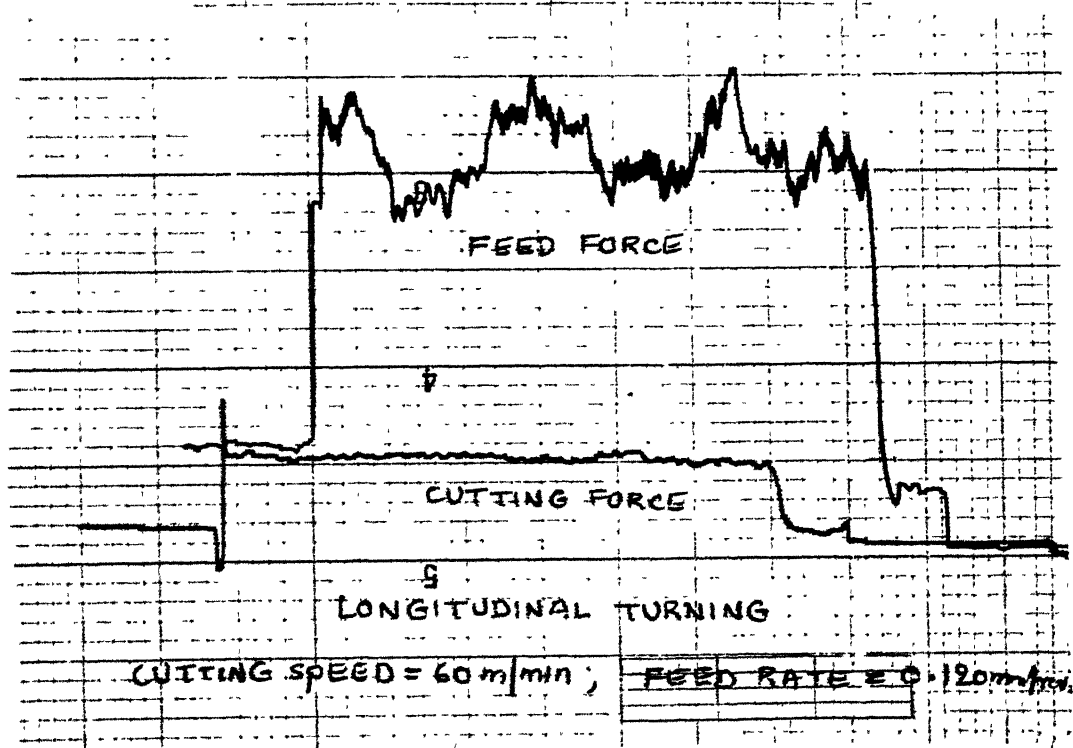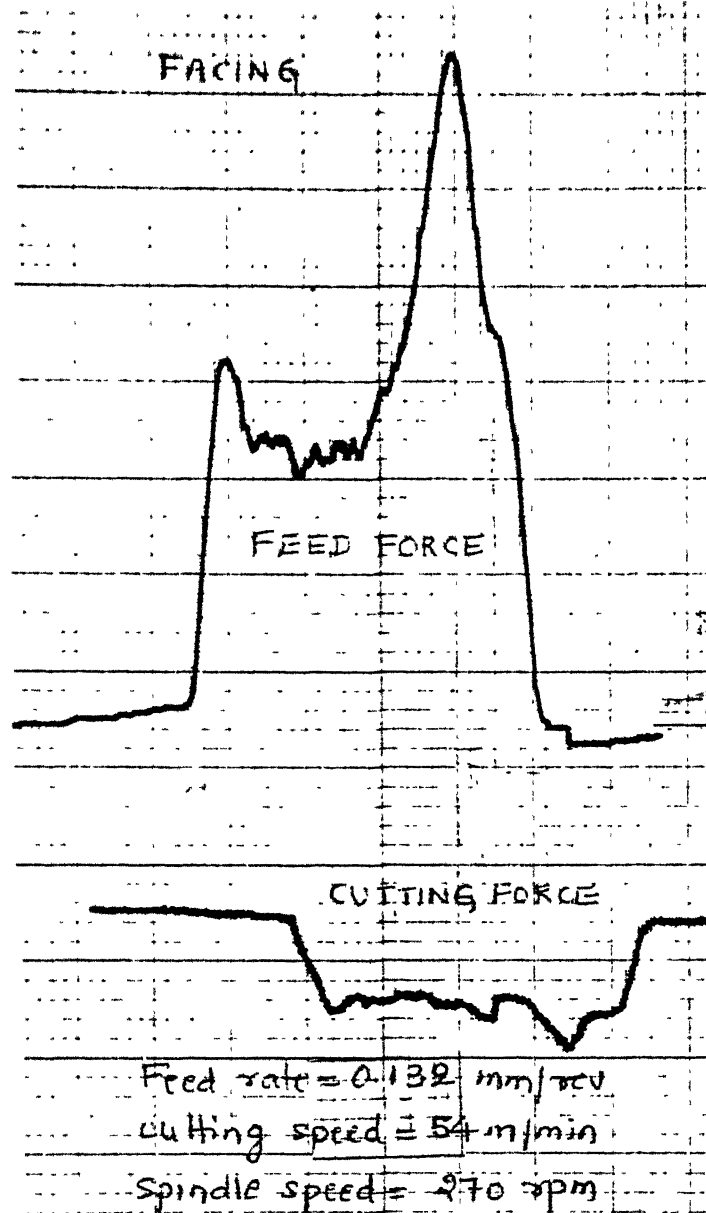
FIG. (2.7). CHARTS OBTAINED BY PEN RECORDERS
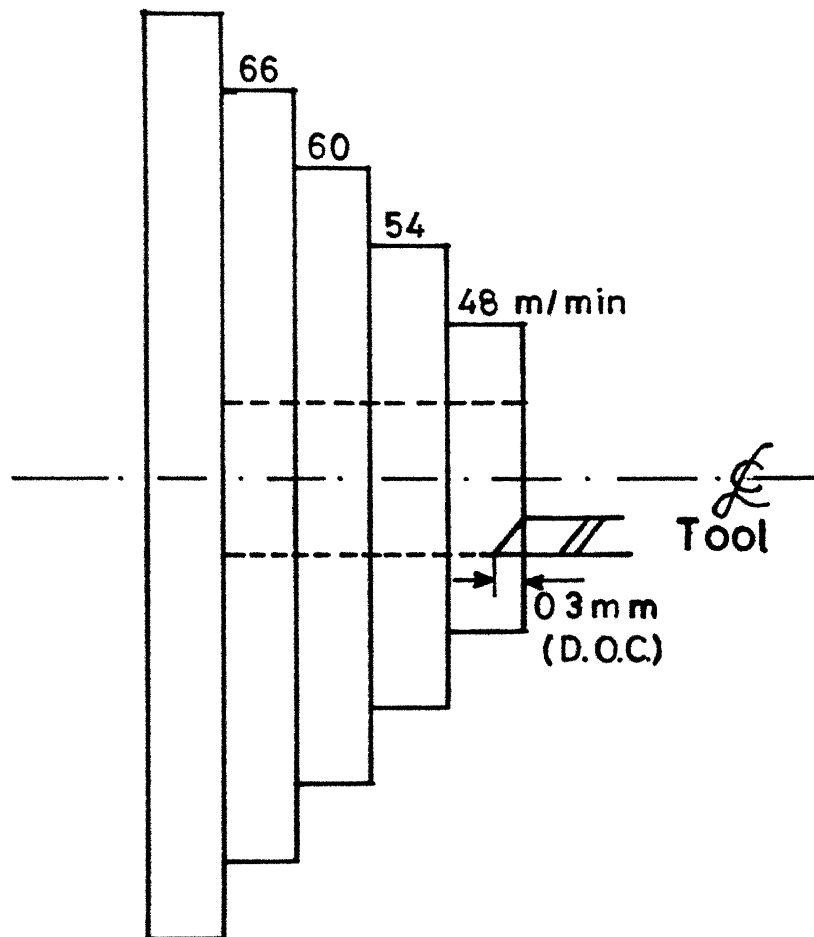
Fig. 2.6 Designed Workpiece for Facing Operation.

CHAPTER-3

RESULTS AND DISCUSSION

The experimental estimations of cutting force, feed force, tool-chip interface temperature, flank wear and crater wear of carbide tool bits were obtained under different cutting conditions (spindle speed, cutting speed, feed rate) for longitudinal turning and facing operations of a composite bar. Depth of cut was kept constant in all the experiments. The response surface Equation (2.5) for machining forces, tool wear and temperature have been established for longitudinal turning. The details of the constants of response surface equation have been given in Table-6. The experimental results obtained from facing are given in Table-5. The experimental results of both the operations were used to analyse the effects of different process parameters on the responses, as discussed below.

3.1 Facing:

3.1.1 Feed Force

3.1.1.1 Spindle Speed and Feed Force

Figures (3.1a,b) show the variation of spindle speed with feed force for constant but different cutting speeds. The feed force is decreasing gradually, with increasing spindle spindle speeds and decreasing cutting speeds. This variation seems due to the less energy required

(a) Feed Rate = 0.132 mm/rev

$V_c=60$ m/min

54

48

42

Feed Force, N.

273 234 195 156 117 78 39 0

Spindle Speed, r.p.m.

180 270 360 450

(b) Feed Rate = 120 mm/rev

$V_c=60$ m/min

54

48

42

Feed Force, N

273 234 195 156 117 78 39 0

Spindle Speed, r.p.m.

180 270 360 450
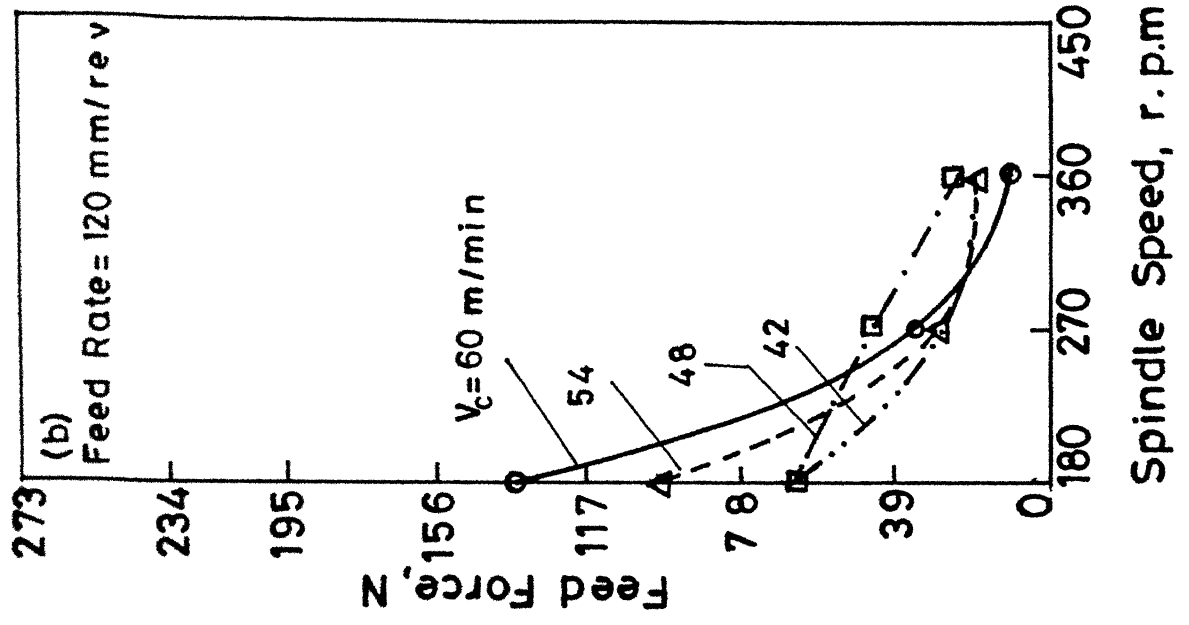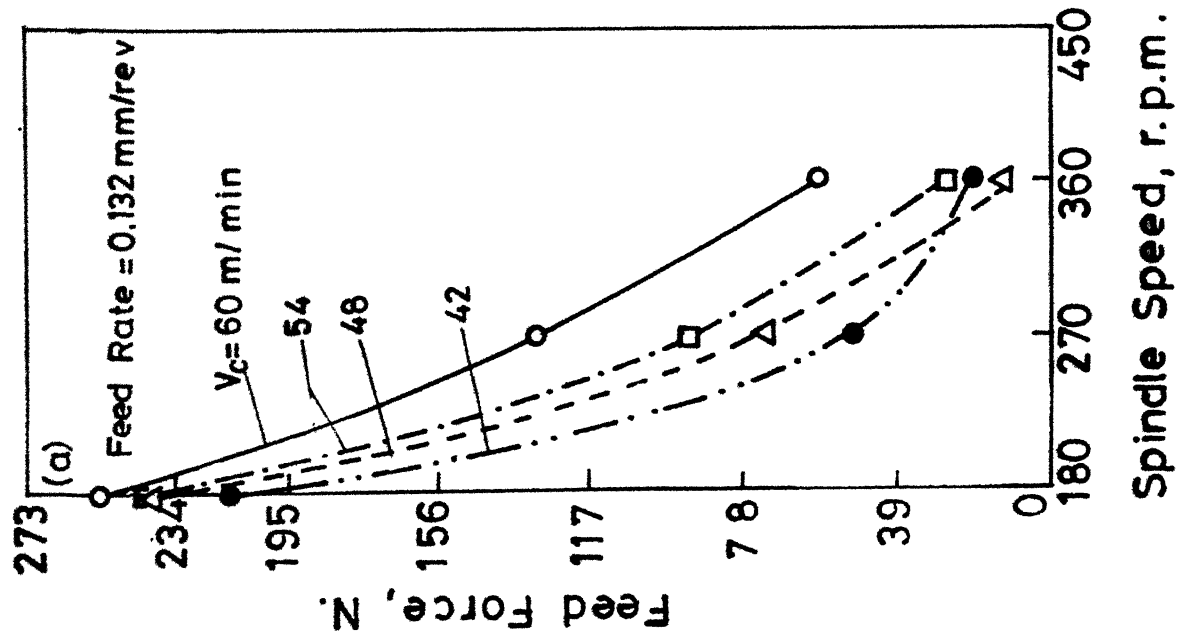
...ce During Facing.

for brittle fracture of glass fibres at higher spindle
speeds (or i.e. higher shear strain rate). As reported
by Rao 34 fracture strain for GFRP (glass fibres
reinforced plastics) decreases with the increase in shear
strain rate and decrease with the increase in spindle
speed.

3.1.1.2 Feed Rate and Feed Force

Figures (3.2a,b) shows the variation of feed
force with feed rate for constant but different spindle
speeds. From figures it is seen that there is gradual
increase in the feed force, with the increase in the feed
rate. As the feed rate increases, the number of fibres to
be cut per unit time increases and hence the resistance
for the cutting increases, thereby increasing the feed
force.

3.1.1.3 Cutting Speed and Feed Force

Figures (3.3a,b) show the variation in feed
force with the cutting speed for different but constant
spindle speeds. From the figures it is seen that there
is a decrease in the feed force for lower range of cutting
speeds and an increasing trend for the higher range of cutting
speed. The increase in feed force for higher values
of cutting speeds may be due to ineffective cutting of
the fibres owing to chipping off or wear out of the
tool.
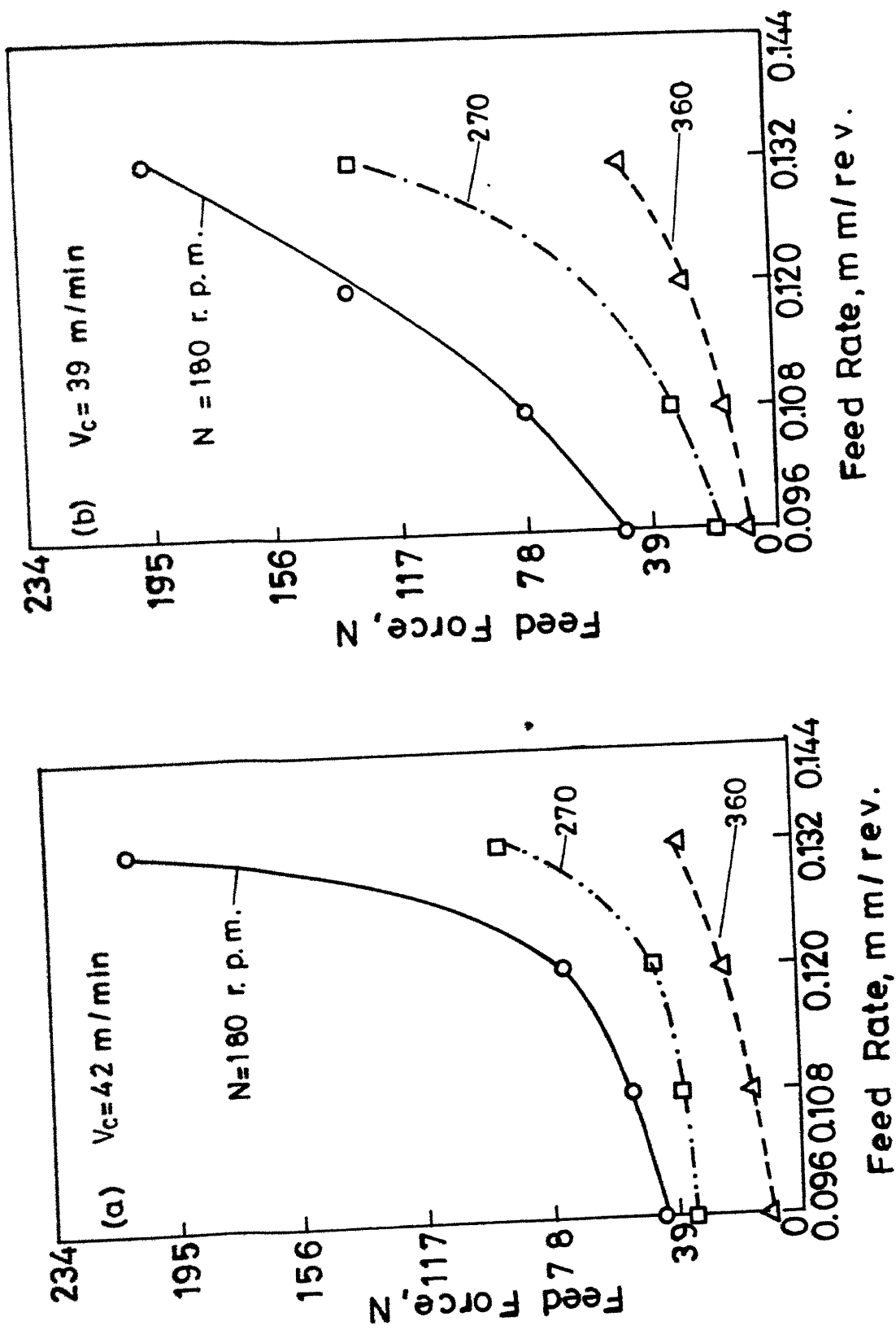
Fig 3.2 Effect of Feed Rate on Feed Force During Facing.
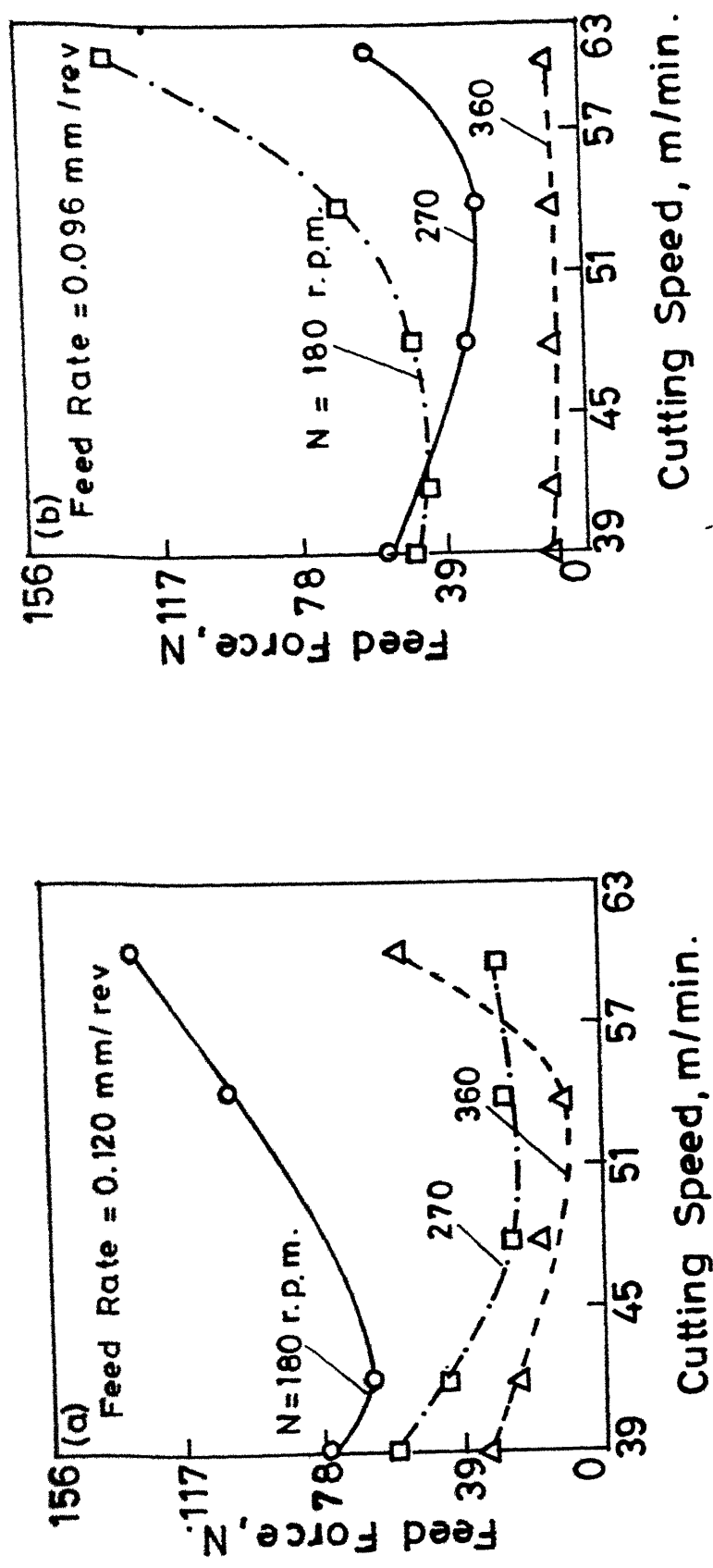
Fig.3.3 Effect of Cutting Speed on Feed Force During Facing.

3.1.2 Cutting Force

3.1.2.1 Spindle Speed and Cutting Force

From the figures (3.4a,b) it is seen that in the beginning, there is a gradual decrease in the cutting force with increasing spindle speeds. But at higher range of spindle speeds, the cutting force is constant. In the cutting force direction, only matrix comes into picture. As the spindle speed increases the energy required to fracture matrix material (epoxy) decreases, thereby decreasing the cutting force. But higher spindle speeds, the effect of spindle speed is not much on the fracture energy and hence there is a constant cutting force.

3.1.2.2 Cutting Speed and Cutting Force

Cutting force is almost unaffected by the cutting speed, as shown in Fig. (3.5a,b). In the cutting force direction (normal to feed direction), the matrix material predominates which requires very less force to cut and hence it is not affected by the cutting speed.

3.1.2.3 Feed Rate and Cutting Force

The graph is plotted in Figs. (3.6a,b). The variations of cutting force with feed rate is not regular. But, because of heterogeniety of the composite bar, there is a increasing and decreasing trend in cutting force with the change in feed rate.

(b) Feed Rate = 0.108 mm/rev

Cutting Force, N

V_c=39 m/min;
42
48,
60

Spindle Speed, r.p.m.

(a) Feed Rate = 0.120 mm/rev

Cutting Force, N

V_c=39 m/min,
42
48
54
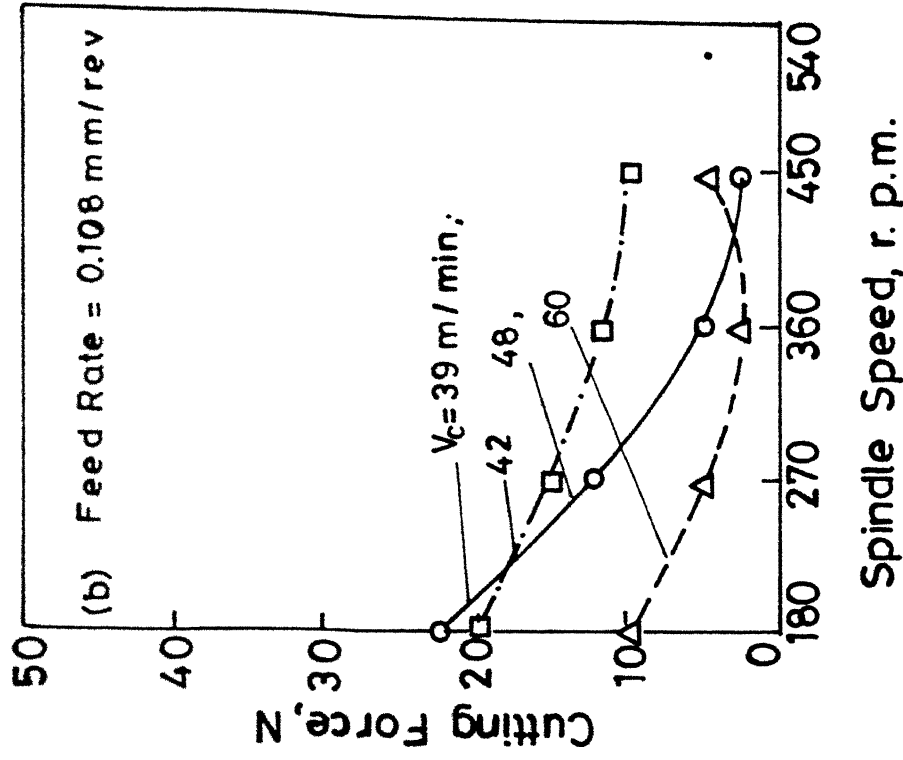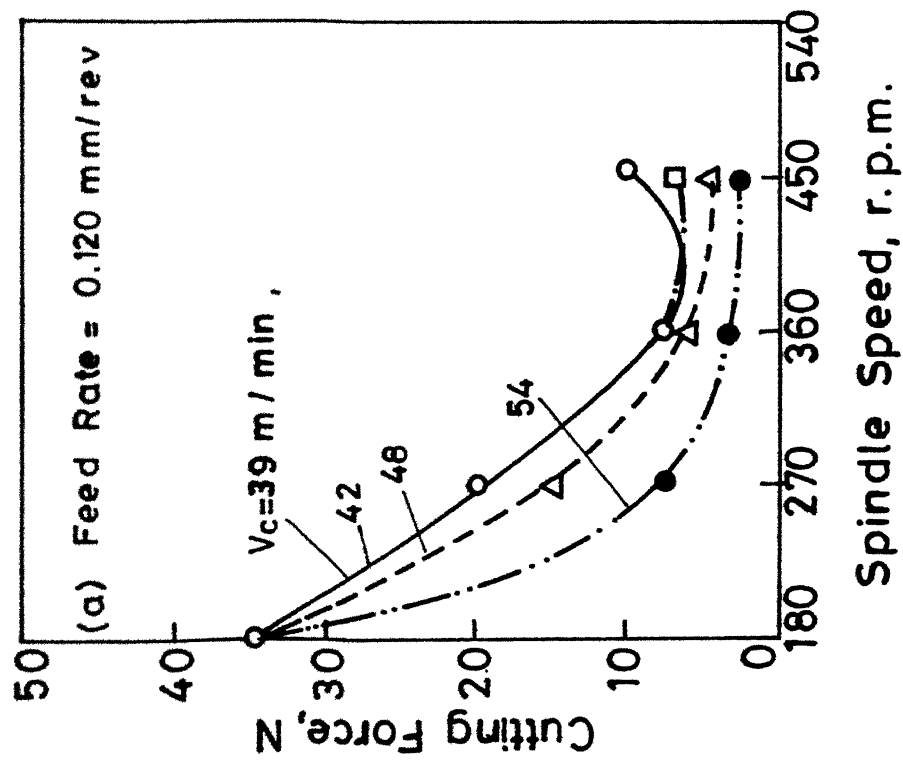
Spindle Speed, r.p.m.

Fig.3.4 Effect of Spindle Speed on Cutting Force During Facing.

(b) Feed Rate = 0.108 mm/rev

N = 180 r.p.m.

270

360

590

Cutting Speed, m/min.

Cutting Force, N

(a) Feed Rate = 0.120 mm/rev

N = 180 r.p.m.

270

360

590

Cutting Speed, m/min.
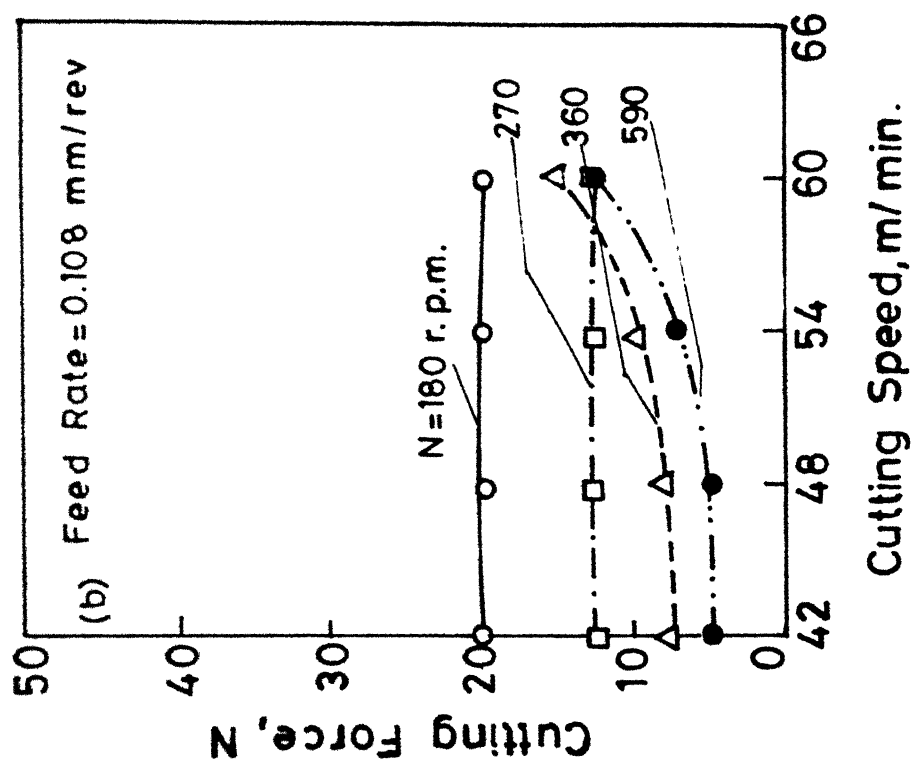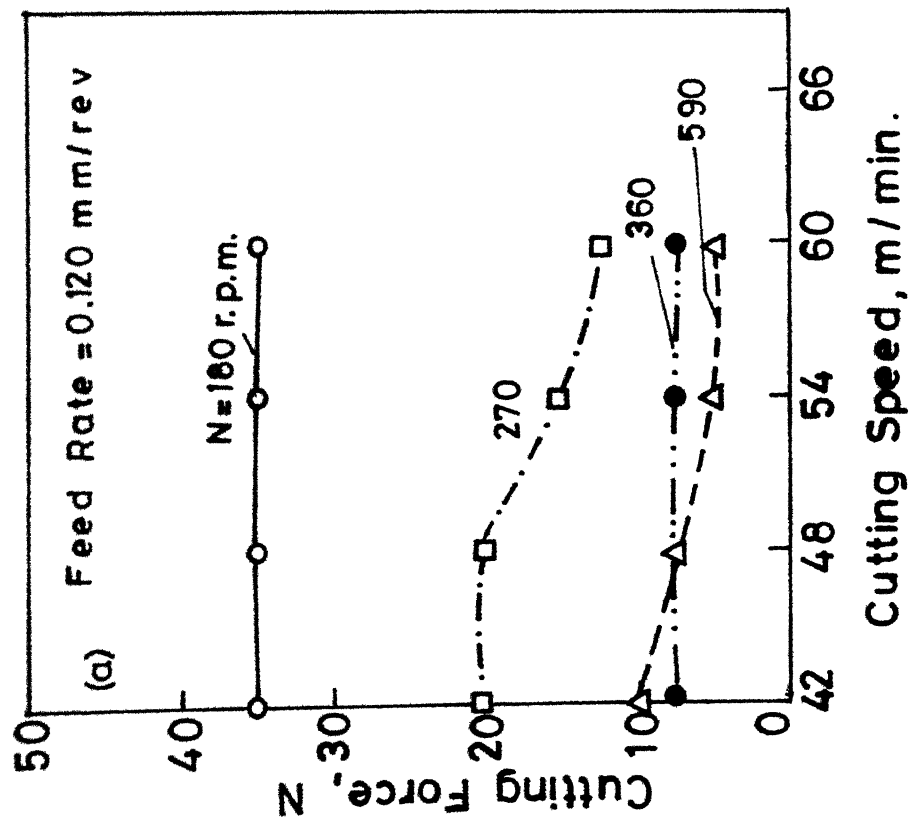
Cutting Force, N

Fig. 3.5 Effect of Cutting Speed on Cutting Force During Facing.
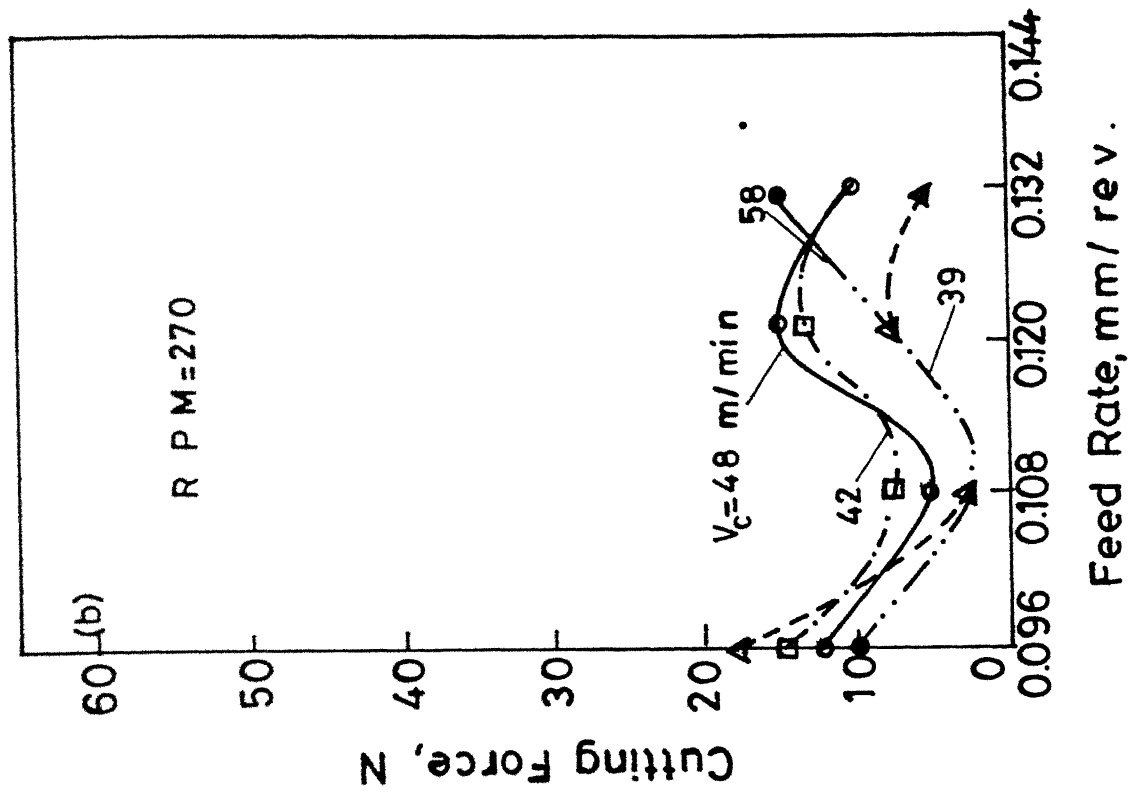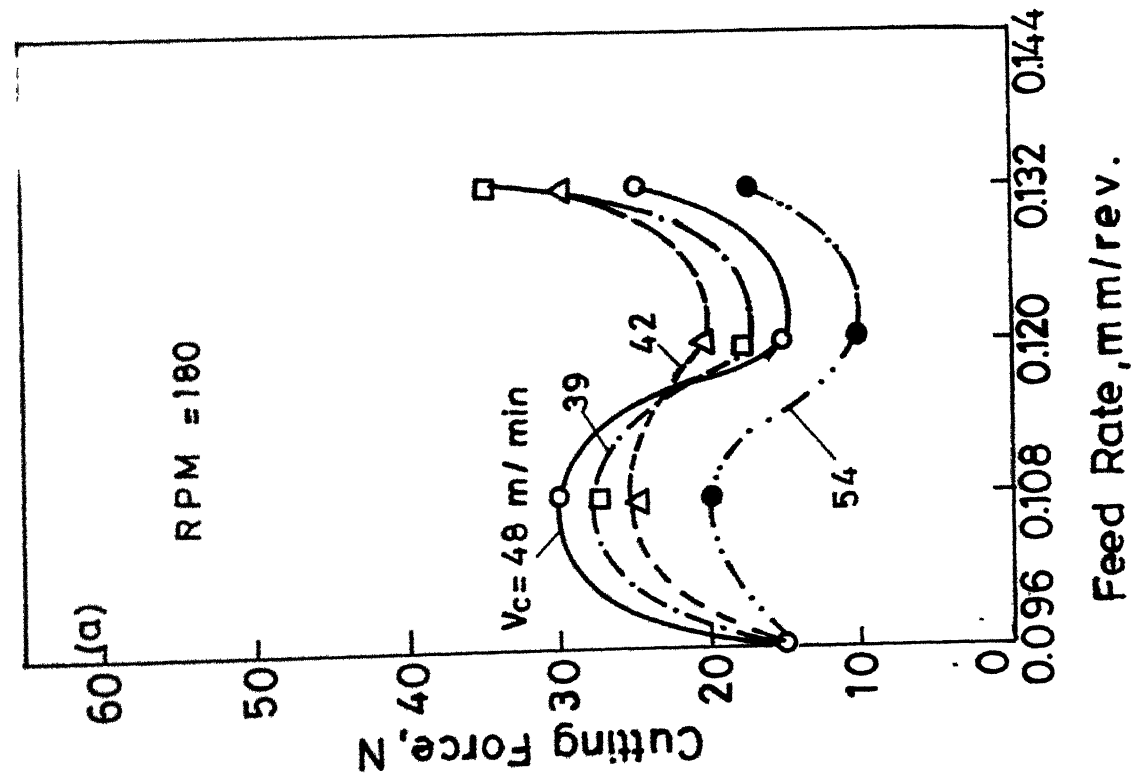
Fig.3.6 Effect of Feed Rate on Cutting Force During Facing.

3.1.3 Temperature

It is to be mentioned that the thermocouple were embedded between the carbide bit and the m.s. anvil of the tool holder. Secondly the temperature values given in the curves are above the room temperature which was measured to be around $32^{O}C$. These are the two basic reasons for low values of temperatures observed during experimentation.

3.1.3.1 Spindle Speed and Temperature

Figures (3.7a,b) show the variation of tool-tip interface temperature with spindle speed for different cutting speeds. From the graph it is seen that there is a minimum value and then rises gradually with decreasing cutting speed.

3.1.3.2 Feed Rate and Temperature

The Figures (3.8a,b) show that there is a gradual increase in temperature, with increasing feed rate and decreasing cutting speed. As the feed rate increases, feed force increases, thereby increasing the temperature.

3.1.3.3 Cutting Speed and Temperature

Figures (3.9a,b) show the variation of temperature with cutting speed for different feed rates.
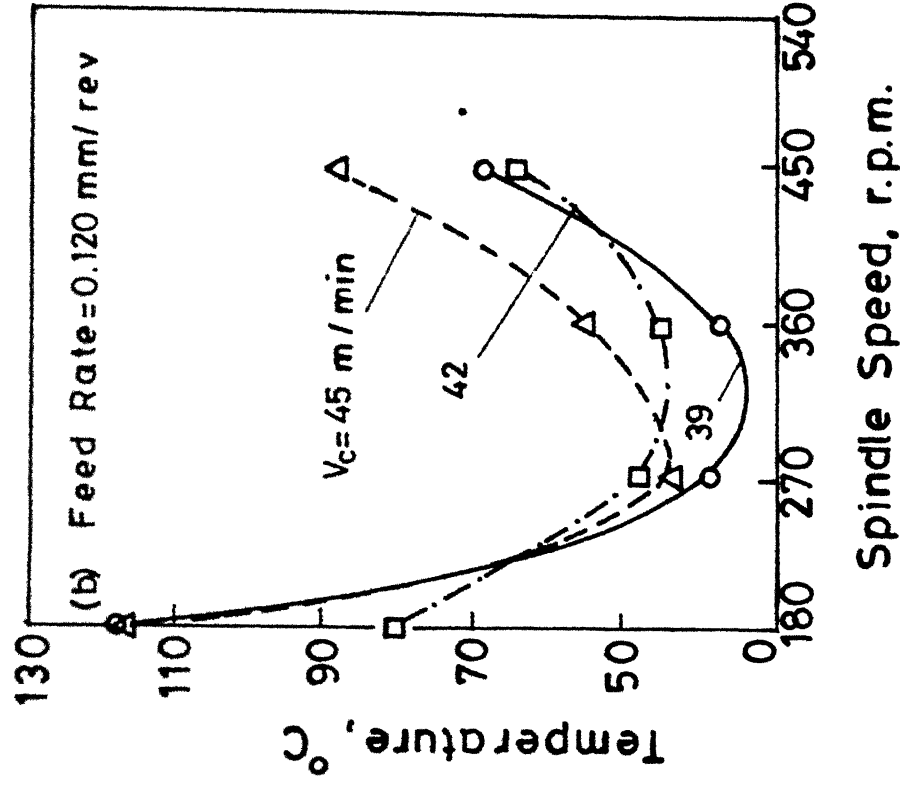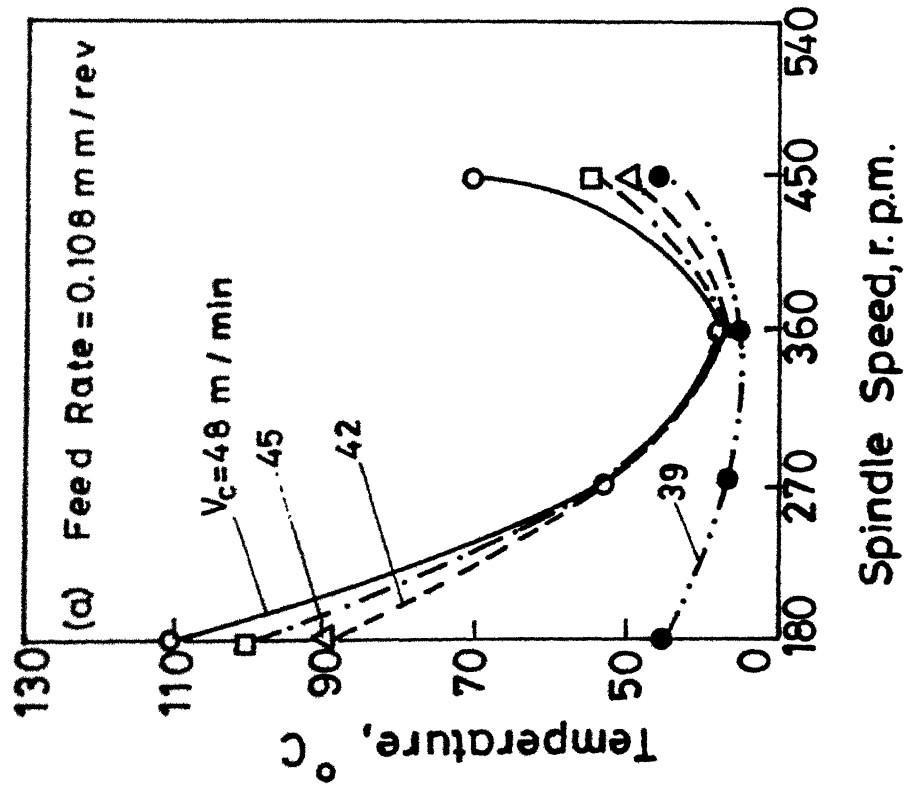
Fig. 3.7 Effect of Spindle Speed on Temperature (without coolant) During Facing.
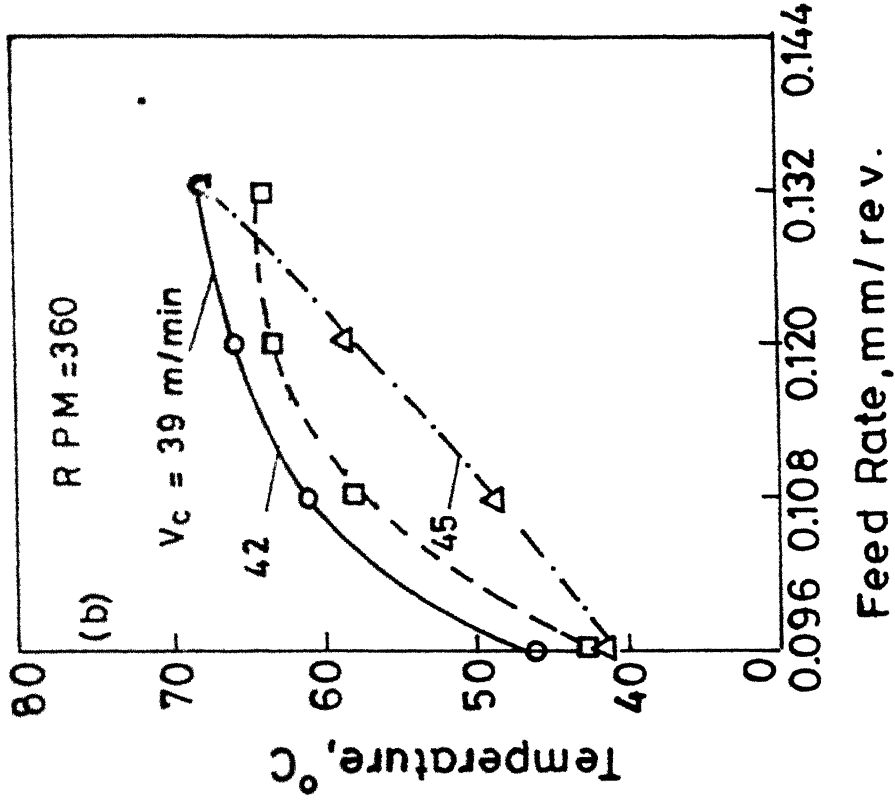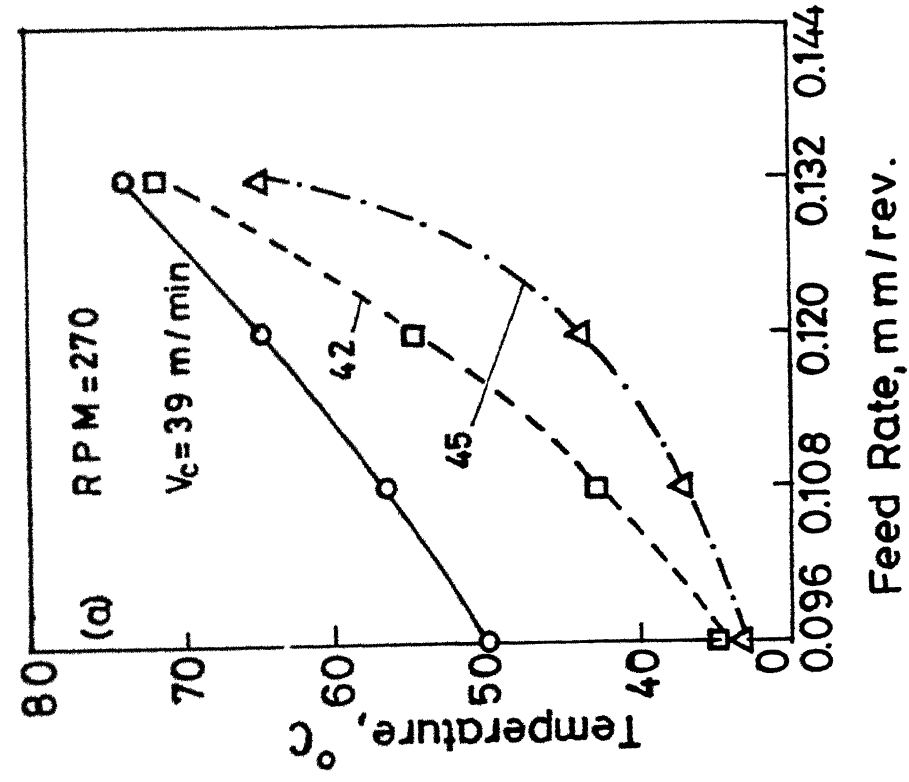
Fig. 3.8 Effect of Feed Rate on Temperature (without coolant) During Facing.

Fig. Temperature (without coolant) During Facing.

(a) RPM = 360

Temperature, °C vs Cutting Speed, m/min.

f = 0.132 mm/rev.
0.120
0.108
0.096

(b) RPM = 270

Temperature, °C vs Cutting Speed, m/min.

f = 0.132 mm/rev
0.120
0.108
0.096
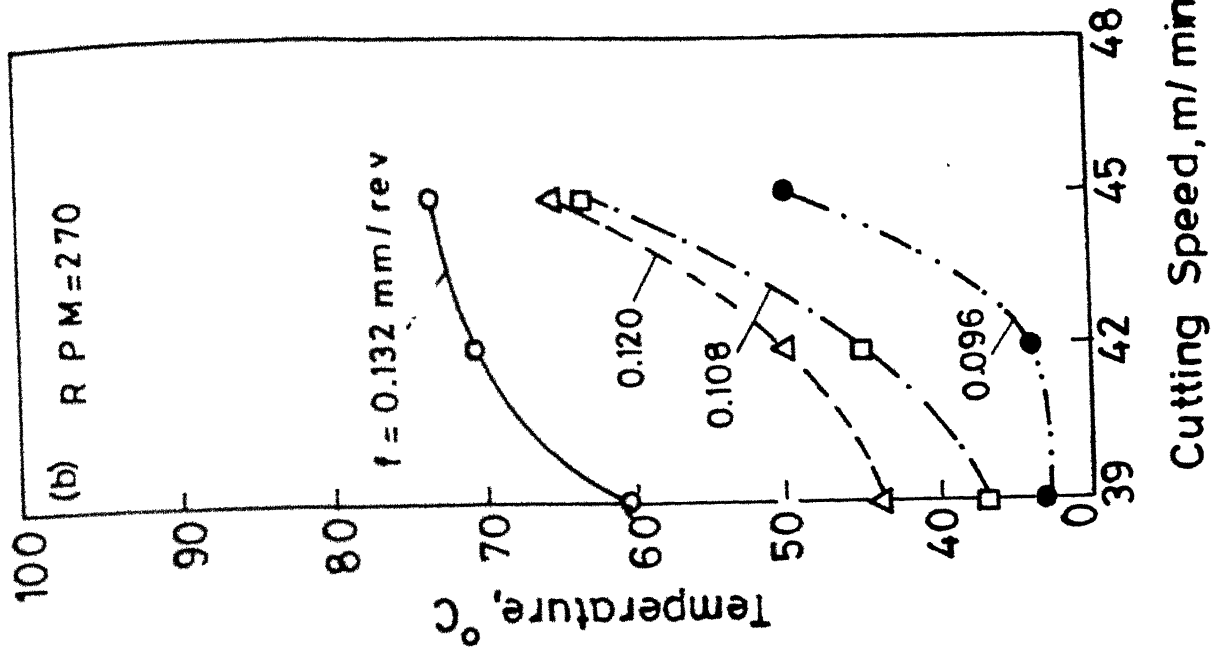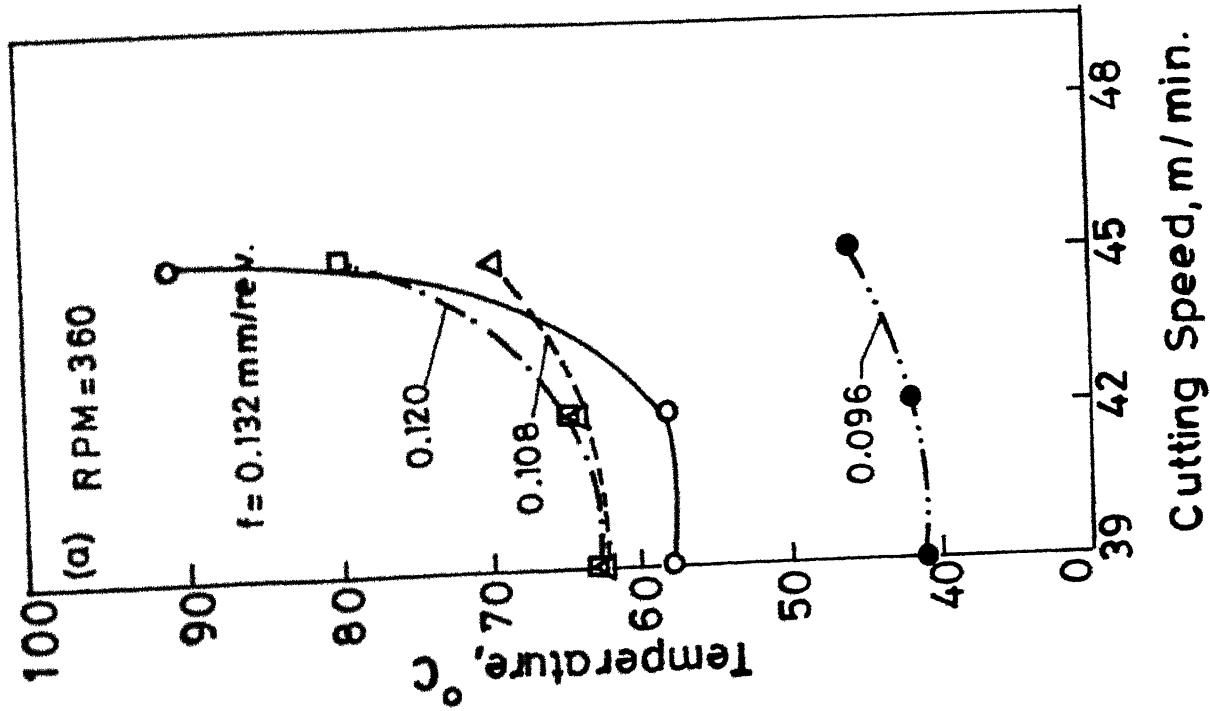
The temperature increases gradually, with increase in the cutting speed and increasing feed rates.

3.1.4 Tool Wear

In the case of facing, flank wear observed was very little,while the other types of wears such as crater wear and chipping of tool-tip were predominant. Hence, in order to investigate and analyse the type of wear,photographs of the wear of carbide tool-tips have been taken and are shown in Figs. (3.10 and 3.11).

From the Figs. (3.10, 3.11) it is seen that in most of the cases crater wear or chipping of the tool bit is present (Crater wear is shown in Fig. (3.10). Most of the crater wear has occurred at higher cutting speeds and lower spindle speeds. From the Fig. (3.11), chipping of the tool bit can be seen and can be observed th chipping has taken place mostly at higher feeds and lower spindle speeds,and is combined with a small amount of crater wear also. And also we can notice very little wear at higher spindle speeds.

During facing, most of the energy spent in cutting is almost entirely converted into heat. This causes a temperature rise of cutting tool. As the thermal conductivity of carbide tool bits is not good, there may be accumulation of heat in the cutting edge which results in its higher temperature. This causes formation of pits called crater on the tool surface near the edges.
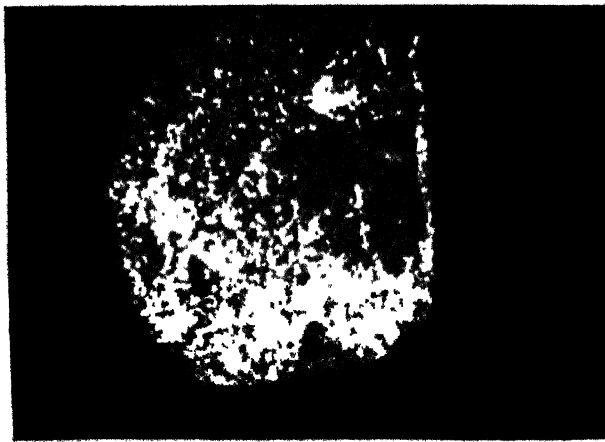
CUTTING SPEED = V_c = 66 m/min
SPINDLE SPEED = N = 270 rpm
FEED RATE = f = 0.096 mm/rev

V_c = 48 m/min
N = 270 rpm
f = 0.096 mm/rev
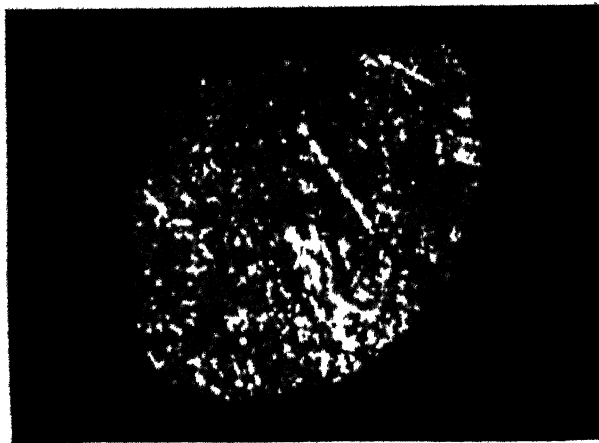
V_c = 60 m/min
N = 180 rpm
f = 0.108 mm/rev

V_c = 60 m/min
N = 180 rpm
f = 0.120 mm/rev

FIG. (3.10) PHOTOGRAPHS OF CRATER WEAR OF
CARBIDE TOOL BITS DURING FACING
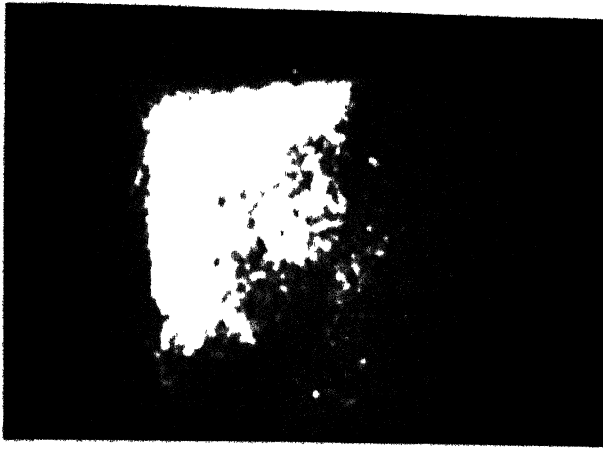
$V_c = 45 \ m/min$
$f = 0.120 \ mm/rev$
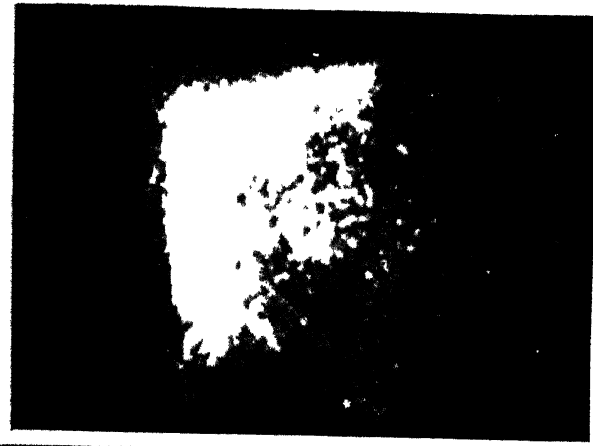
$V_c = 54 \ m/min$
$f = 0.132 \ mm/rev$
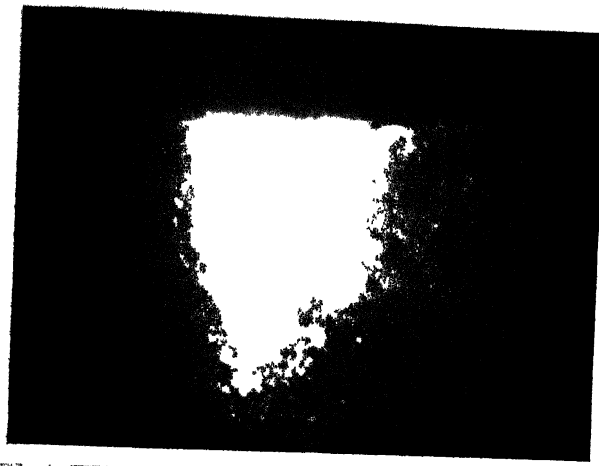
$V_c = 60 \ m/min$
$f = 0.108 \ mm/rev$

FIG. (3.11) FLANK WEAR OF CARBIDE TOOL BITS DURING LONGITUDINAL TURNING

$V_c = 54 \text{ m/min}$
$N = 270 \text{ rpm}$
$f = 0.108 \text{ mm/rev}$
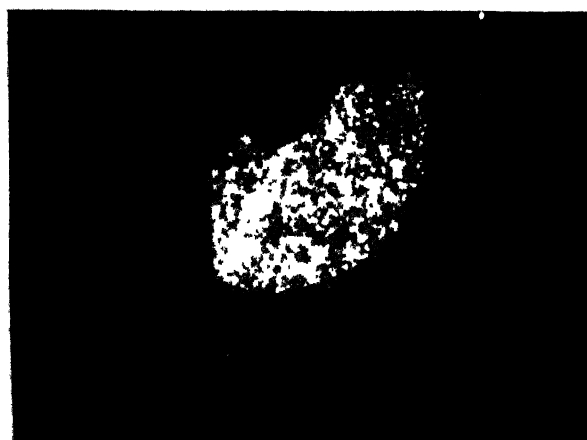
$V_c = 60 \text{ m/min}$
$N = 270 \text{ rpm}$
$f = 0.132 \text{ mm/rev}$

$V_c = 66 \text{ m/min}$
$N = 180 \text{ rpm}$
$f = 0.120 \text{ mm/rev}$
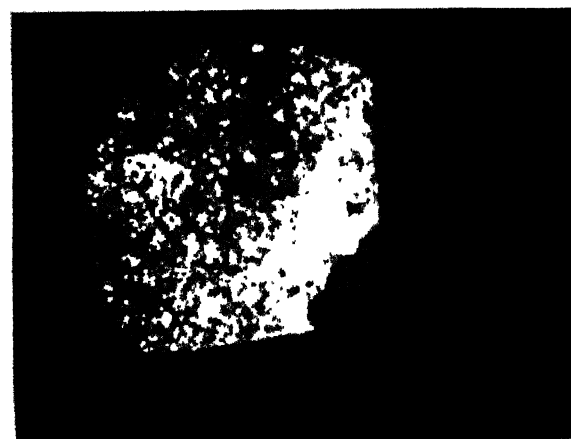
$V_c = 54 \text{ m/min}$
$N = 180 \text{ rpm}$
$f = 0.096 \text{ mm/rev}$

FIG. (3.11). PHOTOGRAPHS OF CHIPPING OF CARBIDE
TOOL BITS DURING FACING

At higher feed rates chipping has occurred. At higher feed rates the tool has to cut more number of fibres which are having high strength and hardness, there is a mechanical impact which may cause the chipping of the tool bits. Mechanical impact may be caused by intermittant cutting due to inhomogenity of composite material and which may lead to chipping of the tool bit.

3.2   Longitudinal Turning:

3.2.1 Feed Force

3.2.1.1 Feed Rate and Feed Force

The Figure (3.12a) shows that feed force continuously increases with increasing feed rate for all values of cutting speed. As the feed rate increases, the number of fibres to be cut increases and hence the force acting on the tool bit rises.

3.2.1.2 Cutting Speed and Feed Force

From the Fig. (3.12b) it is seen that there is gradual decrease in feed force with an increase in cutting speed for all values of feed rates.

3.2.2   Cutting Force

3.2.2.1 Feed Rate and Cutting Force

Figure (3.13a) shows that there is a slight increase in cutting force with an increase in feed rate for all values of cutting speeds. But the cutting force tends to be constant at higher feed rates. In
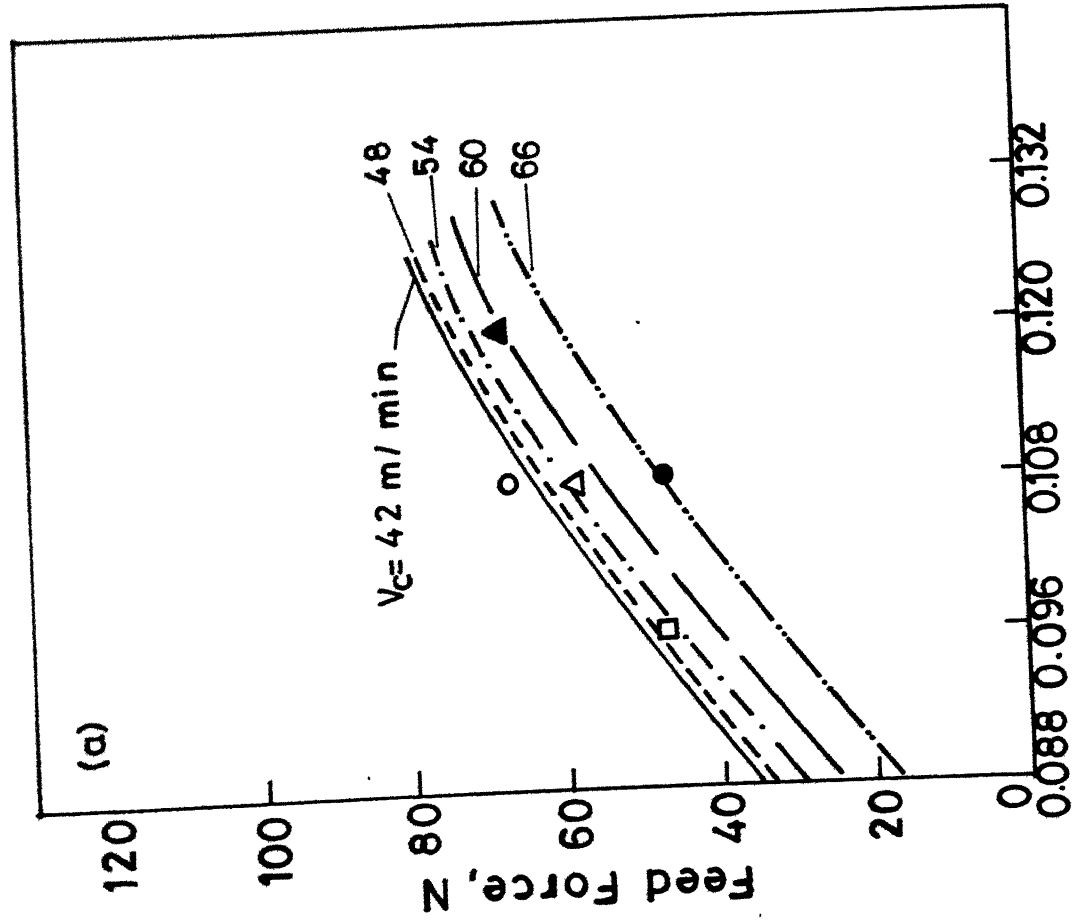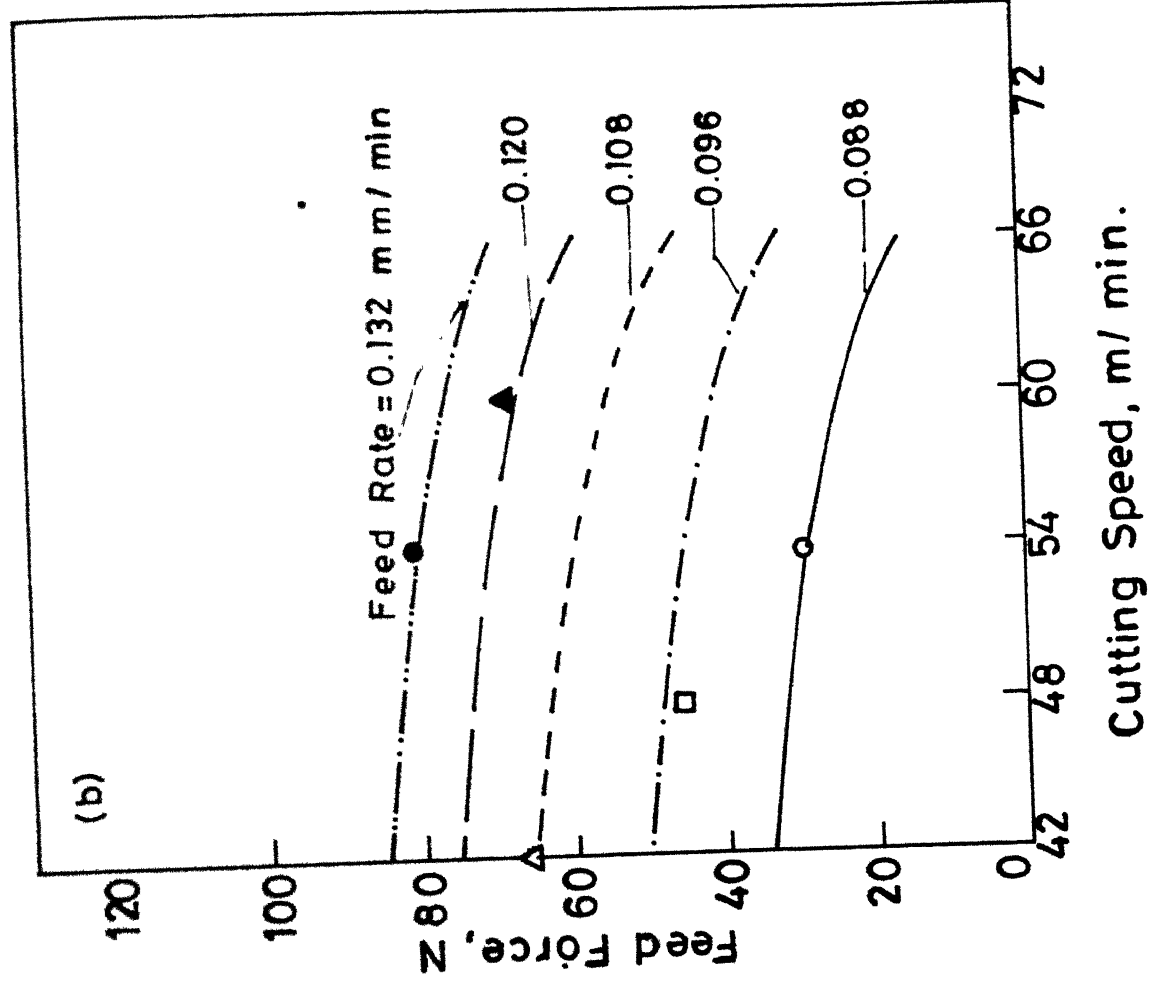
Fig. 3.12 Effect of Feed Rate and Cutting Speed on Feed Force During Longitudinal Turning.

(b)

Feed Rate = 0.132 mm/rev

0.120
0.108
0.096
0.088

Cutting Force, N

Cutting Speed, m/min.

(a)

$V_c = 42$ m/min

48
54
60
66

Cutting Force, N

Feed Rate, mm/rev.
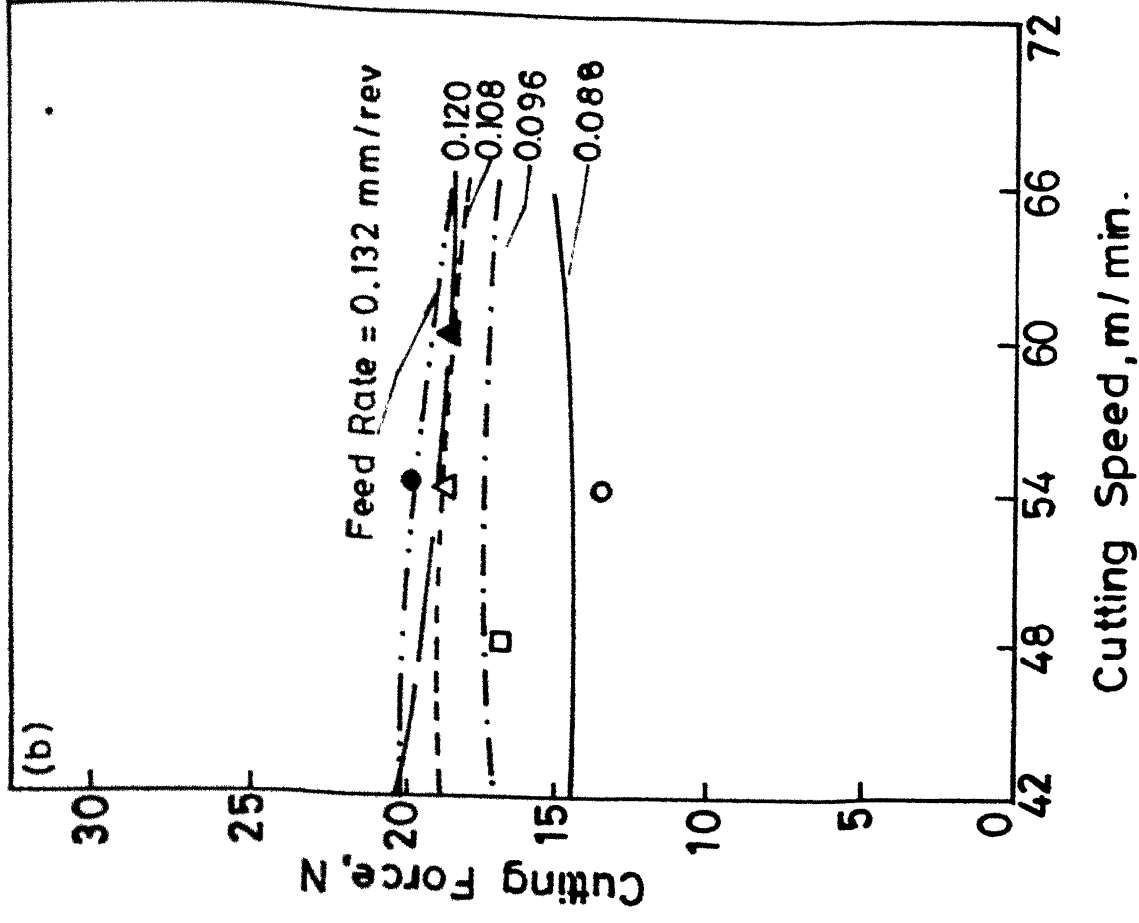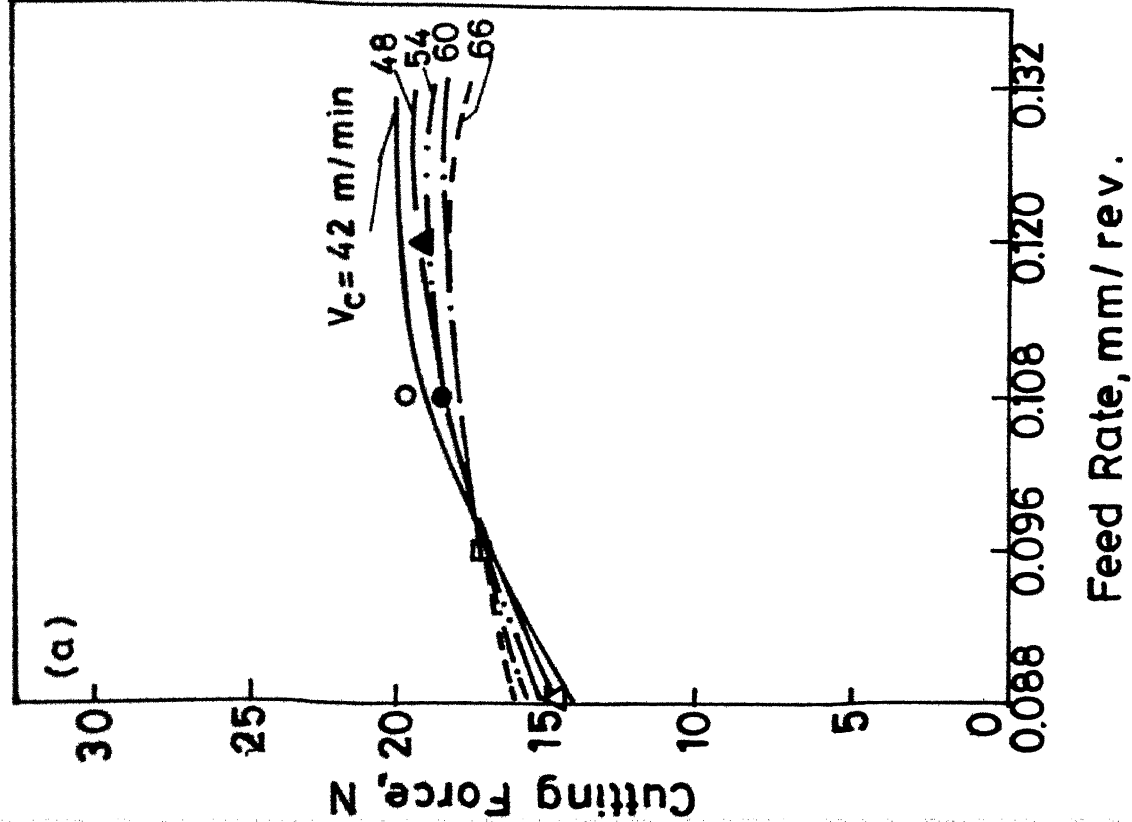
Fig. 3.13 Effect of Feed Rate and Cutting Speed on Cutting Force During Longitudinal Turning.
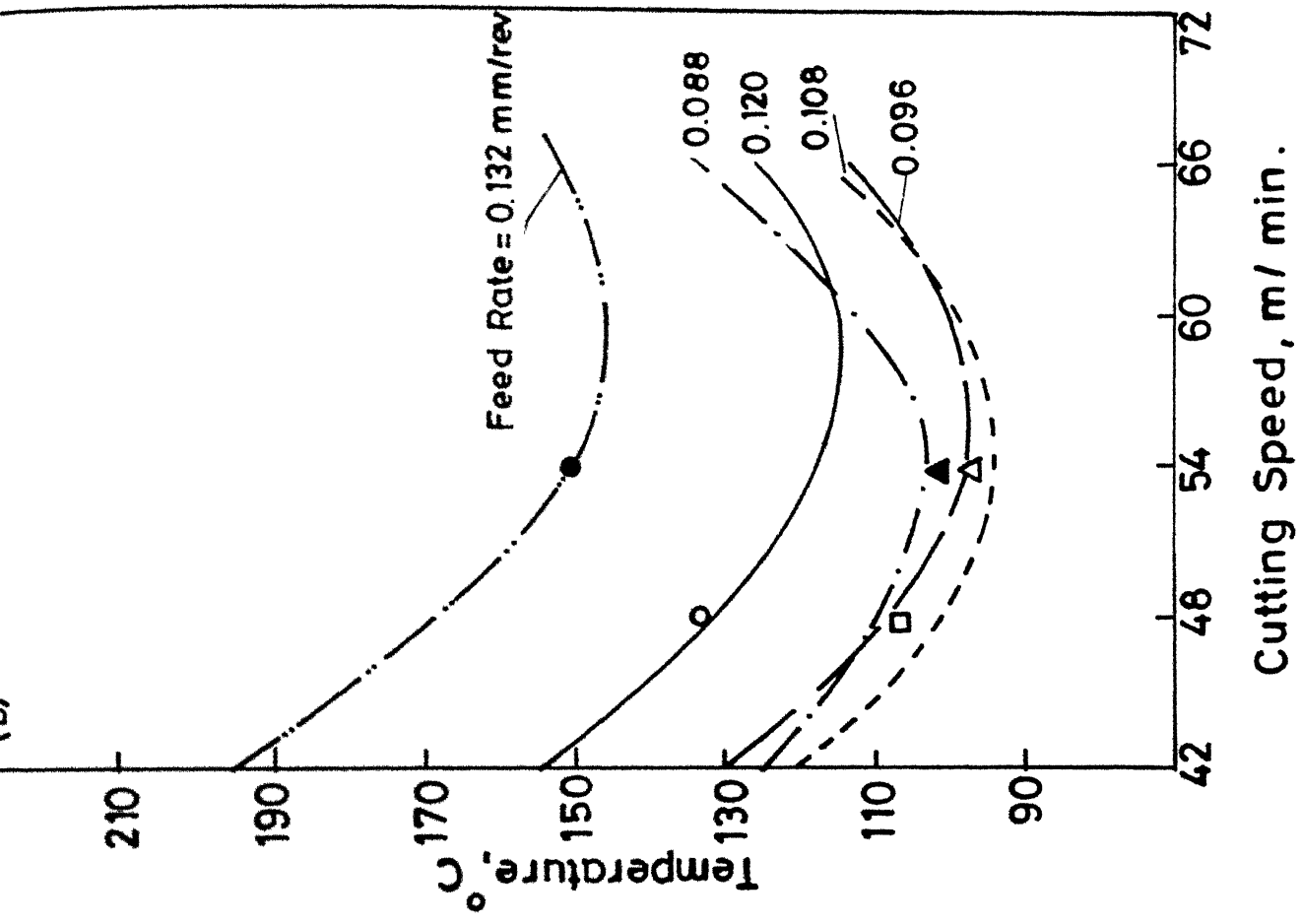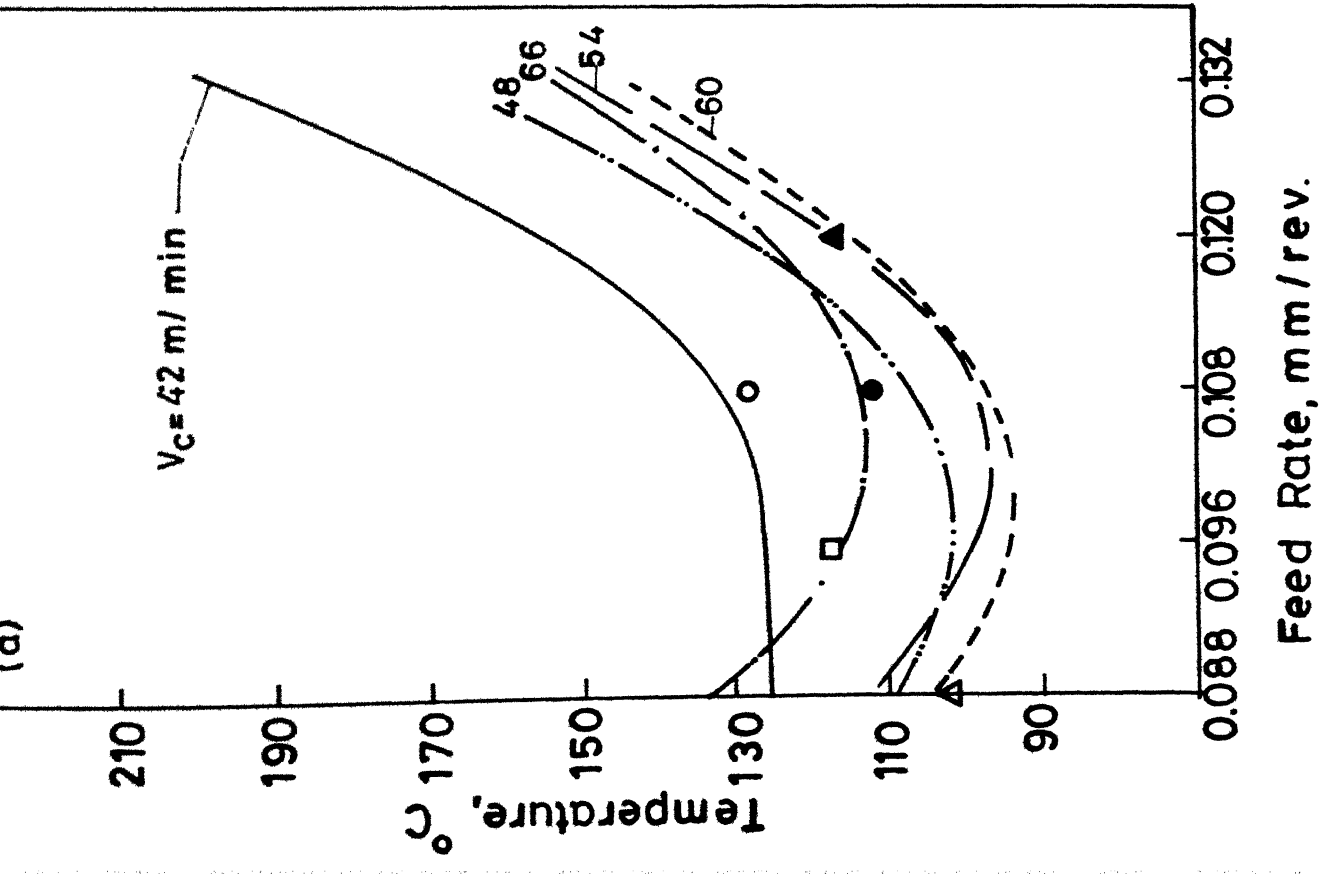
Fig. 3.14 Effect of Feed Rate and Cutting Speed on Temperature (without coolant) During Longitudinal Turning.

fact, in the cutting force direction, the force will
be needed to cut only the matrix material and it seems
that cutting of matrix is not much affected by the feed
rates.

3.2.2.2 Cutting Speed and Cutting Force

From the Figure (3.13b) it is seen that cutting
force is almost constant for all values of cutting speeds.
This shows that cutting force variation is unaltered by
the cutting speeds.

3.2.3 Temperature

3.2.3.1 Feed Rate and Temperature

The variation of the feed rate with temperature
at the bottom of the tool bit for different cutting speeds
is shown in Fig. (3.14a). The figure shows that at lower
range of feed rates there is decrease in temperature,
but at higher values of feed rates, the temperature
increases with increase in feed rates. At lower feed
rates the amount of fibres to be cut will be very less
and hence the tool temperature is less. But as the feed
rate increases the feed force increases, thereby increases
the temperature.

3.2.3.2 Cutting Speed and Temperature

In the beginning the temperature decreases as shown
in Fig. (3.13b), with increase in cutting speeds, but
afterwards, the temperature gradually increases with
increase in cutting speeds.

(a)

Cutting Speed = 54 m/min

Feed Rate = 0.132

0.108

0.088

Flank Wear Land Width, mm ($\times 10^{-1}$)

Machining Time, min.

(b)

Feed and Rate = 0.108 mm/rev.

V_c = 42 m/min

54

66

Flank Wear Land Width, mm ($\times 10^{-1}$)
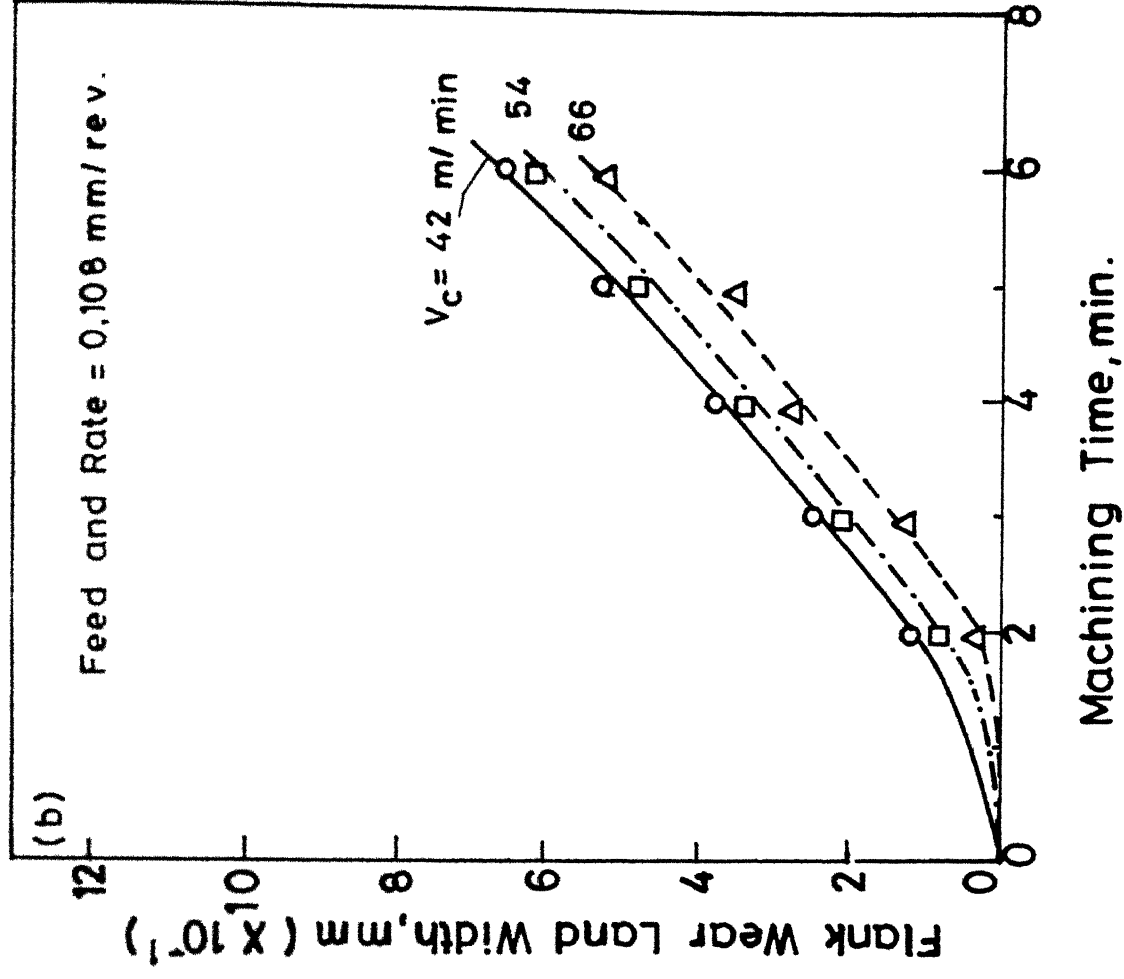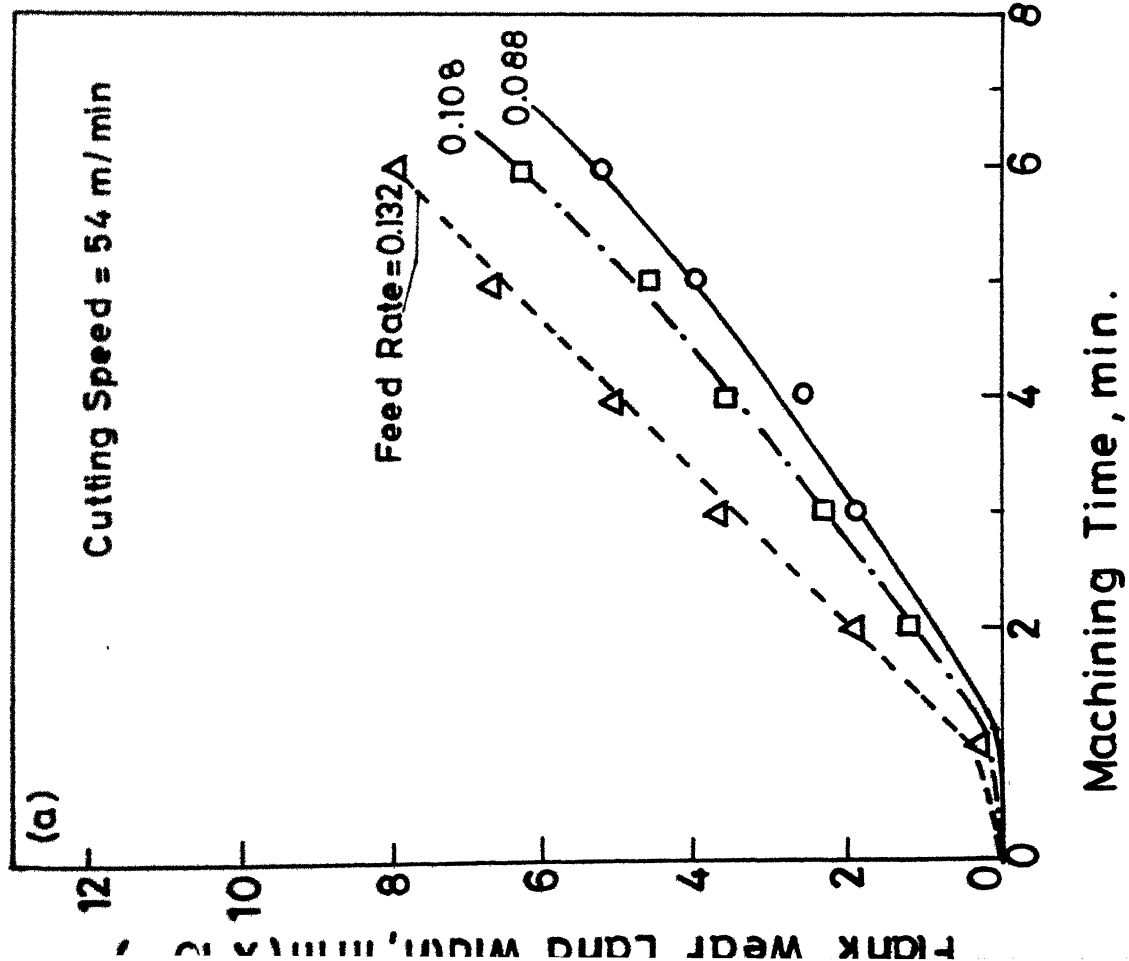
Machining Time, min.

Fig. 3.15 Effect of Machining Time on Flank Wear During Longitudinal Turning.

3.2.4 Tool Wear

3.2.4.1 Machining Time and Flank Wear

Figures (3.15a,b) shows the variation of flank wear land width with machining time for different values of feed rates and cutting speeds. From the figures it is seen that there is almost linear increase in flank wear with increase in machining time; from the figures it is also seen that flank wear land width is less at lower feed rates and higher cutting speeds.

CHAPTER-4

CONCLUSIONS AND SCOPE FOR FUTURE WORK

4.1 Conclusions

On the basis of experimental results and discussion, the following conclusions may be drawn.

4.1.1 Feed Force:

1. The feed force is more compared to cutting force in both longitudinal turning and facing operations on the composite material. But the trend is reverse in case of conventional metals.

2. In facing, the feed force increases with an increase in feed rate, cutting speeds and has low value at lower spindle speeds.

3. In longitudinal turning, the feed force increases with an increase in feed rate, while it decreases with an increase in cutting speeds.

4.1.2 Cutting Force

1. The cutting force is not much affected by the machining parameters such as cutting speed, spindle speed and feed rate in both longitudinal turning and facing operations.

4.1.3 Tool Wear

1. Tool wear is found to be very high in machining of composites compared to machining of conventional metals. This high tool wear may be due to high hardness and abrasive nature of the glass fibres.

2. In longitudinal turning, flank wear is predominant and it increases with increasing feed rate and decreases with increase in cutting speed.

3. In case of facing operation, flank wear is very little while crater wear and chipping of tool bit is predominant which occurs at high feed rates, high cutting speeds and low spindle speeds.

4.1.4 Tool Temperature

1. In facing, temperature is found to increase with increase in all machining parameters except at lower range of cutting speeds, wherein there is a gradual decrease in temperature with increase in cutting speeds.

2. In longitudinal turning, the temperature is found to increase with an increase in feed rates but at lower values of feed rates there is a decrease in temperature. At higher cutting speeds the temperature attains minimum value.

4.2 Scope for Future Work:

1. The mechanism of chip formation in machining of composite materials is not known exactly and work can be carried out in this field.

2. The work can be extended to shaping, milling, to estimate the tool wear, machining forces etc.

3. As the airborne dust is produced while machining of glass fibre epoxy composite which is hazardous to health, a better set-up may be designed for collecting and removing the glass dust.

CHAPTER-5

REFERENCES

1   Rosenhein W. and Sturney A.C., Report in Flow and Rupture of Metals during Cutting, Proc. of Inst. of Mech. Engrs, 1925, p. 441.

2   Koceuoglu D., Shear Strain Rate in Metal Cutting and Its Effects on Shear Flow Stress, Trans. Am. Sci. Mech. Engrs., Vol. 158 (1958).

3   Das S. and Bhattacharya A., Analysis of Stagnant Phenomenon in Metal Cutting by High Speed Drop Tool Trigger Mechanism, J. Inst. Engrs. (India), XLU, 9, Pt. ME 5 (1965).

4   Black J.T., and James C.R., The Hammer QSD-Quick Stop Device for High Speed Machining and Rubbing, ASME Journal, Jan. 14, 1981.

5   Vorm T., Development of a Quick-Stop Device and an Analysis of the 'Frozen-chip' Technique, Int. J. Mech. Tool. Des. Res., Vol. 16, pp. 241-250.

6   Okushima K. and Hitomi K., An Analysis of the Mechanism of Orthogonal Cutting and its Application to Discontinuous Chip Formation, Trans. Am. Soci. Mech. Engrs., J. Engg. Industries, Paper No. 60-WA-79.

7   Heginbotham W.B. and Gogia S.L., Metal Cutting and the Built-up Nose, Proc. Inst. Mech. Engrs., 175, 892 (1962).

8   Hastings W.F., A New Quick-Stop Device and Grid Technique for Metal Cutting Research, Annals. of CIRP, Vol. 15, p. 109 (1957).

9   Ellis J. Kirk R. and Barrow G., The Development of a Quick-Stop Device and Metal Cutting Research, Int. J. Mech. Tool. Des. Res., Vol. 9, p. 321 (1969).

10   Brown R.H., A Double Shear Pin Quick-stop Device for very Rapid Disengagement of a Cutting Tool, Int. J. Mach. Tool Des. Res., Vol. 16, pp. 115-221 (1976).

11   Philip P.K., Study of the Performance Characteristics
      of an Explosive QSD for Freezing Cutting Action,
      Int. J. Mach. Tools Des. Res., Vol. 11, p. 133
      (1971).

12   Brown R.H. and Komanduri R., An Investigation of the
      Performance of a QSD for Metal Cutting Studies,
      Proc. of 13th M.T.D.R. Conf. Birmingham, p. 225.

13   Merchant M.E. and Zlatin N., Proc. of the Soci. of
      Expt. Stress Analysis, Vol. 3, No. 2 (1946), pp.4-7.

14   Boothroyd G., A Metal Cutting Dynamometer, The
      Engineer, Vol. 213 (1962), p. 351.

15   Shaw M.C., Metal Cutting Principles, Oxford and IBH,
      New Delhi (1969).

16   Okushima K. and Hitomi K., A Design of Three Component
      Tool Dynamometer, Trans. of J. Soci. Mech. Engrs,
      Jan. 1961.

17   Albrecht P., Dynamics of Metal Cutting Process,
      Trans. of ASME, Nov. 1965, p. 429.

18   King B. and Foschi R.O., Crossed Ring Dynamometer
      for Direct Force Resolution with Three Orthogonal Compone
      Int. J. of M.T.D.R., Vol. 9, No. 9, 1969, p. 345.

19   Venkatesh V.C. and Chandrasekaran H., Experimental
      Techniques in Metal Cutting, PHI, 1987.

20   William T. Thomson, Theory of Vibration with Applications
      PHI edition.

21   Konig W., Machining of Fibre Reinforced Plastics,
      Annals of CIRP, Vol. 34, 1985, pp. 537-548.

22   Schwartz M.M., Composite Material Hand Book,
      McGraw-Hill Book Company, 1984, Chapter-6.

23   Dastin S.J., Joining and Machining Techniques, Hand Book
      of Composites, edited by George Lubin, pp. 602-632.

24   Rod Docrr, Machining Techniques for Kevlar Reinforced
      Composites, Fabrication of Composite Materials - Source
      Book, Compiled by Mel. M. Schwartz, ASM, 1985.

25   Radhakrishnan T. and S.M. Wu, On Line Hole Quality
      Evaluation for Drilling Composite Material using
      Dynamic Data, ASME J. Eng. Industry, Feb. 1981, Vol. 103,
      pp. 119-125.

26   Everstine G.C., A Theory of Machining of Fibre
        Reinforced Materials, J. Composite Materials,
        Vol. 5 (Jan. 1971), p. 94.

27   Aksel Koplov, Cutting of CFRD with Single Edge
        Tools, Advances in Composite Materials, ICCM-3
        3rd International Conference on Composite Materials,
        France, Vol. 2, pp. 1597-1605.

28   Koplov A., The Cutting Process, Chips and Cutting
        Forces in Machining CFRP, Composites, Vol. 14, No.4,
        Oct. 1983.

29   Preuss and McGinty, Machining Fibre FP/Aluminium,
        American Machinist, August 1985.

30   Bhagwan D. Agarwal and Lawrence J. Broutman,
        Analysis and Performance of Fibre Composites, Wiley
        Interscience Publication, 1980, Chapter 2, pp. 12

31   Markova E.V. et al. The Design of Experiments, Mir
        Publishers, Moscow, 1975.

32   Cochron W.G. and Vox G.M., Experimental Design,
        Asia Publishing House, New Delhi (1962).

33   Jain V.K., and Pandey P.C., Computer Aided Analysis
        of ECBD Process, Proc. of the 23rd IMTDR Conference,
        1982, pp. 257-264.

34   Lukalapu Joga Rao, High Strain Rate Behaviour of
        Glass and Graphite Fibre Epoxy Composites,
        Ph.D. Thesis, IIT Kanpur, 1983.

APPENDIX

Table-1 : Time taken by the tool to withdraw at different
cutting conditions

Sl. No.	Vertical force (N)	Horizontal force (N)	Time taken by the tool to withdraw from tool holder (μs)
1.	107	78	204
2.	147	98	221
3.	245	147	249
4.	341	196	289
5	384	216	226

Table-2 : Cutting conditions at which chip roots are
collected for the study of primary shear
deformation zone

Sl. No.	Cutting speed (m/min)	Feed rate (mm/rev)	Depth of cut (mm)
1	13.7	0.2	0.6
2	17.9	0.15	0.8
3	8.7	0.3	0.6

Table-3 : Levels for different factors for **longitud**inal
turning

Factors	Levels				
	-2	-1	0	1	2
Feed rate, X_1 (mm/rev)	0.084* (0.088)	0.096	0.108	0.120	0.132
Cutting speed, X_2 (m/min)	42	48	54	60	66

* Indicates the feed rate that was not available on the lathe
machine.

The value in the bracket indicates the actual value of feed
rate available on the machine lathe.

Table-4 : Experimental plan and responses for longitudinal turning

| Sl.No. | Order | Feed rate (mm/rev) | CUTTING speed (m/min) | Responses Forces, N | | | | |
				Minimum feed force	Maximum feed force	Mean feed force	Standard deviation	Mean cutting force
1	11	0.096	48	37.3	54.9	46.1	8.8	17.7
2	12	0.120	48	52.9	90.3	71.6	18.7	18.6
3	2	0.096	60	24.5	59.8	42.2	17.7	18.6
4	3	0.120	60	47.1	90.3	68.7	21.6	18.6
5	4	0.088	54	27.5	31.4	29.4	2.7	13.7
6	5	0.132	54	61.8	101	81.4	19.4	19.6
7	13	0.108	42	55.9	77.5	66.7	10.3	19.6
8	1	0.108	66	39.2	52.9	46.1	6.9	17.7
9	6	0.108	54	51.0	78.5	64.7	13.7	18.6
10	7	0.108	54	51.5	66.2	58.9	7.4	18.6
11	8	0.108	54	40.2	48.1	44.1	3.9	18.6
12	9	0.108	54	58.9	66.2	67.7	8.8	18.6
13	10	0.108	54	47.1	80.4	63.8	16.7	18.6

Continued.....

Sl. No.	Order	Factors		Mean Temperature, °C		Responses — Tool wear-Flank wear land width, mm					
		Feed rate (mm/rev)	Cutting speed (m/min)	Without coolant	With coolant	1st min	2nd min	3rd min	4th min	5th min	6th min
1	11	0.096	48	108	60	0.01	0.10	0.20	0.31	0.43	0.59
2	12	0.120	48	134	70	0.02	0.11	0.23	0.37	0.49	0.62
3	2	0.096	60	103.7	44	–	0.02	0.12	0.18	0.30	0.45
4	3	0.120	60	117.2	48.7	0.01	0.16	0.23	0.40	0.51	0.74
5	4	0.088	54	101	50.5	0.01	0.13	0.22	0.31	0.44	0.56
6	5	0.132	54	151	72	0.04	0.20	0.39	0.50	0.67	0.82
7	13	0.108	42	128	68	0.03	0.14	0.25	0.39	0.53	0.70
8	1	0.108	66	112.5	44.2	0.01	0.07	0.19	0.25	0.40	0.54
9	6	0.108	54	122	61	0.02	0.13	0.22	0.38	0.50	0.65
10	7	0.108	54	82	50	0.02	0.13	0.22	0.38	0.50	0.65
11	8	0.108	54	62	46	0.01	0.13	0.22	0.38	0.50	0.59
12	9	0.108	54	105	45	0.02	0.13	0.22	0.38	0.50	0.66
13	1-	0.108	54	112	46	0.02	0.13	0.22	0.38	0.50	0.70

Table-5: Experimental Plan and results for facing operation

Sl. No.	Feed rate (mm/rev)	Spindle speed (rpm)	Cutting speed (mm/min)	Feed Force 39	42	48	54	60	66	Cutting Force 39	42	45	54	60	66
1	0.108	180		137.3	78.5	71.6	201.1			34.3	34.3	34.3	34.3		
2	0.108	270		93.2	83.4	117.7	206			19.6	19.6	14.7	9.8		
3	0.108	360		54	39.2	29.4	39.2			7.4	7.4	7.4	7.5		
4	0.108	540		17.2	17.2	9.8	14.7			9.8	7.4	4.9	9.8		
5	0.108	180		73.6	58.9	39.2	44.1	88.3		19.6	19.6	19.6	19.6	19.6	
6	0.108	270		58.9	58.9	63.8	83.4	147.1		12.3	12.3	19.6	9.8	12.3	
7	0.108	360		17.2	17.2	12.3	22	34.3		4.9	4.9	4.9	9.8	12.3	
8	0.108	540		12.3	147	9.8	7.4	9.8		7.4	7.4	7.4	12.3	14.7	
9	0.108	180		117.7	112.8	88.3	93.2	68.7	73.6	22	22	19.6	14.7	9.8	9.8
10	0.108	270		68.7	63.8	58.9	49	63.8	132.4	19.6	17.2	14.7	14.7	9.8	4.9
11	0.108	360		14.7	14.7	34.3	27	19.6	9.8	4.9	4.9	4.9	12.3	12.3	2.2
12	0.108	540		24.5	17.2	19.6	24.5	24.5	24.5	9.8	9.8	9.8	4.9	4.9	4.9

Table 5 (Continued):

13	0.096	180	49	44.1	34.3	29.4	63.8	14.7	14.7	17.2	17.2	19.6	19.6
14	0.108	180	58.5	93.2	103	132.4	215.8	24.5	26.9	23.4	24.5	19.6
15	0.120	180	77.5	63.8	65.8	103	132.4	19.6	17.2	9.8	9.4	14.7
16	0.132	180	196.2	211	230.5	235.4	245.2	29.4	34.3	24.5	17.2	4.9
17	0.096	270	49	34.3	49	68.7	132.4	12.3	14.7	19.6	14.7	9.8
18	0.108	270	31.9	36.8	9.8	39.2	19.6	7.3	7.3	2.4	4.9	2.4
19	0.120	270	58.9	44.1	24.5	27	29.4	19.6	14.7	7.3	14.7	9.8
20	0.132	270	132.4	93.2	49	73.6	147.1	24.5	17.2	12.3	9.8	4.9
21	0.096	360	98	98	73	9.8	9.8	4.9	4.9	4.9	4.9	4.9
22	0.108	360	14.7	14.7	14.7	9.8	9.8	9.8	9.8	12.3	9.8	9.8
23	0.120	360	29.4	24.5	19.6	9.8	58.9	9.8	7.3	7.3	4.9	7.8
24	0.132	360	49	36.8	19.6	9.8	58.9	7.3	4.9	4.9	4.9	9.8

le 5 (Continued):

0.096	270	29.4	24.5	44.1			9.8	9.8	14.7		
0.108	270	63.8	54	147.2			17.2	17.2	14.7		
0.120	270	73.6	58.7	240.3			19.6	19.6	29.4		
0.132	270	176.6	161.7	201.1			24.5	19.6	24.5		
0.096	270	44.1	19.6	14.7	295		14.7	9.8	9.8		
0.108	270	14.7	14.7	14.7	9.8		7.3	9.8	4.9		
0.120	270	117.8	73.6	98.1	107.9		2.2	19.6	4.9		
0.132	270	93.2	68.7	63.7	186.4		19.6	14.7	19.6		
0.096	270	49	49	49	78.5	93.2	24.5	24.5	19.6	49	49
0.108	270	39.2	49	68.7	39.2	58.7	12.3	9.8	9.8	9.8	9.8
0.120	270	49	44.1	147.1	152	161.7	24.5	24.5	24.5	24.5	24.5
0.132	270	63.8	54	166.8	235.4	284.5	24.5	24.5	88.3	49	14.7
0.096	270	26.9	29.4	83.4	93.2	176.6	166.8	9.8	9.8	24.5	24.5	19.6	27	54
0.108	270	2944	19.6	19.6	39.2	24.5	19.6	12.3	17.1	4.9	4.9	4.9	4.9
0.120	270	58.7	49	54	54	68.7	34.3	19.6	19.6	19.6	19.6	19.6	19.6
0.132	270	83.4	73.6	58.7	107.9	54	73.6	19.6	24.5	24.5	14.7	12.76

Table-5 : Continued

Sl. No.	Feed rate (mm/rev)	Spindle speed (rpm)	Cutting speed (m/min)	Response, Temperature, °C									
				39	42	45	48	51	54	57	60	63	65
1	0.108	180		81	118	62	41	39	35				
2	0.108	270		48	40	43	43	38	36				
3	0.108	360		45	38	56	46	42	39				
4	0.108	540		65	69	89	35	55	34				
5	0.108	180		47	54	58	47	37	37	39	34		
6	0.108	270		40	40	41	42	42	43	38	33		
7	0.108	360		43	44	48	45	50	51	53	53		
8	0.108	540		52	50	52	55	43	41	39	38		
9	0.108	180		45	91	101	111	106	37	40	39	39	34
10	0.108	270		43	53	53	57	33	41	38	34	32	32
11	0.108	360		35	38	38	38	49	50	46	50	52	56
12	0.108	540		46	51	56	71	36	44	39	38	39	38
13	0.096	180		44	59	61	36	42	52	49	39		
14	0.108	180		53	86	43	45	47	42	41	40		
15	0.120	180		60	61	39	38	47	50	53	35		
16	0.132	180		87	96	112	61	41	45	46	37		

Table-5 (Continued):

17	0.132	180	87	96	112	61	41	45	46	37
17	0.096	270	38	40	47	49	35	35	36	35
18	0.108	270	38	48	48	57	37	35	43	40
19	0.120	270	42	48	47	52	49	43	42	43
20	0.132	270	48	54	64	100	45	45	47	43
21	0.096	360	41	42	46	49	52	50	45	33
22	0.108	360	58	58	91	37	44	49	48	41
23	0.120	360	58	63	68	80	53	36	58	34
24	0.132	270	63	64	66	70	54	43	41	33
25	0.096	270	42	47	57	38				
26	0.108	270	52	56	48	44				
27	0.120	270	55	50	35	35				
28	0.132	270	58	60	82	38				
29	0.096	270	31	32	46	72	39	36		
30	0.108	270	38	42	49	39	38	36		
31	0.120	270	45	45	47	40	42	33		
32	0.132	270	46	40	38	38	38	36		
33	0.096	270	33	34	50	59	36	38	37	38
34	0.108	270	37	50	64	40	45	45	43	42
35	0.120	270	44	55	65	45	36	36	37	38

Table-5 (Continued) :

36	0.132	270	65	72	74	38	43	44	47	44		
37	0.096	270	41	51	38	40	36	39	46	51	38	38
38	0.108	270	48	58	65	41	33	36	33	36	37	36
39	0.120	270	48	67	86	92	72	39	38	38	35	35
40	0.132	270	49	85	93	92	42	52	53	39	42	41

Table-6 : The values of coefficients (b_i's) for longitudinal turning

Source (coefficients)	Feed force	Cutting force	Temperature	Flank wear land width
b_o	59.66	18.67	98.21	0.49
b_1	12.98	1.1	11.62	0.06
b_2	-3.98	-2.4	-4.3	-0.03
b_{11}	-1.12	-0.48	7.4	0.01
b_{22}	-0.87	0.02	6.0	-0.01
b_{12}	0.19	-0.22	-3.1	0.04

ME-1988-M-SAT-MAC